December 2015

Alkali-~Activated Fly Ash Binders: Feasibility as a Sustainable Alternative to Ordinary Portland Cement for Pre-~Cast Systems

Kimberly Sierra
University of Nevada, Las Vegas, sierrak@unlv.nevada.edu

ALKALI-ACTIVATED FLY ASH BINDERS: FEASIBILITY AS A SUSTAINABLE ALTERNATIVE TO ORDINARY PORTLAND CEMENT FOR PRE-CAST SYSTEMS

By

Kimberly J. Sierra

Bachelor of Science in Entertainment Engineering Design
University of Nevada, Las Vegas
2012

A thesis submitted in partial fulfillment
of the requirements for the

Master of Science in Engineering – Civil and Environmental Engineering

Department of Civil and Environmental Engineering and Construction
Howard R. Hughes College of Engineering
The Graduate College

University of Nevada, Las Vegas
December 2015

UNLV | GRADUATE COLLEGE

Thesis Approval

The Graduate College
The University of Nevada, Las Vegas

November 13, 2015

This thesis prepared by

Kimberly J. Sierra

entitled

Alkali-Activated Fly Ash Binders: Feasibility as a Sustainable Alternative to Ordinary Portland Cement for Pre-Cast Systems

is approved in partial fulfillment of the requirements for the degree of

Master of Science in Engineering – Civil and Environmental Engineering
Department of Civil and Environmental Engineering and Construction

Nader Ghafoori, Ph.D.
Examination Committee Chair

Kathryn Hausbeck Korgan, Ph.D.
Graduate College Interim Dean

Samaan Ladkany, Ph.D.
Examination Committee Member

Mohamed Kaseko, Ph.D.
Examination Committee Member

Mohamed Trabia, Ph.D.
Graduate College Faculty Representative

ABSTRACT

ALKALI-ACTIVATED FLY ASH BINDERS: FEASIBILITY AS A SUSTAINABLE ALTERNATIVE TO ORDINARY PORTLAND CEMENT FOR PRE-CAST SYSTEMS

By

Kimberly Sierra

Dr. Nader Ghafoori, Advisory Committee Chair
Professor of the Civil and Environmental Engineering Department
University of Nevada, Las Vegas

Fresh, load-dependent, transport, and durability properties of alkali-activated fly ash mortars were studied. The influences of activator concentration, solution-to-binder ratio, curing condition, activator type, and sodium silicate-to-total solution ratio on the properties of the studied alkali-activated mortars were examined. This study was divided in two phases. The first phase dealt with the use of sodium hydroxide as the sole activator. The second phase of the study was divided into two parts, both of which used a combination of sodium hydroxide and sodium silicate as the activator solution. Part I of phase II used elevated temperature curing conditions, whereas part II utilized moist curing at ambient temperature. Fresh properties included workability and setting times. Load-dependent properties included compressive and flexural strengths, as well as modulus of elasticity. The evaluated transport properties were absorption, density, void content, and rapid chloride migration. Durability properties consisted of resistance to abrasion, sulfuric acid, freezing and thawing, and external sulfate attack.

For the phase I of this study, workability and initial and final setting times were found to increase and decrease with increased solution-to-binder ratio and activator concentration, respectively. The effects of different curing conditions were found to be dependent on the

concentration of sodium hydroxide. All mechanical properties tested were found to decrease and increased with increased solution-to-binder ratio and activator concentration, respectively. Absorption and rapid chloride migration were found to increase and decrease with increased solution-to-binder ratio and activator concentration, respectively. Results for density, on the other hand, produced the contrary.

For the phase II of this study, workability was found to decrease with increased sodium hydroxide concentration and sodium silicate-to-total solution ratio. Mechanical properties were found to increase with an increase in sodium hydroxide concentration, as well as increased sodium silicate-to-total solution ratio up to 7.5 M NaOH. Mechanical properties decreased with increases in sodium silicate-to-total solution ratio when 10 and 12.5 M NaOH were used. Transport properties, namely absorption, void content and rapid chloride migration, results were found to decrease with increased sodium hydroxide concentration as well as sodium silicate-to-total solution ratio up to 7.5 M sodium hydroxide. The named transport properties were found to increase with increased sodium silicate-to-total solution ratio for the mortars activated by 10 and 12.5 M NaOH. Mass losses induced by acid attack and freezing and thawing cycles experienced the same trends as transport properties, whereas the depth of wear results produced the contrary. Strength losses due to acid and sulfate attacks were minimal throughout the entire immersion duration; with the mortars having lower sodium hydroxide concentrations experienced larger losses as compared to the mortars containing higher sodium hydroxide concentrations.

ACKNOWLEDGEMENTS

I would like to thank my advisor, Dr. Nader Ghafoori, for his guidance on this research project and pushing me into the right direction. His persistence on quality and delivery of results helped me to develop this project to a level I didn't think was possible.

I would also like to thank my laboratory colleagues, particularly Meysam Najimi, for always being willing to help me to evaluate my results from a different point of view and helping me understand things better. I would also like to mention the help I received from our summer interns, whom without them, I wouldn't have been able to batch multiple mixtures in one day.

Finally, I would like to thank my family. With their encouragement and endless support, such as their willingness to help me cut out what seemed like millions of wax paper cutouts for my molds, I was able to batch much more mixtures and samples than I could imagine. Their support helped me to see the light at the end of the tunnel and motivated me to complete this study.

TABLE OF CONTENTS

LIST OF TABLES

LIST OF FIGURES

CHAPTER 1

INTRODUCTION

1.1. Background

Concrete is known as the most used construction material in the world, accounting for about 1.35 billion tons made per year (Hardjito et al., 2004). Ordinary Portland cement (OPC) is typically used in the production of concrete as a binder. In the production of OPC, per every ton produced, another ton of carbon dioxide (CO_2) is also produced (Pacheco-Torgal et al., 2008; Meyer, 2009). Collectively, OPC is responsible for approximately 7% of the total CO_2 emissions released into the atmosphere per year worldwide (Pacheco-Torgal et al., 2012; Hardjito et al., 2004; Meyer, 2009). According to the EPA's website, is classified as a greenhouse gas, CO_2 attributes to approximately 82% of total greenhouse gas emissions in the United States (EPA, 2014). Greenhouse gases are gases that cannot escape the atmosphere, thus harming the environment and contributing to global warming. Due to many environmental concerns, the need to develop a new, sustainable alternative for OPC is needed.

Another problem faced by OPC concrete is related to its durability issues. In Norway, approximately 25% of its bridges that were built after 1970 have begun to present corrosion problems. In the United States, 40% of its 600,000 bridges also present corrosion problems, with a total repair cost estimated to be 50 billion dollars (Pacheco-Torgal et al., 2008). OPC has a relatively high permeability, thus allowing water and other harmful media to penetrate concrete, causing corrosion and carbonation problems (Pacheco-Torgal et al., 2012; Pacheco-Torgal et al., 2008; Ma et al., 2013).

Recently, alkali – activated binders have shown to be a potential solution to OPC concrete concerns. Alkali – activated binders are seen to be a more sustainable choice due to its use of waste by-products, such as slag from the production of iron or fly ash from the burning of coal. Fly ash, when combined with an alkaline activator such as sodium hydroxide (NaOH) or sodium silicate, has been seen to produce not only a strong concrete binder but also more durable, in comparison to OPC, when exposed to harsh environments.

1.2. History of Alkali-Activated Binders

The development of alkali – activated binders began in the 1940s with the studies done by Purdon (Pacheco-Torgal et al., 2008). Purdon used blast furnace slag with the addition of a sodium hydroxide solution to create cement. Purdon suggested that the hydration of this cement took place in two steps, with the first step consisting of the separation of silica aluminum and calcium hydroxide. The second step consisted of the formation of silica and alumina hydrates along with a regeneration of the alkaline solution. Ultimately, Purdon concluded that alkaline hydrates served as a catalyst, supported by results obtained from leaching the same alkaline hydroxides used in the cement mix which also pointed to the same conclusion.

Glukhovsky sought to investigate the cement binders used in ancient Roman and Egyptian buildings (Pacheco-Torgal et al., 2008). His investigation led him to conclude that the binders consisted of aluminosilicate calcium hydrates, similar to that found in OPC, as well as crystalline phases of analcite, a natural rock. Glukhovsky developed a new kind of binder which he named “soil-cement”; the soil to represent a ground rock and cement to represent its cementitious properties. The “soil-cement” consisted of ground aluminosilicate and rich alkalis in industrial wastes.

The majority of the work in alkali – activated binders deals with alkali – activated blast furnace slag. Blast furnace slag is a waste by-product from the production of iron. Calcium carbonate is used in calcination procedures and therefore, blast furnace slag has a high calcium content. With the addition of an alkaline activator, blast furnace slag can produce high compressive strength (Pacheco-Torgal et al., 2008). Glukhovsky's work involved the activation of blast furnace slag. He was able to identify the hydration product, consisting of calcium silicate hydrates as well as calcium and sodium aluminosilicate hydrates. Glukhovsky also found that when clay materials are activated by alkalines, aluminum silicate hydrates, referred to as zeolites, forms as a hydration product.

The work done by Davidovits has caused a great interest in alkali – activated binders. Davidovits developed and patented binders containing alkali – activated metakaolin, which comes from kaolinite, typically used to make porcelain. He named these binders "geopolymers" in 1978 (Pacheco-Torgal et al., 2008). According to Davidovits, this binder is similar to that of binders used by the Romans and Egyptians. Chemical and mineralogical studies of pyramid blocks have shown to contain limestone sand, calcium hydroxide, sodium carbonate, and water. X-ray diffraction analysis of the pyramid blocks show that $CaCO_3$ was a major crystalline phase as well as an amorphous material containing aluminosilicates and a zeolite-like material, $Na_2O{\cdot}Al_2O_3{\cdot}4SiO_2{\cdot}2H_2O$. Davidovits also defined geopolymers as polymers, due to the fact that at low temperatures, geopolymers transform, polymerize and harden. Geopolymers are also considered inorganic, stable at high temperatures, and non-flammable.

1.3. Alkali-Activated Fly Ash Binders

1.3.1. Fly Ash Background

In addition to blast furnace slag, fly ash is also seen to be very promising in the development of an alkali – activated binders. Fly ash is produced during coal combustion and contains high amounts of silicon dioxide (SiO_2), amorphous and crystalline alike, and calcium hydroxide (CaO). Fly ash is typically stored at coal power plants or landfills, with approximately 49% of it being disposed of in landfills (Yang et al., 2008). Fly ash is often used as a supplement for Portland cement in concrete production; it is seen to significantly improve workability of the concrete mix as well as to reduce the water demand, resulting in improvements in compressive strength, chemical resistance, and physical durability.

ASTM C 618 classifies coal-produced fly ash into two groups, class F and class C (Yang et al., 2008). The main difference between the two types of fly ash deals with the amount of calcium, silica, alumina, and iron oxides present within the fly ash. The chemical properties of fly ash is determined by the chemical content of the coal being burned as well as its type, whether it is anthracite, bituminous, or lignite. Class C fly ash is produced when younger lignite or sub-bituminous coal is burned. It has some pozzolanic properties as well as some self-cementing properties. It also contains more than 10**%** of lime (CaO). Class F fly ash is produced when harder and older anthracite and bituminous coal is burned. It contains less than 10% of lime (CaO), pozzolanic in nature, and with the addition of a chemical activator, such as sodium hydroxide, calcium hydroxide or sodium silicate, it is able to form a geopolymer.

The development of alkali – activated binders using fly ash as its starting material has recently taken off. Fly ash is seen to possess great potential due to its pozzolanic properties and when mixed with an alkaline activator, it becomes a cementitious material capable of producing

high compressive strength and good durability. Due to its early development stage, there are many unanswered questions related to alkali – activated fly ash. There are currently no standards set in relation to alkali – activated fly ash. This includes no standard curing conditions and mixing procedures. Another unknowns about alkali – activated fly ash deals with its properties, such as reaction products formed, compressive and flexural strengths, porosity characteristics, microstructural characteristics, and durability properties.

1.3.2. Main Reaction Product of Alkali-Activated Fly Ash Binders

The main reaction product formed from alkaline activation is an alkaline aluminosilicate hydrate gel, referred to as N-A-S-H gel or geopolymer. Glukhovsky has broken down the process of alkaline activation into three stages: "destruction-coagulation", "coagulation-condensation", and "condensation-crystallization" (Shi et al., 2011). The first stage, "destruction-coagulation", begins with the breakdown of the following bonds in the starting material: Me-O, Si-O-Si, Al-O-Al, and Al-O-Si. The alkaline when serves as a neutralizer leading to the creation Si-O-Na^+ bonds. These bonds are helpful in the development of the reaction product molecular structure. Aluminates also form complexes, for example $Al(OH)_4^-$ or $Al(OH)_6^{3-}$, which are dependent on the pH level of the system. The second stage, "coagulation-condensation", involves the formation of a coagulated structure, accompanied by polycondensation. The rate of polycondensation is dependent on the conditions needed for gel precipitation. For example, for a pH greater than 7, the disaggregation of the Si-O-Si bond are more likely to form hydroxylated complexes such as $Si(OH)_{4-}$. The third stage, "condensation-crystallization", can be best described by using a model proposed in 2005 by Fernandez-Jimenez and Palomo named the microstructural development of alkaline aluminosilicate cements. This model begins with the vitreous/amorphous component of the solid material coming into contact with the alkaline

solution and thus aluminates and silicates are released. Smaller particles begin to coagulate and form larger particles that ultimately begin to form a gel. This gel contains Si and Al bonds that aid neutralizing the electrical charge generated from replacing a Si with Al. With that said, there is a high aluminum content in this gel, named Gel 1, with a Si/Al ratio approximately equal to 1. As the reaction continues, more Si-O bonds are broken down, allowing for a change from Gel 1, which is an Al-rich phase, to Gel 2, a Si-rich phase with a Si/Al ratio approximately equal to 2. An increase in the Si/Al ratio allows improvements in the mechanical properties of the aluminosilicate gels. The main reaction product formed on the microstructural level is an amorphous alkali aluminosilicate gel, often referred to as N-A-S-H gel or geopolymer. The chemical composition of the gel will vary with different raw materials, alkaline activator solutions and curing conditions (Shi et al., 2011).

For the purpose of this thesis, the variation of N-A-S-H gel or geopolymer formed by using solely sodium hydroxide as the activator will be discussed as well as the reaction product formed by using both sodium hydroxide and sodium silicate as activators. The type of geopolymer formed by the use of sodium hydroxide is referred to as poly(soalate-siloxo) while the type of geopolymer formed by the use of both sodium hydroxide and sodium silicate is referred to as poly(sialate-disiloxo) (Weng and Sagoe-Crentsil, 2007; Sagoe-Crentsil and Weng, 2007). When sodium hydroxide is used as the activator, the overall silicate content of the system is low, while the silicate content of the system is high when sodium silicate is also used in the activator solution. Regardless of which activator is used, the alkaline activation process is still the same, similar to the process explained previously by Glukhovsky. For simplicity, the chemical formation process will be referred to as dissolution, hydrolysis, and condensation, as labeled in (Weng and Sagoe-Crentsil, 2007; Sagoe-Crentsil and Weng, 2007).

1.3.2.1. Reaction Product for Sodium Hydroxide as the Main Alkaline Activator

As stated, poly(sialate-siloxo) is the reaction product formed when sodium hydroxide is the sole activator (Weng and Sagoe-Crentsil, 2007). Once the activator is added to the starting material, the dissolution process begins instantly in order to supplement the aluminate ions needed for the rest of the activation process. Al^{3+} and Si^{4+} ions result from the dissolution process in addition to water. The amount of Al^{3+} and Si^{4+} ions made available is dependent on the concentration of the activator, with the amount increasing with increase in the concentration of the activator. The next step, referred to as the hydrolysis process, the water, Al^{3+} and Si^{4+} ions from the previous step are used to develop $[Al(OH)_4]^-$ ions as well as $[SiO_2(OH)^2]_{2-}$ and $[SiO(OH)_3]^-$ ions. These can be expressed by the following chemical equations when only the mass and charge equilibriums are taken into account:

$$Al_2O_3 + 3H_2O + 2OH^- \rightarrow 2Al(OH)_4^- \quad \text{(Eq. 1.1)}$$

$$SiO_2 + H_2O + OH^- \rightarrow [SiO(OH)_3]^- \quad \text{(Eq. 1.2)}$$

$$SiO_2 + 2OH^- \rightarrow [SiO_2(OH)_2]^{2-} \quad \text{(Eq. 1.3)}$$

The mechanisms of the condensation step is not as simple as the previous two steps because of its dependency on the evolutions of silicate ions $[SiO_2(OH)^2]_{2-}$ and $[SiO(OH)_3]^-$. In general, the condensation step involves the condensation between $[Al(OH)_4]^-$ and$[SiO_2(OH)^2]_{2-}$ and of $[Al(OH)_4]^-$ and $[SiO(OH)_3]^-$. The dependency relies on the concentration $[SiO_2(OH)^2]_{2-}$ and $[SiO(OH)_3]^-$, which is dependent on the pH of the system or the concentration of the activator. With that said, the end reaction varies with the concentration of the two silicate ions, but in general, equations 4 and 5 depict the chemical reactions of the condensation process between $[Al(OH)_4]^-$ and$[SiO_2(OH)^2]_{2-}$ and $[SiO(OH)_3]^-$, respectively.

$$[Al(OH)_4]^- + [SiO(OH)_3]^- \rightarrow [(OH)_3Al - O - SiO(OH)_2]^{2-} + H_2O \quad \text{(Eq. 1.4)}$$

$$[Al(OH)_4]^- + [SiO_2(OH)_2]^{2-} \rightarrow [(OH)_3Al - O - SiO_2(OH)]^{3-} + H_2O \quad \text{(Eq. 1.5)}$$

With lower concentration in the activator, there is a higher concentration of $[SiO(OH)_3]^-$, leading to further condensation of $[Al(OH)_4]^-$ and ultimately lowering the rate of reaction product production. On the other hand, too high of activator concentration leads to an abundance of $[SiO_2(OH)^2]_{2-}$, negatively affecting the condensation process because of the increased possibility of forming unstable reactions.

1.3.2.2. Reaction Product for Sodium Hydroxide and Sodium Silicate as the Main Alkaline Activator

Poly(sialate-disiloxo) is formed when both sodium hydroxide and sodium silicate are used as the alkaline activator (Sagoe-Crentsil and Weng, 2007). As far as the dissolution and hydrolysis steps, these steps stay the same as discussed for the use of solely sodium hydroxide in the previous section. With the addition of sodium silicate, sodium silicate provides more $[Al(OH)_4]^-$ ions, ultimately improving the condensation process due to their increased reactivity. The condensation process is further broken down into two steps, with the first step being the quick condensation process between $[Al(OH)_4]^-$ and both $[SiO_2(OH)^2]_{2-}$ and $[SiO(OH)_3]^-$, and the second step being the slow condensation process between $[SiO_2(OH)^2]_{2-}$ and $[SiO(OH)_3]^-$, similar to the process described previously.

Overall, higher $[OH]^-$ concentration allows for a faster dissolution rate. $[Al(OH)_4]^-$ controls the condensation rate as well as setting times, however, it is also highly sensitive to the pH of the activator solution, lower pH leads to lower concentration of $[Al(OH)_4]^-$. Sodium silicate, although proven to be highly beneficial to strength development of alkali-activated binders, has a lower pH than sodium hydroxide, hindering the development of $[Al(OH)_4]^-$. In

addition to the pH, the concentration of the activator as well as curing temperature affect the rate of condensation.

1.3.3. Parameters

There are many parameters that can alter the performance of alkali-activated fly ash, including curing condition, solution-to-binder ratio, type of alkaline activator, and concentration of alkaline activator. As stated in the previous section, all of the named parameters can alter the chemical composition of the N-A-S-H gel produced. With that said, it is critical to determine the effects of each parameter on the performance of the finished concrete mix.

1.3.3.1. Curing Conditions

The temperature, moisture exposure, curing method, and duration are the main variations in terms of curing conditions. The temperature during the curing period plays a major role when it comes to alkali-activated fly ash binders, although, the temperature has been seen to be more critical in the early stages of curing. The amount of moisture available during the curing period has also been seen to have a dramatic effect on the performance of the mix. Referred to as the relative humidity, the amount of moisture available can aide in the further development of the N-A-S-H gel. The curing type deals with the method of storage of samples during the curing period. The two main curing types, referred to as “exposed” and “sealed”, can alter the performance of the mix. Exposed samples are left without any protection during the curing period meanwhile sealed samples are sealed in plastic during the curing period. The duration of the curing period dictates the time alkali-activated fly ash has to develop its reaction products.

1.3.3.2. Solution-to-Binder Ratio

The solution-to-binder ratio is similar to the water-to-cement ratio used for OPC concrete. The amount of alkaline solution, the water equivalent for alkali-activated binders, can

change the performance of the mixture. Similar to that seen in OPC concrete, solution-to-binder ratio can change its fresh and hardened properties.

1.3.3.3. Type of Alkaline Activator

Dependent on the starting material, hydroxides or silicates, sodium or potassium, are used to produce the best results. For alkali-activated fly ash, both NaOH and sodium silicate have been seen to work best while solely NaOH-activated mixtures have been able to perform above OPC mixtures, the addition of sodium silicate at the right ratio further intensified these results.

1.3.3.4. Concentration of Alkaline Activator

The concentration of NaOH as well as the ratio of NaOH to sodium silicate alters the performance of alkali-activated fly ash. With a higher concentration, more alkalis are available to react with the starting material, ultimately producing more of the reaction product, thus increasing its performance results. Although higher concentrations benefit the mix, there is an optimum concentration and ratio in terms of performance as well as economic.

1.4. Fresh Properties

Fresh properties deal with the workability of concrete, such as the ability of being able to work with the concrete before it sets and hardens. The two main properties are the flow and setting times.

1.4.1. Test Methods

Although specific standards for alkali-activated binders are not available, the American Society for Testing and Materials (ASTM) has developed standards for hydraulic cements. With that said, such standards are used for the purpose of this thesis.

1) ASTM C 1437-01: Standard Test Method for Flow of Hydraulic Cement Mortar. This standard details how to measure the flow for hydraulic cement mortars using a flow table

apparatus. Mortar is placed in two steps before lowering the mortar rapidly 25 times. The diameter is then measured at four different locations and averaged; the diameter of the ring is subtracted from the measurements.

2) ASTM C 807-03a: Standard Test Method for Time of Setting of Hydraulic Cement Mortar by Modified Vicat Needle. This standard details the procedure for measuring the initial and final setting times for hydraulic cement mortars using a modified vicat needle apparatus. A sample of roughly 30 to 35 mm tall is made and used for this standard. The depth of the vicat needle penetration is measured every 30 minutes until the depth is 25 mm or less. At that time, the depth is measured every 10 minutes until the depth is less than 10 mm. Using linear interpolation, the initial and final setting times can be determined.

1.4.2. Effects due to Changing Parameters

Due to the recent increased interest into alkali-activated fly ash, there is a limited amount of past studies dealing with the flow and setting time of alkali-activated products. In the study by Joseph and Mathew (2012), the compacting factor was used to evaluate the workability of the mixtures tested. In this study, the influence of the aggregate content on certain engineering properties of fly ash-based geopolymer concrete was investigated. The study was broken down into three parts, labeled M1, M2, and M3, with all using class F fly ash and 10 M NaOH and sodium silicate. For M1, the following the following parameters were used: alkali-to-fly ash ratio of 0.55; sodium silicate-to-NaOH ratio of 2.5; water-to-geopolymer solid ratio of 0.25; 100°C curing temperature; total aggregate content, by volume, of 65, 70, and 75%; and fine aggregate-to-total aggregate mass ratio of 0.20, 0.25, 0.30, 0.35, and 0.40. For M2, the following parameters were used: alkali-to-fly ash ratio of 0.35, 0.45, 0.55, and 0.65; sodium silicate-to-NaOH ratio of 1.5, 2.0, 2.5, 3.0, and 3.5; water-to-geopolymer solid ratio of 0.25; total aggregate

content of 70%; fine aggregate-to-total aggregate mass ratio of 0.35; and 100°C curing temperature. For M3, the following parameters were used: alkali-to-fly ash ratio of 0.35, 0.45, 0.55, and 0.65; sodium silicate-to-NaOH ratio of 2.5; water-to-geopolymer solid ratio of 0.24, 0.26, 0.28, 0.30, and 0.32; 70% total aggregate content; fine aggregate-to-total aggregate mass ratio of 0.35; and 100°C curing temperature. The compacting factor increased with increased water-to-geopolymer solid ratio. The compacting factor was also higher with increased alkali – to – fly ash ratio. A higher compacting factor corresponded to a lower workability.

Ryu et al. (2013) also tested the flow of fly ash-based geopolymer concretes. The main focus of this study was to evaluate the changes in strength of fly ash-based geopolymer concretes with varying alkaline activator concentrations and NaOH-to-sodium silicate ratios. The study was broken down into two series, labeled series 1 and series 2. Series 1 used three concentrations of NaOH, namely 6, 9 and 12 M. Series 2 used 9 M NaOH and sodium silicate with NaOH-to-sodium silicate ratios of 0:100, 25:75, 50:50, 75:25, and 100:0. For both series, class F fly ash was used as well as a liquid-to-fly ash ratio of 0.6 and sand-to-fly ash ratio of 1.5. Samples were cured at 60˚C for 24 hours before being cured at 20˚C for 1, 3, 7, 14, 28, 56, and 91 days. Mini-cone slump test was used to obtain the flow of mixtures tested. In terms of alkaline activator concentration, the slump decreased with increased NaOH concentration. For NaOH-to-sodium silicate ratios, 100/0 had the highest flow and 0/100 had the lowest flow. 50/50 flow was, however, higher than both 25/75 and 75/25. The decreased slump was attributed to the increased severance of the glassy chain of fly ash caused by the increased concentration of NaOH.

Lastly, Lee and Lee (2013) studied the setting time of alkali-activated fly ash/slag concrete, in addition to its mechanical properties. Class F fly ash and slag, with slag replacement of 10, 15, 20, 25, and 30%, were activated with 4, 6, and 8 M NaOH and sodium silicate, with a

sodium silicate-to-NaOH ratio of 0.5, 1.0, and 1.5. Solution – to – binder ratios of 0.38 and 0.56 were used for paste and concrete samples, respectively. 85% phosphoric acid was added as a set-retarding admixture. All samples were cured at 20°C with 60% relative humidity until time of testing and de-molding occurring after 1 day. For setting time, testing was conducted at 17 and 28°C. Setting times were found to decrease with increased NaOH concentration, slag content, and sodium silicate content. The setting time also decreased with increased temperature. Ultimately, the decreased setting time with increased NaOH, slag content and sodium silicate content was attributed to the interaction that took place between NaOH and sodium silicate. In the case of temperature, it was concluded that the decreased setting time proved that the alkali-activated fly ash/slag paste was extremely sensitive to the temperature.

1.5. Strength Properties

Strength properties of interest are the following: compressive strength, flexural strength, and modulus of elasticity. These three engineering properties are critical in the possible use of alkali-activated binders to produce concrete.

1.5.1. Test Methods

Concrete is known for performing great under a compressive load; therefore, investigating compressive strength of alkali-activated fly ash is critical. In addition to the compressive strength, flexural strength and modulus of elasticity are two critical engineering properties for concrete. Both flexural strength and modulus of elasticity test standards are described below.

1) ASTM C 78-02: Standard Test Method for Flexural Strength of Concrete (Using Simple Beam with Four-Point Loading). This standard outlines the procedure for testing the

flexural strength of concrete beams by dividing a single load point into two points, each along one-third of the length of the beam being tested.

2) ASTM C 469-02: Standard Test Method for Static Modulus of Elasticity and Poisson's Ratio of Concrete in Compression. This standard depicts the testing procedure for determining static modulus of elasticity by loading samples up to 40% of their ultimate strength and recording the change in length at this point. Stress is also recorded when strain is 50 millionth and, thus, with both points being able to calculate the modulus of elasticity.

1.5.2. Effects due to Activator Concentration

Katz (1998) studied the mechanical and microstructural properties of alkali-activated fly ash. The study itself was broken into three parts, with the first part being the investigation of the effect of NaOH concentration with the use of four different NaOH concentrations, namely 1, 2, 3, and 4 M. A constant water-to-fly ash ratio and curing temperature was used, 0.8 and 90°C, respectively. Compressive strength was tested after 7 days of curing. For a given water-to-fly ash ratio and curing temperature, the compressive strength increased with increased solution concentration. This was attributed to the increased degree of reactivity with increased solution concentration.

Hardjito et al. (2004) studied the compressive strength and manufacture of fly ash-based geopolymer concrete and how they were impacted by several variables. 8 and 14 M NaOH in combination with sodium silicate were used as the alkaline activators, at sodium silicate-to-NaOH mass ratios of 0.4 and 2.5. Concrete samples were cured in plastic bags at 60˚C for 6 to 96 hours. Compressive strength was tested after 7 days of curing. Improvements in compressive strength were seen with increased NaOH concentration, as well as increased sodium silicate-to-

NaOH ratio. It was determined that increased compressive strength was due to the interaction caused between the oxides found in the alkali-activated system.

Fernandez-Jimenez et al. (2006) evaluated various engineering properties of alkali-activated fly ash concrete and how it compared to Portland cement concrete. Two activator solutions were used to activate class F fly ash, 8 M NaOH and 85% 12.5 M NaOH and 15% sodium silicate. The following ratios were used: coarse aggregate-to-fine aggregate ratio of 1.26, aggregate and sand-to-fly ash ratio of 4, solution 1 (8 M NaOH)-to-fly ash ratio of 0.4, solution 2 (85% 12.5 M NaOH and 15% sodium silicate)-to-fly ash ratio of 0.55, and water-to-cement ratio of 0.5. All concrete samples were cured at 85˚C for 20 hours. Compressive strength, static modulus of elasticity, and pull-out test methods were used. Compressive strength results showed that alkali-activated fly ash concrete outperformed Portland cement concrete. Strength development was very high during the first 24 hours, followed by a reduction in strength development rate with minimal increase over time. The addition of sodium silicate in the activator solution improved strength development. The static modulus of elasticity of alkali-activated fly ash concrete was lower than that for Portland cement concrete. Pull-out test results showed that the maximum load required as well as adherence tension for alkali-activated fly ash concrete was higher than for Portland cement concrete. The high strength development in the early stages was attributed to the rapid reaction time that occurred between the activator and fly ash. The lower modulus of elasticity and higher tension in alkali-activated concrete was found to be caused by the bonding strength; increased tension caused increased stress within the concrete, ultimately resulting in premature cracking. The microstructure of alkali-activated concrete, although responsible for its good mechanical strength, is also susceptible to cracking within the silicate chains formed.

Komljenović et al. (2010) studied the microstructural and mechanical properties of alkali-activated fly ash-based geopolymers using different types of class F fly ash as well as different types of alkaline activators. Six different sources of class F fly ash were evaluated and activated with four different activators, namely $Ca(OH)_2$, NaOH, KOH, and sodium silicate. For mixtures containing $Ca(OH)_2$, an activator-to-fly ash-to-sand-to-water mass ratio of 1: 2: 9: 1.8. Sand-to-binder ratio of 3: 1 was used for all mixtures. Once casted, molds were cured in plastic bags at room temperature for 24 hours before curing at 55 ± 2°C for 6 days. Compressive strength was tested on mortar samples only. Samples containing liquid sodium silicate produced the best strength, followed by NaOH samples. Increased activator concentration led to increased compressive strength. Sodium silicate was found to be the best alkaline activator due to its silicon content, which reacts more easily and thus, increased reaction product content and ultimately, higher strength. Higher activator concentration also allowed for higher reaction product formation, resulting in higher strength.

Ravikumar et al. (2010) used various activator concentrations and activator-to-binder ratios for fly ash or ground granulated blast furnace slag (GGBFS)-based cement free concrete to study its influence on structure and strength characteristics. Class F fly ash and type 100 GGBFS were separately activated with three NaOH concentrations, namely 4 M, 6 M, and 8 M. Three activator-to-binder ratios were tested, 0.40, 0.50, and 0.60, with a total aggregate content ranging between 65 and 70%. All concretes were cured at 75°C for 48 hours; concretes were de-molded after 24 hours. Compressive strength was tested after 12, 24, and 48 hours of curing. Compressive strength was seen to increase with increased activator concentration. Activator concentration has a greater influence on fly ash-based cement free concrete as compared to GGBFS-based cement free concrete. Higher activator concentration allowed for higher

production of reaction product that led to increased strength; fly ash was better utilized with higher activator concentration.

Vargas et al. (2011) studied the effects of varying Na_2O/SiO_2 molar ratio, curing temperature and age on the morphology and microstructure of fly ash-based geopolymers. Class F fly ash was activated with NaOH with three Na_2O/SiO_2 (N/S) ratios, namely 0.2, 0.3, and 0.4. Both paste and mortar samples were produced. For paste samples, water-to-binder ratios of 0.55, 0.502, and 0.458 were used for Na_2O/SiO_2 ratios of 0.2, 0.3, and 0.4, respectively. For mortar samples, water-to-binder ratios of 0.622, 0.566, and 0.522 were used for N/S ratios of 0.2, 0.3, and 0.4, respectively, along with constant sand-to-fly ash ratio of 3. Both paste and mortar samples were cured for 24 hours at 50, 65, and 80°C before being stored at 24 ± 1°C and 50% relative humidity until time of testing. Compressive strength was evaluated after 1, 7, 28, 91, and 180 days. Ultimately, the N/S had the most significant effect on compressive strength development, with N/S ratio of 0.40 having the highest compressive strength. Higher N/S ratio allowed for faster strength development due to higher amounts of aluminosilicate gel, also known as the reaction product for alkali-activated fly ash.

Rajamma et al. (2012) investigated the use of biomass fly ash as a starting material in alkali-activated binders. Biomass fly ash used in this study contained 24% of CaO and used as a starting material in combination with metakaolin. Four concentrations of NaOH, namely 8, 10, 12, and 18 M, were used as the alkaline activator in combination with sodium silicate. For paste samples, an activator-to-binder ratio of 0.66 and four sodium silicate-to-NaOH ratios were evaluated, namely 2:1, 1:0.5, 1:1, and 1:2.5. Samples were sealed cured at 60˚C and 95% relative humidity for 2 days before curing at 20˚C until testing. For mortar samples, a binder-to-activator ratio of 3.2 was used, as well as a binder-to-aggregate ratio of 1.3, 1% by binder content of super

plasticizer, and a NaOH-to-sodium silicate ratio of 1.2. Mortar samples implemented the same curing procedure as that for paste samples. Compressive strength was tested after 10 days of curing. Increased NaOH concentration as well as sodium silicate content caused an increase in strength development for samples containing biomass fly ash. Microstructural development was determined to be the cause of increased strength development, however, the exact mechanisms was not determined in this study.

Arioz et al. (2012) investigated the use of 3 different concentrations of NaOH and sodium silicate as an activator in fly ash-based geopolymers. Class F fly ash was activated with 4 M, 8 M, and 12 M NaOH combined with sodium silicate. Mixtures were cured at 80˚C for 15 hours before de-molded and allowed to cure further at room temperature for up to 28 days. Compressive strength was tested after 7 and 28 days of curing. Ultimately, the compressive strength was found to increase with increased NaOH concentration. Along with increased compressive strength, degree of reaction also increased with increased NaOH concentration. With that said, it could be said that increased NaOH concentration allowed for increased reaction product formation and thus increased degree of reaction and compressive strength.

Chi and Huang (2013) studied the binding mechanisms and various properties of alkali-activated binders containing slag and fly ash. Class F fly ash and GGBFS, with fly ash-to-slag ratios of 100/0, 70/30, 50/50, 30/70, and 0/100, were activated with NaOH and sodium silicate, with Na_2O concentrations of 4 and 6% and a liquid-to-binder ratio of 0.5. Samples were cured at 25˚C and 80% relative humidity until testing. Compressive and flexural strength was tested after 7, 14, and 28 days of curing. Compressive strength was seen to increase with increased Na_2O content. Similar conclusions were made based on flexural strength results. Higher strength development was due to the increased formation of reaction product.

First discussed in section 1.4.2, Ryu et al. (2013) studied the changes in strength of fly ash-based geopolymers containing various activator concentrations and NaOH-to-sodium silicate ratios. Compressive strength was tested at 1, 3, 7, 14, 28, 56, and 91 days. Compressive strength increased with increased NaOH concentration. Higher SiO_2/Na_2O and Al_2O_3/Na_2O ratios caused a decrease in compressive strength. The difference in compressive strength was attributed to the degree of reaction.

Lee and Lee (2013), first mentioned in section 1.4.2., studied the setting and mechanical properties of slag/fly ash-based alkali-activated concrete. Compressive strength along with modulus of elasticity was tested at 3, 7, 14, 28, and 56 days and splitting tensile strength was tested at 28 days. Increased NaOH concentration caused an increase in compressive strength, with the contrary occurring with increased NaOH-to-sodium silicate ratio. Elastic modulus was lower when compared to OPC-based concrete, with the same result seen for splitting tensile results. Differences in compressive strength was found to be attributed to the amount of NaOH and sodium silicate; higher NaOH and sodium silicate content could deteriorate the strength development rather than improving it.

1.5.3. Effects due to Type of Activator

Criado et al. (2005) studied the effects of different curing conditions on polymerization reactions of alkali-activated fly ash. Class F fly ash was activated with NaOH and sodium silicate with a liquid-to-solid ratio of 0.25. Mixtures were cured at 85°C for 5, 12, and 20 hours, as well as 7 days. As mentioned, two curing methods were used. The first method placed mixtures in an air-tight container with water, although not in contact with the mixtures. The second method placed the mixtures directly in the oven with a water-filled porcelain capsule alongside them. Compressive strength was tested after 5, 12, and 20 hours, as well as 7 days of curing. By adding

sodium silicate to the activator solution, further polymerization of the reaction product was allowed as compared to an activator solution with solely NaOH. The increased polymerization of the reaction product allowed when sodium silicate was added to the activator solution resulted in increased mechanical strength. When NaOH was the sole activator, less polymerization of the reaction product occurred and thus had lower mechanical strength.

Panias et al. (2007) studied the influence of water as well as NaOH and sodium silicate on the development of class F fly ash geopolymer. Various concentrations of NaOH were used as well as sodium silicate. Mixtures were cured at 60°C for 72 hours before switching to room temperature for 7 days. The addition of sodium silicate allowed for compressive strength to increase. Sodium silicate allowed for total soluble silicate content to increased and thus favored strength development.

Komljenović et al. (2010), as mentioned in the previous section 1.5.2., investigated different types of class F fly ashes from different sources as well as four different alkaline activators and its effects on the mechanical and microstructural properties for use in fly ash-based geopolymers. The type and concentration of the activator proved to be the most important factors for the reaction of fly ash, however, all activators produced reaction products that were amorphous with zeolites in certain mixtures. Sodium silicate was found to be the best activator, due to its increased content of dissolved silicon which had higher reactivity and resulted in higher reaction product formation. Increased content of reaction product allowed for increased strength development.

1.5.4. Effects due to Curing Conditions

Katz (1998), as mentioned previously in section 1.5.2., studied the mechanical and microstructural properties of alkali-activated fly ash in three distinct parts. For the second part of

the study, the effect of the curing temperature was studied. Three curing temperatures were tested: 20, 50 and 90°C. A constant water-to-fly ash ratio of 0.4 and sodium hydroxide concentration of 4 M were implemented. An increase in curing temperature allowed for an increased compressive strength. For temperatures up to 50°C, a lower water-to-fly ash ratio had a higher compressive strength. For a 90°C curing temperature, a water-to-fly ash ratio of 0.8 had a greater compressive strength than that corresponding to a water-to-fly ash ratio of 0.4. At higher temperatures, reaction products are allowed to form and ultimately improve compressive strength development.

Hardjito et al. (2004), as discussed in section 1.5.2, studied the compressive strength of fly ash-based geopolymer concrete. In addition to the results discussed, compressive strength also improved with increased curing temperature and duration. Further discussion was not given in terms of curing temperature and duration results.

As discussed in the previous section, Criado et al. (2005) studied different curing conditions for alkali-activated fly ash. Curing method 1 was shown to have better strength development than curing method 2. Curing method 2 favored the development of carbonation and thus hindered strength development. This was primarily due to the increased humidity during curing for method 1. Increased humidity favored reaction product formation.

Kovalchuk et al. (2007) investigated curing conditions for optimum polymerization reactions in alkali-activated fly ash. Class F fly ash was activated with sodium silicate, with NaOH added to obtain Na_2O/Al_2O_3 ratios of 3.5 and 4.0. Silica fume was also added to obtain SiO_2/Al_2O_3 ratios of 0.5 and 1.0. A constant water-to-solid ratio of 0.18 was used throughout. Three curing methods were evaluated, labeled curing in covered molds (CCM), dry curing (DC), and steam curing (SC). CCM, also referred to as sealed curing, entailed placing molds in sealed

plastic bags and placed in an oven at 95°C for 8 hours. DC-placed molds we placed directly in the oven at 95°C for 2 hours, after which samples were taken from room temperature to 150°C for 3 hours, maintained at 150°C for 6 hours, and lastly allowed to cool to room temperature in 3 hours. SC entailed placing molds directly in the oven at 95°C for 2 hours, maintained at 95°C for 6 hours, and then allowed to cool to room temperature in 3 hours. For SC only, a relative humidity of 100% was maintained throughout the entire curing process. Mechanical strength was tested after 24 hours of curing. Samples cured in covered molds produced the best strength, followed by steam curing and lastly, dry curing. The amount of water present during curing was found to be immensely important for microstructural development, as well as degree of reaction and engineering properties. Increased water content allowed for better microstructural development, leading to higher degree of reaction and compressive strength.

Criado et al. (2010) studied the effects of relative humidity on the physical and mechanical properties of alkali-activated fly ash. Class F fly ash was activated by 8 M NaOH and 0.4 liquid-to-solid ratio. Two curing methods were used, labeled method 1 and method 2, with both methods entailing 80˚C curing temperature for 8 and 20 hours, and 28 and 60 days. Method 1 involved enclosing molds in air-tight containers with water, producing relative humidity greater than 90%. Method 2 involved placing molds directly in the oven with a container of water, with relative humidity of approximately between 40 and 50%. Compressive strength was measured at each curing age. Curing method 1 samples portrayed higher compressive strength as compared to samples cured using method 2. Method 1 continued to have an increase in strength over time, whereas curing method 2 samples had minimal strength development over time. Higher relative humidity favored the development of alkali-activated fly ash and resulted in a more dense material with higher amounts of the reaction product.

Mentioned in the previous section 1.5.2., Ravikumar et al. (2010) investigated the strength and structural properties of fly ash and ground granulated blast furnace slag-based cement-free concretes with different alkaline activator concentrations and solution-to-binder ratios. The curing temperature was found to have a significant impact on compressive strength; compressive strength increased with increased curing temperature. Increased curing time also increased compressive strength. Mentioned results indicate that strength development continued over time. Increased temperature also helped with the strength development process.

Mustafa Al Bakri et al. (2011) studied the influence of various curing temperatures on the chemical and physical properties of fly ash-based geopolymers. Class F fly ash was activated with 12 M NaOH combined with sodium silicate along with a fly ash-to-activator ratio of 2 and sodium silicate-to-NaOH ratio of 2.5. Samples were cured for 24 hours at five different temperatures: room temperature, 50, 60, 70, and 80˚C. Compressive strength was tested after 7 days. 60˚C was found to produce the highest compressive strength. Increasing the temperature after 60˚C did not provide substantial increase in compressive strength. Higher temperatures allowed for samples to experience significant moisture loss, ultimately hindered compressive strength.

As mentioned in section 1.5.2., Vargas et al. (2011) investigated the morphology and microstructure of fly ash-based geopolymers when different Na_2O/SiO_2 molar ratio, curing temperature, and age. Increased temperature and age allowed for increased compressive strength for samples containing 0.30 and 0.40 N/S ratios. Increased curing duration allowed for further continuation of reaction product formation and thus, furthered compressive strength development.

Criado et al. (2012) sought to determine a relationship between the relative humidity used during curing and soluble silica in the activator solution on the reaction products formed in alkali-activated fly ash. Class F fly ash was activated with a solution containing 85% 10 M NaOH and 15% sodium silicate. Two curing methods were used, with both methods using 85˚C as a curing temperature for 12 hours, and 7 and 30 days. Curing method 1 involved placing samples in air tight containers; relative humidity was approximately 90%. Curing method 2 involved placing samples in the oven alongside a porcelain vial containing water; relative humidity was approximately between 40 and 50%. Compressive strength was tested at each age. Relative humidity was seen to influence compressive strength development significantly. Higher relative humidity produced higher compressive strength and development rate over time as compared to lower relative humidity. Decreased compressive strength when cured at a lower relative humidity was caused by the decreased pH that occurred as well as the lack of moisture. Both a lower pH and lack of moisture favored the formation of carbonation and thus, hindered compressive strength.

Joseph and Mathew (2012), first mentioned in section 1.4.2, studied the influence of the aggregate content on various engineering properties of fly ash-based geopolymer concrete. Compressive strength was found to increase with increased curing temperature up to 100˚C before decreasing. The sudden decrease in compressive strength was attributed to the lack of moisture.

Xin et al. (2012) studied alkali-activated slag-fly ash paste characteristics such as strength, setting and hardening. Slag and class C fly ash were activated with NaOH and sodium silicate, along with a fly ash-to-slag ratio of 0.6, a 6% alkali content, and proportion of composite alkali of 1.6. For paste samples, samples were cured at 20°C and relative humidity over 95% for

28 days. For temperature stimulating characteristics, samples were cured at 20, 30, 40, 50, 60, 70, 80, and 95°C for 28 days. Compressive and flexural strength was tested. Temperature was found to have a significant effect on strength properties, indicating the importance of establishing a curing temperature for future research studies.

Görhan and Kürklü (2014) studied various NaOH concentrations and its effects on the physical and mechanical properties of fly ash-based geopolymer mortars. 3, 6, and 9 M NaOH concentrations were used to activate class F fly ash. Dependent on the NaOH concentration, different solid-to-liquid and liquid-to-fly ash ratios were used: for solid-to-liquid ratios, 3.92, 4.14, and 4.37 for 3, 6, and 9 M, respectively; for liquid-to-fly ash ratios, 1.04, 1, and 0.97 for 3, 6, and 9 M, respectively. Samples were cured at 65 or 85˚C for 2, 5, and 24 hours. Compressive and flexural strength was tested at 7 days. Increased curing temperature was seen to increase compressive and flexural strength. 6 M NaOH produced the highest strength when cured at 85˚C, followed by 9 M and 3 M, however, further discussion for such results was not given.

1.5.5. Effects due to Solution-to-Binder Ratio

Hardjito et al. (2004) also studied the effects of water-to-geopolymer solid mass ratio, in addition to the previously mentioned properties for fly ash-based concrete. Compressive strength decreased with increased water-to-geopolymer solid mass ratio. Such results were consistent with previous studies. This concluded the importance of mixture proportions for water content in relation to strength development.

Panias et al. (2007), as discussed in section 1.5.3., studied the effects of water content and NaOH and sodium silicate contents on fly ash-based geopolymer. Compressive strength improved with decreased water content. Decreased water content was found to improve the geopolymerization process.

Ravikumar et al. (2010), as mentioned in the previous sections, investigated the use of different alkaline activator concentrations and activator-to-binder ratios for fly ash or ground granulated blast furnace slag (GGBFS)-based cement free concretes and the influences on the strength and structural characteristics. Compressive strength increased with decreased activator-to-binder ratio. Although the amount of alkaline activator increased with higher activator-to-binder ratio, the porosity also increased and thus, caused lower compressive strength.

Xie and Kayali (2013) studied the effect of water content on ambient-cured fly ash-based geopolymers. Class F fly ash was activated with three different activators, all containing sodium silicate and NaOH with the following concentrations: 8.7 M, 10.8 M, and 14.3 M. Three water-to-geopolymer ratios were used as well as three fly ash-to-activator ratios: 0.22, 0.24, and 0.26 and 2.28, 2.16, and 2.06, respectively. Once molded, samples were placed in the environmental control room, 20˚C and 50% relative humidity, for 6 hours. Samples were divided into two groups, referred to as heat curing samples and controlled ambient curing samples. For heat curing samples, samples were sealed and cured at 60˚C for 4 to 24 hours before being placed in the environmental control room. For controlled ambient curing samples, samples were sealed and kept in the environmental control room for 7 days before being divided into three different curing conditions, unsealed, sealed, and dried in a desiccator over anhydrous silica gel, all three for another 7 days. Compressive strength testing was conducted at 7 and 14 days. Strength increased with decreased water content in ambient-cured samples; heat-cured samples were not significantly impacted by a lower water content. It was determined that the increase in strength development with decreased water-to-geopolymer ratio was attributed to the geopolymerization process. Lower water content allowed for further continuation of the geopolymerization process as compared to when a higher water content was used.

1.6. Transport Properties

Transport properties are related to the ability of liquids to flow through concrete. This is an extremely important property for concrete, as it relates to the possibility of corrosion to occur in permeable concretes, ultimately hindering its durability properties and failing before the end of its design service life. Water absorption falls under this category, as well as void content, porosity, and density.

1.6.1. Test Methods

Although little research has been conducted on transport properties of alkali-activated fly ash binders, there are three main test methods that will be used for the purpose of this thesis and are listed below.

1) ASTM C1202-97: Standard Test Method for Electrical Indication of Concrete's Ability to Resist Chloride Ion Penetration. Referred to it as RCPT, this test evaluates the amount of current to pass through a concrete sample. This test is used to determine the concrete's ability to resist chloride penetration and thus avoiding corrosion to any steel reinforcement within the concrete. The higher the amount of current, the more permeable the sample is.

2) NT BUILD 492: Concrete, Mortar and Cement-Based Repair Materials: Chloride Migration Coefficient from Non-Steady-State Migration Experiments. Referred to as RMT, this test is similar to RCPT, however, the chloride depth is measured for this test. After a certain amount of time, dependent on the initial current when the voltage is set at 30 V, the samples are broken in two to reveal the inside profile and then sprayed with silver nitrate. The silver nitrate reacts with the sodium chloride that is present within the sample, producing a white line. This white line is the depth of chloride penetration of the sample. The white line is measured at various locations and averaged to give an average chloride depth.

3) ASTM C 642-97: Standard Test Method for Density, Absorption, and Voids in Hardened Concrete. Referred to as Water Absorption, this test calls for various masses to be taken of the tested samples and with the measured masses, different densities and absorptions can be calculated. Void content is also determined.

1.6.2. Effects due to Activator Concentration

Ravikumar et al. (2010), first mentioned in section 1.5.2., studied the changes in strength and structure of cement-free concretes containing fly ash or GGBFS with changes in alkaline activator concentrations and activator-to-binder ratios. Porosity of tested samples were studied using the procedure set by RILEM CPC 11.3, referred to as the vacuum saturation method, as well as image analysis techniques. Porosity was seen to decrease with increased alkaline activator concentration, attributed to the increased reaction product formation. This trend correlated well with those found in compressive strength, see section 1.5.2.

In the study by Chi and Huang (2013), discussed first in section 1.5.2., a combination of fly ash and slag were used in alkali-activated mortar to study the binding mechanisms and properties. Water absorption was determined according to ASTM C642. Increased Na_2O content caused a decrease in water absorption. These results were due to the formation of the reaction product, similar to the discussion seen in section 1.5.2.

Ma et al. (2013) investigated the correlation between the water permeability and pore structure of alkali-activated class F fly ash. NaOH and sodium silicate were used as the alkali activators such that the following five alkali solutions were achieved: 0.5 mol SiO_2 and 1.5 mol Na_2O, 1.0 mol SiO_2 and 1.5 mol Na_2O, 1.0 mol SiO_2 and 1.3 mol Na_2O, 1.0 mol SiO_2 and 1.0 mol Na_2O, and 1.5 mol SiO_2 and 1.5 mol Na_2O. A water-to-fly ash ratio of 0.35 was implemented for all mixtures. Two curing methods were used, labeled method 1 and method 2.

Method 1 sealed-cured samples at 40˚C for 7 days before curing at 20˚C with relative humidity over 98% for 3 and 6 months. Method 2 sealed-cured samples at 40˚C for 28 days. An increase in silica content caused a decrease in water permeability; the same trend occurred with increased alkali content. Water permeability decreased was attributed to the increased amounts of uniform aluminosilicate gel with increased silica and alkali content.

1.6.3. Effects due to Curing Conditions

Mentioned in section 1.5.4., Kovalchuk et al. (2007) studied various curing conditions that create the optimum polymerization reaction of alkali-activated fly ash. Mercury intrusion porosimetry (MIP) techniques were implemented to study the porosity of the tested samples. Curing in covered molds provided the least total porosity followed by dry curing and steam curing. There results corresponded with the compressive strength results discussed previously, see section 1.5.4. Porosity influences strength development; therefore a lower porosity would correspond with higher compressive strength. With that said, curing in covered molds had the highest strength and lowest porosity, due to the amount of water available during curing that allowed for higher degree of reaction.

Xie and Kayali (2013) studied the changes in ambient-cured fly ash-based geopolymers with varying water content, as discussed in section 1.5.5. Water displacement method was implemented to determine the density of samples tested. Density decreased with increased curing age, regardless of curing type and water-to-geopolymer ratio. Heat cured samples had a lower density than ambient-cured samples. This was contributed to the amount of water that was released. While heat cured, more water was released as compared to curing at ambient temperature. With increased curing time, more water was released and thus, had a lower density.

Görhan and Kürklü (2014), discussed in section 1.5.4., evaluated fly ash-based geopolymer mortars in terms of physical and mechanical properties. Principle of Archimedes was implemented to determine to water absorption, porosity, bulk and apparent densities. Increased curing time and temperature reduced the apparent porosity; similar trends were found for water absorption. Bulk density increased with corresponding increase in curing time. Trends in relation to NaOH varied with curing time. Bulk density and water absorption properties are inversely related; increased porosity allowed for higher void content and thus a lower density. Results correlated well with those discussed for compressive strength in section 1.5.4.

1.6.4. Effects due to Solution-to-Binder Ratio

Ravikumar et al. (2010), in addition to studying the effects of alkaline activator concentration, studied the effects of activator-to-binder ratio. Using the same procedure discussed in section 1.6.2., porosity increased with corresponding increase in activator-to-binder ratio. This trend correlated well with the results discussed for strength, see section 1.5.5. With that said, compressive strength and porosity were determined to be inversely related.

Xie and Kayali (2013), as discussed in the previous section, used a water displacement method to determine the density of ambient-cured fly ash-based geopolymers. Density increased with increased water-to-geopolymer ratio. Following the discussion presented in the previous section, the authors determined that more water content allowed for lower porosity and thus, higher density. With that said, a higher water-to-geopolymer ratio allowed for more water to stay within the system and thus, density increased.

1.7. Durability Properties

Minimal research has been conducted on the durability properties of alkali-activated fly ash binders. As stated previously, OPC concrete has shown to have alarming durability issues,

therefore, a more durable alternative binder to OPC is needed, in addition to being more sustainable. Four test methods are used for investigating the durability of alkali-activated fly ash binders for this study, see below.

1.7.1. Test Methods

1) ASTM 1012-04: Standard Test Method for Length Change of Hydraulic Cement Mortars Exposed to a Sulfate Solution. This test method measures the length change of samples immersed in a sodium sulfate solution. The length change is tracked over a 15 week period.

2) Acid Resistance. Although a set standard has not been developed, this test method dealt with the immersion of samples in a sulfuric acid solution for a total of 8 weeks. At four different ages, samples are not only tested for compressive strength, but also for mass loss.

3) Sulfate Resistance. In addition to the test method mentioned above, samples are also immersed in a sodium sulfate solution and its compressive strength is measured over an 8 week period, similar to that described for acid resistance testing.

4) Freeze-Thaw Resistance. Dependent on the climate, freeze-thaw resistance of concrete is an important property to know. Samples are immersed in distilled water for a total of 50 freeze-thaw cycles, where one cycle is defined as 24 hours in a freezer set at -4˚C and then left out to thaw at room temperature for another 24 hours. The mass loss is measured at 10 cycle intervals.

1.7.2. Effects due to Changing Parameters

Hardjito et al. (2004), first mentioned in section 1.5.2., tested several variables in order to study their influence on the strength and production of fly ash-based geopolymer concrete. Sulfate resistance was tested over a 12 week time period. After 12 weeks, minimal changes in

compressive strength and length was seen. This indicated a great sulfate resistance for the tested geopolymers.

Bakharev (2005) studied the durability of fly ash-based geopolymers in an acid environment. The first geopolymer used sodium silicate as the activator, meanwhile the second geopolymer used sodium hydroxide, and lastly the third geopolymer used a combination of sodium hydroxide and potassium hydroxide. A water-to-binder ratio of 0.30 was used and a total of 8-9% of Na content. Mixtures were cured at room temperature for 24 hours before being cured at 95°C for another 24 hours. Mixtures were then allowed to cool down to room temperature for 2 days before being subjected to compressive strength and immersion testing. Immersion in acetic and sulfuric acids were implemented. Minimal change in appearance was witnessed in the geopolymers after being immersed in both solutions for 5 months. Samples activated with NaOH had the best resistance against both acids, followed by samples activated with sodium silicate. Samples activated with KOH performed well in acetic solution but performed poorly in sulfuric solution. Ultimately it was determined that the stability of geopolymers was reliant on the composition of the reaction product, aluminosilicate gel. NaOH was found to be more stable in an acidic environment than sodium silicate.

Fernandez-Jimenez et al. (2006) evaluated various engineering properties of alkali-activated fly ash concrete and how it compared to Portland cement, see section 1.5.2. Drying shrinkage tests were conducted. The alkali-activated fly ash concrete experienced minimal shrinkage, much less than that of Portland cement concrete. This result was attributed to the microstructural development of alkali-activated fly ash. The main reaction product is a zeolite-type phase and zeolite has been proven to not be affected by loss of water because they are able to absorb water from the humidity present in the environment.

1.8. Research Objectives

Although great effort has been made by previous research, there are still many unanswered questions in relation to the development of alkali-activated fly ash binders. This study aimed to help further the knowledge of alkali-activated fly ash as a sustainable binder in production of non-cement concrete. Specifically, this study was broken down into two phases, each with its own objectives.

Phase I examined the influence of activator concentration, solution-to-binder ratio, and curing method on the fresh, mechanical and transport properties of alkali-activated fly ash mortars. Class F fly ash was used as the main binder and a fine aggregate-to-fly ash ratio of 2 for all trial mixtures. Sodium hydroxide was used as the main activator. Five sodium hydroxide concentrations, three curing conditions, and three solution-to-binder ratios were used. 2.5, 5, 7.5, 10, and 12.5 M sodium hydroxide concentrations and 0.42, 0.46 and 0.50 were the solution-to-binder ratios were tested. The three curing conditions tested, referred to as air, moisture exposed, and sealed curing, called for a consistent temperature of 60˚C for the first three hours of curing, followed by de-molding and curing at 80˚C. For the first three hours, all samples, regardless of curing type, were sealed cured with four layers of plastic. Once de-molded, samples were separated according to their curing type. Air curing samples were exposed in the oven. Moisture exposed curing samples were placed in a water-filled container within the oven, however, not immersed. Sealed curing samples were sealed with four layers of plastic, similar to the procedure used prior to de-molding. Fresh, mechanical, and transport properties were the main focus for this phase. For fresh properties, the workability and initial and final setting times were tested. Mechanical properties evaluated were compressive and flexural strengths, and modulus of elasticity. For transport properties, chloride depth, density and absorption were determined.

Phase II studied the influence of activator concentration and sodium silicate replacement levels on the fresh, mechanical, transport, and durability properties of alkali-activated fly ash mortars. Phase II was broken down into two parts, with the first part having samples cured at elevated temperatures and the second part involved curing samples at room temperature. Similar to phase I, class F fly ash and a fine aggregate-to-fly ash ratio of 2 were used throughout the study. For this phase, both sodium hydroxide and sodium silicate were used as the activator. For part 1, four sodium hydroxide concentrations and three sodium silicate-to-total solution ratios by mass were tested, 5, 7.5, 10, and 12.5 M NaOH and 0.20, 0.40 and 0.60. Described in phase I, sealed curing was implemented for all samples, with the first three hours at 60˚C followed by 80˚C for the remainder of curing duration. Workability was the fresh properties tested. For mechanical properties, compressive and flexural strength were determined as well as modulus of elasticity. Chloride depth, density, absorption, and void content were established as the transport properties to be tested. Durability properties tested were resistance to acid and sulfate attacks, as well as resistance to freeze-thaw and abrasion. For the part 2 of this phase, 10 M sodium hydroxide was used as well as the three sodium silicate-to-total solution ratios listed in part 1. Room curing was implemented, with samples being de-molded one day after casting, sealed with four layer of plastic, and completely immersed in water for up to 28 days. Just as part 1, same testing procedures were implemented with the exception of fresh properties. Ultimately, results from part 1 and 2 were compared to discuss the possibility of alkali-activated fly ash binders being cured at room temperature, thus eliminating the need for elevated temperatures when curing.

This thesis presented the findings of this study in six distinct chapters. Chapter 1 reviewed the available literature on alkali-activated fly ash binders as well as the main reaction

product. The objectives of the two phases of the investigation were discussed as well as variables tested, curing conditions, and test procedures.

Chapter 2 explains the experimental program used for this study at great length. Mixture proportions, test equipment and methods, mixture parameters, and properties evaluated are further discussed.

Chapter 3 presents the results obtained for phase I of this study. Fresh, mechanical and transport properties of the studied alkali-activated mortars are discussed as functions of activator concentration, curing conditions and solution-to-binder ratio.

Chapter 4 presents the results obtained for part I of the phase II of this investigation. Fresh, mechanical, transport and durability properties are evaluated as functions of sodium hydroxide concentration and sodium silicate-to-total solution ratio.

Chapter 5 presents the results obtained for part II of the phase II of this study. Mechanical, transport and durability properties are discussed as functions of curing at room temperature. Furthermore, comparisons between results obtained in part I and II are discussed.

Chapter 6 contains conclusions for this study as well as recommendations for further research related to alkali-activated fly ash binders.

The appendix contains conversion factors as well as additional tables and figures not presented in chapters 3 through 5.

1.9. Research Significance

As stated previously, Ordinary Portland cement (OPC) is considered to be the dominant binder presently used in concrete production, with concrete being the most widely used

construction material in the world. Unfortunately, manufacturing of OPC poses environmental concern with respect to green house effects, as well as concerns for longevity of concrete products. As such, there is a pressing need to find a sustainable and more durable alternative to OPC. Alkali-activated binders have emerged as a promising alternative binder for use in concrete production. Although recent research has made a great effort in understanding alkali-activated binders, there are still many unanswered questions. The purpose of this study was to further the knowledge of alkali-activated fly ash mortars in terms of curing conditions, activator type and concentration, and solution-to-binder ratio and their effects on fresh, mechanical, transport, and durability properties of alkali-activated mortars. These properties provide a better insight to the behavior of alkali-activated binders and expand the state-of-the-art knowledge for its potential to be a binder of future use for the concrete industry.

CHAPTER 2

EXPERIMENTAL PROGRAM

The study was broken down into two phases, labeled Phase I and Phase II. Using sodium hydroxide as an activator, Phase I sought to examine the effects of activator concentration, curing method, and solution-to-binder ratio on fresh, mechanical, and transport properties of alkali-activated fly ash mortars. Phase II, which used sodium hydroxide and sodium silicate as activators, sought to establish the role of activator concentration and combination on fresh, mechanical, transport, and durability properties of the studied alkali-activated fly ash mortars. In the following sections, specific details into the experimental program to achieve the stated objectives are discussed.

2.1. Mixture Proportions

Table 2.1. Mixture Proportions for Phase I

Solution-to-Binder Ratio	Fly Ash (kg/m^3)	Sand (kg/m^3)	Liquid (kg/m^3)
0.42	0.602	1.204	0.253
0.46	0.595	1.191	0.274
0.50	0.589	1.178	0.294

Table 2.2. Mixture Proportions for Phase II

Sodium Silicate-to-Total Solution Ratio	Fine Aggregate (kg/m^3)	Fly Ash (kg/m^3)	Liquid (kg/m^3)	NaOH Solution (kg/m^3)	Sodium Silicate (kg/m^3)
0.20	1.127	0.564	0.259	0.207	0.052
0.40	1.127	0.564	0.259	0.155	0.104
0.60	1.127	0.564	0.259	0.104	0.155

Table 2.3. Amount of Water and Sodium Hydroxide per 1 Liter of Solution

NaOH Concentration (M)	Distilled Water (g)	Sodium Hydroxide (g)
2.5	995.62	100
5	973.91	200
7.5	950.25	300
10	903.44	400
12.5	858.79	500

For both phases, a constant fine aggregate-to-fly ash ratio by mass of 2 was used. Different solution-to-binder ratios were used for phase I while a constant solution-to-binder ratio or 0.46 was used for phase II. Table 2.1 and 2.2 document the selected mixture proportions for phases I and II, respectively, while Table 2.3 displayed the selected sodium hydroxide solution mixture proportions as needed to create one liter of solution.

2.1.1. Fly Ash

Class F fly ash was used throughout this study; its physical-chemical properties are shown in Table 2.4. This fly ash was classified according to its calcium oxide (CaO) content and total pozzolan oxides (SiO_2+Al_2O_3+Fe_2O_3) which were less than 10% and more than 70%, respectively.

Table 2.4. Physical Chemical Composition of Class F Fly Ash

Silicon Dioxide (SiO_2)	Aluminum Oxide (Al_2O_3)	Iron Oxide (Fe_2O_3)	Sulfur Trioxide (SO_3)	Calcium Oxide (CaO)	Moisture	Loss on Ignition
59.93%	22.22%	5.16%	0.38%	4.67%	0.04%	0.32%

2.1.2. Fine Aggregate

Fine aggregate used was obtained from a quarry in Southern Nevada. It met specifications set by ASTM C 117 and C 136. ASTM C 117 was the standard for determining the amount of aggregates finer than a 75-µm (No. 200) sieve size while ASTM C 136 was the

standard for determining the particle size distribution of the tested aggregates. The specific gravity and absorption of fine aggregate evaluated in accordance to ASTM C 128, is shown in Table 2.5. Figure 2.1 displays the mass percent of fine aggregate that passed each sieve size as well as the minimum and maximum values allowed per ASTM standards.

Table 2.5. Specific Gravity and Absorption of Fine Aggregate

Relative Density (Specific Gravity) Oven-Dry	2.755
Relative Density (Specific Gravity) Saturated-Surface-Dry	2.777
Apparent Relative Density (Apparent Specific Gravity)	2.818
Absorption	0.81%

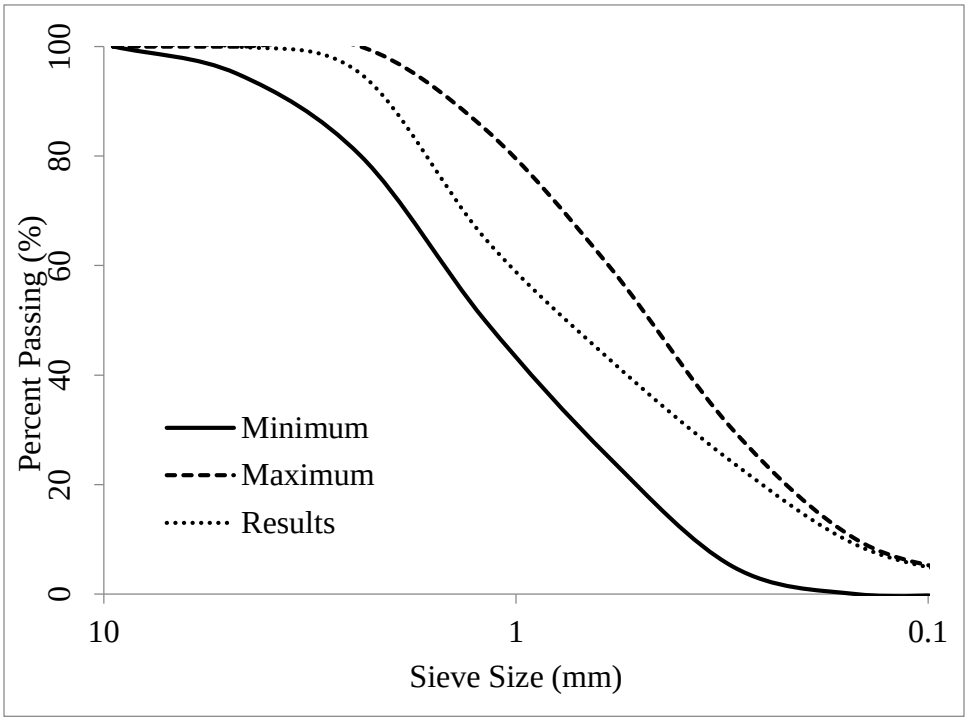

Figure 2.1. Size Distribution for Fine Aggregate Used

2.1.3. Alkaline Activator

Many different alkaline activators have been used in various studies, however, the most common have been sodium hydroxide (NaOH) and sodium silicate. Phase I of this study used NaOH only, while Phase II utilized both NaOH and sodium silicate.

2.1.3.1. Sodium Hydroxide

Sodium hydroxide used for this study was supplied by Duda Diesel, LLC, in solid form. Sodium hydroxide was composed of between 97 and 98.2% of sodium hydroxide, up to 1.2% of sodium chloride and between 0.4 and 1.0% of sodium carbonate.

2.1.3.2. Sodium Silicate

Type D Sodium Silicate solution, supplied by PQ Corporation, was used for this study. Sodium silicate was composed of 55.9% by weight of water and 44.1% by weight of a combination of silicic acid, and sodium salt; silicic acid and sodium salt make sodium silicate.

2.2. Test Equipment

2.2.1. Mortar Mixer

Two different mixers were utilized in this study. Phase I, due to smaller batch size, used a smaller mixer as compared to phase II. To follow are the descriptions of both mixers used for this study.

2.2.1.1. Phase I Mortar Mixer

The mixer used for phase I was a 20-quart capacity mixer, as shown in Figure 2.2. The mixer has three speeds, low, intermediate and high corresponding to 107, 198 and 361 RPM, respectively. For the purpose of this study, speed was kept uniform at the intermediate speed of 198 RPM.

2.2.1.2. Phase II Mortar Mixer

The mixer used for phase II of this study was a 0.0283 m^3 (1 ft^3) capacity counter-current pan mixer as displayed in Figure 2.3. A different mixer was used for phase II due to the increased batch size and quantities. The mixer had a rotating cylindrical pan with rotating blade. The speed of the mixer was kept constant at 60 RPM.

Figure 2.2. Mixer used for Phase I

Figure 2.3. Mixer used for Phase II

2.2.2. Slump Flow

Slump flow was measured by using the flow table pictured in Figure 2.4. The flow table was hand driven with a 254 mm (10 inch) diameter table and 69.85 mm (2.75 inch) top diameter, 50.8 mm (2 inch) high by 101.6 mm (4 inch) bottom diameter flow mold, both of which were made of brass.

Figure 2.4. Flow Table used for Slump Flow Measurements

2.2.3. Setting Time

A modified vicat apparatus was used to measure the setting time, as pictured in Figure 2.5, with a 10 mm (0.4 inch) plunger and 100 gram (0.22 lb) weight. It also had a 0-50 mm (0-2 inch) scale to read the depth the needle penetrated into the test sample. The needle used had a 1 mm (0.04 inch) diameter.

Figure 2.5. Modified Vicat Apparatus used to Measuring Setting Time

2.2.4. Strength

The machine used to evaluate strength in compression and flexure, and stiffness (elastic modulus) is shown in Figure 2.6. The testing machine has a 2, 224 kN (500 M lbf) load capacity. For compressive strength testing, the loading rate was kept uniform between 0.034 and 0.048 MPa-per-second (5 and 7 psi-per-second). Flexural strength utilized a loading rate between 0.014 and 0.034 MPa-per-second (2 and 5 psi-per-second). To determine elastic modulus of the studied alkali-activated mortars, the rate of loading of approximately 0.14 MPa-per-second (20 psi-per-second) was used.

2.2.5. Resistivity to Rapid Chloride Migration Test

DC power supplies were used to evaluate rapid chloride migration of the studied alkali-activated mortars. The test set-up is shown in Figure 2.7. The power supply had a maximum

voltage and amperage of 60 V and 5 A, respectively. While the voltage and amperage could be adjusted, per the limitations of the samples, the voltage was kept constant at 10 V.

2.2.6. Sulfate Length Change

A length comparator and digital indicator were used to determine the length expansion of the studied mortars under exposure to a sodium sulfate environment. The test set-up is shown in Figure 2.8. The digital indicator's accuracy was to the nearest 0.00254 mm (0.0001) inch. It also read in millimeter and inch units, dependent on the user's preference.

2.2.7. Freeze-Thaw Resistance

The freezer, as pictured in Figure 2.9, was used for freeze-thaw resistance testing. The temperature of the freezer was set at approximately -4°C. Temperature was adjusted weekly, dependent on the amount of samples in the freezer at one time.

Figure 2.6. Strength and Stiffness Testing Machine

Figure 2.7. Rapid Chloride Migration Test Set-Up

Figure 2.8. Length Comparator and Digital Indicator used for Sulfate-Induced Expansion Measurements

Figure 2.9. Freezer used for Freeze-Thaw Resistance Test

2.2.8. Abrasion Resistance

The test apparatus shown in Figure 2.10 was used for abrasion resistance testing, modeled after the one used in the thesis study by Tays (2002). The test apparatus was composed of a dymodrills motor attached to a rig assembly. Although retrofitted with an air-water combination, for the purpose of this study, only air was used to aid in the removal of loose particles from the testing surface. A retainer ring with twelve 12 mm (0.5 inch) diameter steel balls was used as the abrasion action surface. A rubber ring was mounted to the bottom of the bearing as to minimize the movement of the ball bearings caused by the vibration of the test apparatus. Similarly, a rubber sheet was attached with adhesive to the bottom surface of the cantilever flange, the area where the needle pointer of the dial gage was placed such to minimize any fluctuations during the experiment. The drive shaft of the test apparatus was constructed from a bronze metal core of smaller length in order to minimize any vibration caused by the

circular rotation of the drive shaft, bearing plate and ball bearings. A total load of 82.88 kg (37 lb) was carried by the ball hearings. The drive shaft operated at 1000 rpm.

Figure 2.10: Abrasion Resistance Test Apparatus

2.2.9. Oven

For this study, two ovens were used for the curing regime of test samples, as shown in Figure 2.11. The oven on the left was utilized for the first three hours of curing, with the oven set at 60°C while the oven on the right was utilized for the remainder of the curing period, set at 80°C.

2.3. Test Program

The testing program was devised to evaluate four main properties; namely fresh, mechanical, transport, and durability. Both phases of this study addressed fresh, mechanical, and transport properties with phase II also investigated the durability properties of alkali-activated mortars.

Figure 2.11. Ovens used for Curing

2.3.1. Fresh Properties Test Procedures

The fresh properties of the studied alkali-activated mortars were evaluated for workability (slump flow) and setting time. Slump flow, as a measure of workability, was used to determine mixture consistency, whereas setting time was used to determine the initial and final setting times. Both of these properties are vital to determine the ability of alkali-activated mortars to be workable for construction applications. ASTM C 1437-01 was used for evaluation of slump flow. Once batching was complete, half of the flow mold was filled followed by tapping the mortar 15 times. The flow mold was then filled and leveled such that the mortar was flush with the top of the mold prior to the flow mold being removed. Using the rotating handle, the flow table was lifted up 25 times in approximately 30 seconds. The diameter of the mortar

flow was measured in four different locations and averaged. The averaged diameter was recorded and noted as the slump flow the evaluated mixture.

ASTM C 807-03a was used to evaluate the setting times. Once batched, a 100 mm (4-inch) diameter by 50 mm (2-inch) high cylinder mold was filled approximately three-fourths of the way with mortar and the sides were tapped approximately 15 times. The mold was then placed under the needle of the apparatus and zeroed such that the needle was flush with the top of the mortar. The needle was then released and needle depth that penetrated the sample in 30 seconds was recorded along with the time. This was repeated every 30 minutes, at maximum, until the needle depth was less than or equal to 25 mm (1inch). Once the needle depth was less than 25 mm (1 inch), measurements were repeated every 10 minutes, at maximum, until the needle depth was less than or equal to 10 mm (0.4 inch). Using the depth and time duration for a measurement greater than 25 mm (1 inch) and less than 25 mm (1 inch), the time at which the depth was 25 (1 inch), was found by interpolation. This time was taken as the initial setting time. The same process was done for 10 mm (0.4 inch). That time was considered as the final setting time.

2.3.2. Load-Bearing Properties Test Procedures

Compressive strength, flexural strength, and elastic modulus were the evaluated mechanical properties. Compressive strength was evaluated after 1, 3, and 7 days. Flexural strength and modulus of elasticity were determined after 7 days of oven curing. For room temperature curing, compressive strength was tested after 7, 14 and 28 days of curing while flexural strength and modulus of elasticity were tested after 28 days of curing.

Two (2) different sample sizes were evaluated, dependent on the phase the study. Phase I of this study utilized sample sizes of 50-mm (2-inch) cubes while phase II utilized 50-mm (2-

inch) diameter by 100-mm (4-inch) high cylinders. Compressive strength testing consisted of the application of a constant rate compressive load, approximately 0.041 to 0.048 MPa-per-second (6 to 7 psi-per-second), until the sample failed. Once failure occurred, the maximum load, measured when failure occurred, was taken and divided by the cross section area of the sample. For each mixture evaluated, a total of four (4) samples were used. Once tested, the calculated strengths were averaged and the final compressive strength was given.

ASTM C78-02, four-point loading was used to evaluate flexural strength of the beam-shaped samples, as shown in the schematic drawing in Figure 2.12. Each beam was 200 mm (8 inches) long with a 50-mm (2-inch) square cross-section. The bottom supports were placed after 25 mm (1 inch) from each side, such that the distance in between was 150 mm (6 inches). The top support was centered on top of the tested sample such that each support was 25 mm (1 inch) from the center and the distance in between was 50 mm (2 inches). The flexural load was applied at a constant 0.014 MPa-per-second (2 psi-per-second) rate until failure occurred. The load measured when the sample failed was then multiplied by the length of the beam within the two bottom supports and divided by 6. In this study, the length between the two supports was approximately 150 mm (6 inches). Then the value was multiplied by the length between the beam supports and divided by 8. The end value was then taken as the flexural strength of the sample. A total of three (3) samples were evaluated until failure and averaged to obtain an average flexural strength for each mixture being tested.

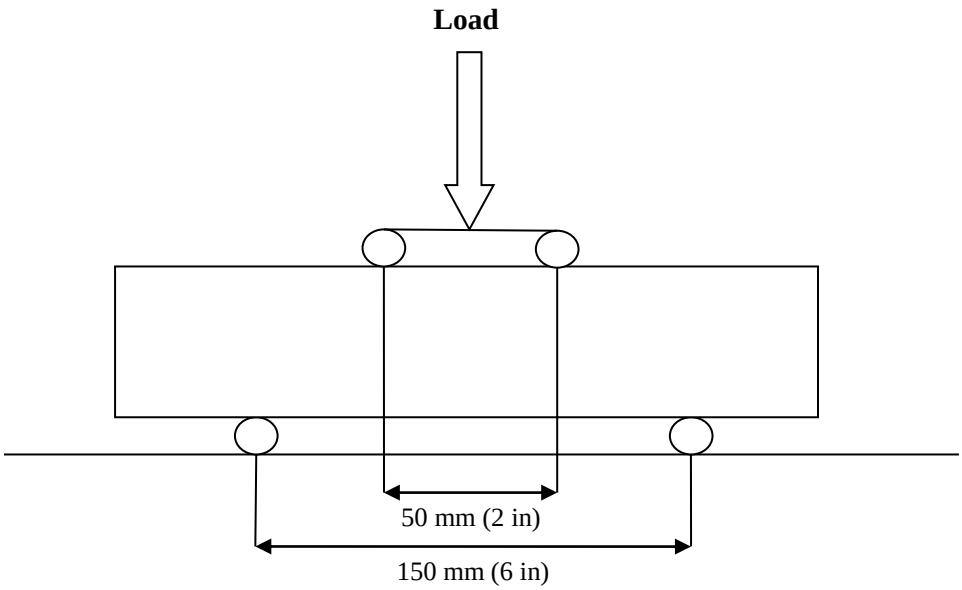

Figure 2.12. Schematic for Four-Point Flexural Strength Testing

Figure 2.13. Four-Point Flexural Strength Test Set-Up

As stated, the modulus of elasticity was evaluated for all mixtures. Two different testing procedures were utilized for modulus of elasticity evaluation, dependent on the phase of the study.

For phase I, the beam samples used for flexural strength testing were utilized to also calculate the modulus of elasticity. Two beam samples were retrofitted with strain gauges in order to record the strain simultaneously with the load applied during flexural strength testing. Measurements were recorded every second until failure. The stress for each load was calculated and plotted against the strain recorded for each sample. Two strains and their corresponding stresses corresponding to a linear increase in the plot were selected, typically approximately to 30% of the ultimate strain and used to interpolate the modulus of elasticity. The difference between the two stresses was divided by the difference between the two strains and multiplied by 10^3. The value obtained corresponded to the modulus of elasticity of the evaluated mixture.

ASTM C469-05 was used to determine the static modulus of elasticity of the studied mixtures for phase II. The standard outlined how to determine the modulus of elasticity using the load recorded when strain in the sample is at 50 millionths and also the load equivalent to 40% of the ultimate load determined by compressive strength and its corresponding strain. By taking the four values recorded, the modulus of elasticity can be found by means of determining the average slope when stress was plotted against strain. 100-mm (4-inch) diameter by 200-mm (8 inch) tall cylinders were used for testing the elastic modulus of evaluated mixtures. Once the device that measured the strain of samples was attached, samples were subjected to a constant compressive load of approximately 0.14 to 0.21 MPa-per-second (20 to 30 psi-per-second). Once the stain began to read, the initial strain and corresponding load was recorded. Based on the compressive strength results obtained previously, the load corresponding to 40% of the ultimate

load was calculated and used as the end load for modulus of elasticity testing and the corresponding strain was recorded. The two load values obtained were then divided by the area cross section of the sample and the stress value was determined. The difference between the two stress values were then divided by the difference between the two strain values, with the end result being the modulus of elasticity. A total of three (3) samples were tested and their results were averaged to obtain the final modulus of elasticity value of the evaluated mixture.

2.3.3. Transport Properties Test Procedures

Transport properties were tested in order to determine the sample's capability to resist penetration from liquids, such as sodium chloride. This is an important property due to its correlation with the possibility of steel corrosion in reinforced concrete and durability of concrete itself. With that said, two procedures were used to determine the transport properties, namely resistivity to rapid chloride ion migration (RMT) which measured the amount of chloride allowed to pass through a sample over a set test period, and water absorption which measured the mass of samples to determine absorptions, densities and void content of the studied alkali-activated mortars.

2.3.3.1. Resistivity to Rapid Chloride Migration Test Procedure

NT Build 492 was the standard used to determine the chloride depth of a sample exposed to sodium chloride and sodium hydroxide with a charge. The chloride depth was measured and correlated to the resistivity to corrosion, the lower the chloride depth the higher the resistivity. In the test standard, the samples, three 100-mm (4-inch) diameter by 50-mm (2-inch) tall cylinders were placed into a vacuum dessicator without any water for three hours before adding calcium hydroxide diluted in water until the samples were completely covered. The vacuum dessicator was left on for another hour before being shut off. The samples were left in the dessicator

without removing the lid for at least 14 hours. For the purpose of this study and time limitations, samples were left in the dessicator until the following morning. Once samples were ready to be removed from the dessicator, samples were surface dried and placed into rubber tubes and secured with metal rings such that the bottom surface of the sample was flush with the edge of the rubber ring. Once secured, samples were placed in a bin filled with sodium chloride water on a plexi-glass fabricated table with wire mesh on the bottom. This plexi-glass table was angled such that the bottom was at 45° to the bottom of the bin. Figure 2.13 displays an actual set-up of the test sample placed in the sodium chloride water. Sodium chloride water used as prepared prior to removing samples from the dessicators such that the salt water was 900 grams of water per 100 grams of sodium chloride (salt). Sodium hydroxide was also another solution used for this test procedure such that 50 grams of sodium hydroxide were mixed with 900 grams of water.

Once samples were placed in sodium chloride water, the top portion of the sample was filled with sodium hydroxide such that the top of the sample was immersed. A metal mesh was placed inside the top of the sample and a red wire was connected to it and to the positive end of the device supplying power. A black wire, also connected to the ground end of the device supplying power, was connected to the wire mesh that was linked to the bottom of the plexi-glass table inside the bin.

With the test apparatus set up, the device supplying power was turned on and set to 10 V. The corresponding current, in mA, was recorded as well as the temperature of the sodium hydroxide. Dependent on the current, the sample was left in the bin for either 6 or 24 hours. For this study, phase I samples were left for 24 hours and phase II samples were left for 6 hours. Once the test duration was completed, the final current and temperature of the sodium hydroxide were recorded. Samples were then removed from the rubber ring and surface dried.

The samples were then split open in half from the top of the sample to the bottom. Silver nitrate solution was sprayed onto the split samples and left to dry for approximately 15 minutes. The silver nitrate sprayed reacted with the sodium chloride that penetrated the sample and produced a white line. The white line was then measured in up to 7 locations throughout the sample and recorded. All measurements were then averaged and this was taken as the chloride depth for the evaluated mixture.

Figure 2.14. Rapid Chloride Migration Sample Test Set-Up

2.3.3.2. Water Absorption

Referred to as water absorption, ASTM C 642-97 was used to calculate various absorptions, densities, and the void content of tested samples. Three (3) 100-mm (4 inch)

diameter by 50-mm (2-inch) tall cylinders were dried in an oven set at 60°C such that the different between two consecutive mass measured after every 24 hours was less than 0.5%. The final mass measured as labeled as the oven-dried mass (A). For oven-cured samples, it was assumed that the mass measured after being removed from the oven was oven-dried. Samples cured at room temperature in phase II-part II followed this procedure. Samples were then immersed in water. After 24 hours, the mass of each sample was measured after being surface-dried. Samples were then immersed in water and measured its mass after 24 hours. Once the mass measured between two 24-hour periods was less than 0.5%, the final mass was labeled as mass after immersion (B).

Samples were then boiled in water for 5 hours and allowed to cool for at least 14 hours before measuring its mass. The mass measured was labeled as mass after immersion and boiling (C). Each sample was then placed in a basket hung from the scale displayed in Figure 2.14 and immersed in water. The mass was then recorded and labeled as mass in water (D).

Once all masses have been measured, the following equations were used to calculate absorption, density and void contents. Please note, ρ is equal to 1 g/cm^3. Once all calculations were made, the results were averaged.

$$Absorption\ after\ immersion = \left[\frac{(B-A)}{A}\right] \cdot 100\% \quad \text{(Eq. 2.1)}$$

$$Absorption\ after\ immersion\ and\ boiling = \left[\frac{(C-A)}{A}\right] \cdot 100\% \quad \text{(Eq. 2.2)}$$

$$Dry\ bulk\ density\ (g_1) = \left[\frac{A}{(C-D)}\right] \cdot \rho \quad \text{(Eq. 2.3)}$$

$$Density\ after\ immersion = \left[\frac{B}{(C-D)}\right] \cdot \rho \quad \text{(Eq. 2.4)}$$

$$Density\ after\ immersion\ and\ boiling = \left[\frac{C}{(C-D)}\right] \cdot \rho \quad \text{(Eq. 2.5)}$$

$$Apparent\ Density\ (g_2) = \left[\frac{A}{(A-D)}\right] \cdot \rho \quad \text{(Eq. 2.6)}$$

$$Void\ Content = \left[\frac{(g_2 - g_1)}{g_2}\right] \cdot 100\% \quad \text{(Eq. 2.7)}$$

Figure 2.15. Scale used for the Measure Mass of Test Sample in Water

2.3.4. Durability Properties Test Procedures

The durability of alkali-activated fly ash is critical for possible alternative to OPC. Therefore, there were four main properties that were evaluated: sulfate resistance in terms of length expansion and strength, acid resistance in terms of mass loss, freeze-thaw resistance in terms of mass loss, and lastly abrasion resistance in terms of abrasion depth.

For oven-cured samples, once removed from the oven, each sample was labeled according to their sample number and property. For acid and freeze-thaw resistance samples only, the mass of each sample was recorded and before it was immersed in water for 7 days. The

mass of sulfate resistance samples were not measured, samples were simply immersed in water for 7 days. After 7 days, samples were surface dried and the mass for acid and freeze-thaw resistance samples were recorded. For room temperature cured samples, the mass of each sample was measured once curing was complete. Abrasion resistance testing samples were not immersed in water following their respective curing period.

2.3.4.1. Strength

Acid and sulfate resistance was determined by measuring compressive strength of samples after being immersed in sulfuric acid and sodium sulfate solutions, respectively for 1, 2, 4, and 8 weeks. A total of twelve (12) 55-mm (2-inch) diameter by 100-mm (4-inch) tall cylinder type samples were utilized for strength loss testing per each resistance type.

A sulfuric acid solution was used for acid resistance testing. 1.5 parts distilled water along with 1.0 parts of 5 N sulfuric acid was the ratio used for the sulfuric acid solution. Acid resistance samples, once their masses were recorded, were placed in labeled bins and immersed in the sulfuric acid solution. The pH of the solution was adjusted weekly such that the pH of 1.0 was maintained. For sulfate resistance testing, a sodium sulfate solution of 50 g of sodium sulfate powder to 900 g of distilled water was used. . The pH of the sodium sulfate solution was adjusted weekly with the sulfuric acid solution used for acid resistance such that the pH was between approximately 6 and 8.

When tested, three samples were removed and placed in a dry bin and left to air dry for at least one hour. Acid resistance samples were then lightly brushed in a forward and backward matter two times around and twice on the top and bottom of the sample. The mass of each sample was measured prior to measuring its strength. The mass of sulfate resistance samples were not measured. Strength testing procedure was the same as that used for compressive

strength testing, see section 2.3.2. Once compressive strength was calculated, the three values were averaged and taken as the compressive strength.

2.3.4.2. Length

Two (2) bar samples, 355-mm (14-inch) long with 25-mm (1-inch) square cross section, were immersed in sodium sulfate solution, the same solution used for sulfate resistance in terms of strength. Length was measured after being immersed for 1, 2, 3, 4, 8, 13, and 15 weeks, with the length measured at each age. ASTM 1012-04 was used to determine the length change of samples immersed in sodium sulfate. Similar to the other durability samples, bar samples were immersed in water for 7 days prior to testing. Once removed from the water, bar samples were surface dried and measured for their initial length. Bar samples were then immersed in sodium sulfate solution. Just as done for sulfate strength resistance, the pH of the sodium sulfate solution was adjusted with sulfuric acid solution used for acid resistance testing, such that the pH was approximately between 6 and 8. When tested, samples were removed from the solution and surface dried prior to measuring and placed back in sodium sulfate solution. The percent difference between the initial length and the measured length at a given age was calculated for each sample and averaged. The value was then plotted against time to observe length expansion over time.

2.3.4.3. Mass Loss

In addition to strength, acid resistance was also measured in terms of mass loss. Mentioned first in section 2.3.4., the mass of each sample was recorded prior to immersion in water and in sulfuric acid solution as well as after being immersed for up to 8 weeks. Mass of each sample was recorded prior to strength testing after being brushed as described in section 2.3.4.1. For each testing age, the mass of three (3) samples were recorded. The difference

between the sample prior to immersion and the mass recorded at the testing age was found and averaged. This was noted as the mass loss of the given testing age. The percentage of mass loss was used to determine the resistance to acid attacks; the fewer the mass loss the better the resistance.

Once removed from water, freeze-thaw resistance samples were placed in individual containers and immersed in distilled water leaving 3.175-mm (0.125-inch) of excess water above the sample. Samples were not touching the bottom of the container. In addition to mass recorded prior to testing, masses were measured prior to the immersion, and after 10, 20, 30, 40, and 50 freeze-thaw cycles. One freeze-thaw cycle was as follows: being in a freezer set at -4˚C for 24 hours, followed by being left to thaw at ambient temperature for another 24 hours. The percentage of mass loss between the initial mass measured prior to immersion and the mass measured after a given testing period was used to determine the resistance to freezing and thawing, with its level of importance being dependent on the climate. Harsh winters quickly deteriorate concrete, a combination of freezing water and salt used to de-ice roadways, and can cut the service life of pavements dramatically. A higher freeze-thaw resistance is desired to expand the service life and therefore require less repairs or full restorations of concrete structures.

2.3.4.4. Abrasion Resistance

Two (2) 150-mm (6-inch) cube samples were utilized per each matrix tested during phase II for abrasion resistance testing. ASTM C 779 Procedure C, standard for assessing the abrasion resistance of horizontal concrete surface, was implemented for abrasion resistance testing with slight modifications, to follow are the testing procedures.

The cube sample was fixed in place with the use of clamps and attached to steel plate under the drive shaft of the test apparatus, as shown in Figure 2.10. The steel plate was leveled once the sample was placed to aid in maintaining the sample positioned horizontally throughout the test duration. Once the sample was placed and fixed, twelve (12) 13 mm (0.5 inch) diameter steel ball bearings were positioned on the bottom of the bearing plate on the test apparatus. The drive shaft was then lowered until the ball bearings came into contact with the top surface of the sample. An air supply was supplemented in order to aid in the removal of loose particles during testing. With that said, the air valve with approximately 40 psi air pressure was opened. A dial gage was then fixed such that the needle made contact with the cantilever flange. The dial gage and a digital stopwatch were then set to zero.

Once the set up was completed, the power was turned on. Measurements were taken from the dial gage every 30 seconds for either 20 minutes or until the depth of total abrasion was 3 mm (0.12 inch), whichever came first. Dependent on the consistency of measurements, two (2) to four (4) sides of the sample were tested.

2.3.5. Phase I Procedures

Phase I tested the effects of activator concentration, curing method, and solution-to-binder ratio of alkali-activated fly ash mortars using solely sodium hydroxide on the fresh, mechanical, and transport properties.

The activator was prepared one day prior to mixing to allow for the activator to cool to room temperature. Activator preparation procedure was similar to that done in the study by Rajamma et al. (2012); solution was prepared and placed in a tub of water to prevent the solution from boiling. Both the fine aggregate and fly ash were mixed for 2 minutes prior to adding the

activator. Once added, the mixture continued for another 2 minutes. If needed, mixing continued until consistency.

2.3.5.1. Curing Method

Three curing methods were implemented for Phase I of this study, labeled air curing, moisture exposed curing, and sealed curing. Once samples were casted, molds were wrapped in four layers of plastic and placed in an oven set at 60˚C before being de-molded. Once de-molded, samples were divided into the three curing methods, all of which were placed in an oven set at 80˚C. Air curing called for samples to be exposed in the oven. Moisture exposed curing left samples exposed in a closed container with water; however, samples were not immersed in water. Sealed curing, similar to how samples were during the first three hours of curing, were sealed in four layers of plastic and left in the oven. Samples were taken out of the oven at the designated testing period.

2.3.5.2. Mixture Parameters

Three solution-to-binder ratios were used, as well as five activator concentrations: 0.42, 0.46, and 0.50; 2.5, 5, 7.5, 10, and 12.5 M NaOH. A constant fine aggregate-to-fly ash ratio of 2 was used for all mixtures. Mixture proportions are shown in Table 2.1. As stated in the previous section, three curing methods were implemented.

2.3.5.3. Test Procedures

Fresh, mechanical, and transport properties were tested for Phase I. For fresh properties, the slump flow and setting time were tested immediately following mixing.

Mechanical properties to be tested were compressive strength, flexural strength, modulus of elasticity, and modulus of toughness. Compressive strength was tested after 1, 3, and 7 days of curing for each curing method. Flexural strength was tested after 7 days of curing; sealed curing

was the only curing method used. After 7 days of curing, strain gages were implemented to the samples and the strain was measured throughout the loading process. Once completed, the strain was plotted versus the stress at each interval and through calculations, the modulus of elasticity was determined as described in section 2.3.2.

Transport property test procedures to be implemented were RMT and water absorption as described in section 2.3.3. As stated previously, disk samples were molded for the purpose of transport property procedures and sealed cured for 7 days, similar to that used for flexural strength testing.

2.3.6. Phase II Procedures

Phase II was broken down into two parts, collectively focused on the use of sodium silicate in combination with sodium hydroxide as the alkaline activator solution. The main objective for phase II-part I focused on the influence of the concentration of sodium hydroxide as well as use of sodium silicate as partial replacement of total solution on the fresh, mechanical, transport, and durability properties of alkali-activated fly ash mortars. In addition, the feasibility of curing alkali-activated fly ash mortars at room temperature was also investigated, labeled as part II.

Similar to the procedure used for phase I, sodium hydroxide solution was prepared one day prior to mixing and placed in a container with water in order to prevent the solution from boiling. Fine aggregate and fly ash were first mixed for 2 minutes prior to the addition of the activator solution and further mixing for 2 minutes. Once completed, samples were molded.

2.3.6.1. Curing Method

2.3.6.1.1. Part I

Unlike phase I, phase II-part I only utilized one curing method, referred to as sealed curing. Once molded, samples were wrapped in two to four layers of plastic and placed in an oven set at 60˚C for 3 hours prior to de-molding. Once de-molded, samples were wrapped in four layers of plastic and placed in an oven set at 80˚C until testing.

2.3.6.1.2. Part II

As stated, phase II-part II sought to investigate the feasibility of curing alkali-activated fly ash mortars at room temperature. Using the same molding procedure as part I, samples were wrapped in two to four layers of plastic and left in the molds for 24 hours prior to de-molding. Once de-molded, samples were wrapped in four layers of plastic and submerged in water until testing. The same types of samples were molded for part II as for part I.

2.3.6.2. Mixture Parameters

2.3.6.2.1. Part I

Four concentrations of sodium hydroxide were tested as well as three sodium silicate-to-total solution ratios by mass: 5, 7.5, 10, and 12.5 M; 0.20, 0.40 and 0.60 by mass. A constant fine aggregate-to-fly ash ratio was used as well as a constant solution-to-binder ratio, 2 and 0.46, respectively. Table 2.2 details the designed mixture proportions.

2.3.6.2.2. Part II

Only one sodium hydroxide concentration was used for part II, namely 10 M NaOH. 4, 1.5 and 0.667 sodium hydroxide-to-sodium silicate ratios by mass were utilized. Fine-aggregate-to-fly ash and sodium-to-binder ratios were kept constant at 2 and 0.46, respectively. The same mixture proportions were used for 10 M sodium hydroxide as that for part I, refer to Table 2.2.

2.3.6.3. Test Procedures

2.3.6.3.1. Part I

Fresh, mechanical, transport, and durability properties were to be determined in phase II-part I. Similar to phase I procedures, the slump flow was tested immediately following mixing. For mechanical properties, compressive strength was tested after 1, 3, and 7 days of oven curing. Flexural strength was tested after 7 days of curing, as well as the modulus of elasticity.

Just as in phase I, RMT and water absorption was tested as the transport properties after 7 days of oven curing. For the durability properties, abrasion, acid, freeze-thaw, and sulfate resistance was tested. Abrasion resistance testing measured the total depth loss after up to 20 minutes of abrasion. Samples were evaluated after the 7 days of curing. For acid resistance, both strength and mass loss was measured after being immersed in sulfuric acid for 1, 2, 4, and 8 weeks. For sulfate resistance, strength was measured after 1, 2, 4, and 8 weeks of sodium sulfate immersion. Additionally, length expansion was also measured after 1, 2, 3, 4, 8, 13, and 15 weeks of sodium sulfate immersion. Freeze-thaw resistance testing was measured using mass loss measurements after 10, 20, 30, 40, and 50 freeze-thaw cycles. For durability testing with the exception of abrasion resistance, samples were cured in the oven for 7 days before being immersed in water for a further 7 days. Once this time was completed, samples were immersed in their respective mediums.

2.3.6.3.2. Part II

Mechanical, transport and durability properties were tested for part II of phase II. The same procedures were conducted as those described for part I with the test period differing. Fresh properties were not tested because these properties are not affected by curing methods.

Compressive strength was tested after 7, 14 and 28 days of curing. Flexural strength and modulus of elasticity were tested after 28 days of curing.

RMT and water absorption testing was carried out after 28 days of curing. Differing from the procedure set in part I, durability samples were not immersed in water prior to testing but rather samples were immersed in their respective mediums after 28 days of curing. Strength and mass loss were determined for acid resistance, with measurements occurring after 1, 2, 4, and 8 weeks of being immersed in sulfuric acid. Strength was tested for sulfate resistance after 1, 2, 4, and 8 weeks after being immersed in sodium sulfate. Mass loss was measured for freeze-thaw resistance testing, with measurements made after 10, 20, 30, 40, and 50 freeze-thaw cycles. Abrasion wear depth was measured after 28 days of curing.

CHAPTER 3

PHASE I: EFFECTS OF SOLUTION-TO-BINDER RATIO, ACTIVATOR CONCENTRATION, AND CURING CONDITION ON ALKALI-ACTIVATED FLY ASH MORTARS

The main objective of phase I of the study was to examine the effects of curing condition, solution-to-binder ratio, and activator concentration on the fresh, mechanical and transport properties of alkali-activated fly ash mortars. The fresh properties evaluated were workability and setting times. Compressive strength was tested to determine the effects of curing conditions. In addition, compressive and flexural strength were tested to determine the effects of solution-to-binder ratio and activator concentration. Rapid chloride migration, absorption, and density were the transport properties tested to evaluate the effects of solution-to-binder ratio and activator concentration. In total, 15 different mortar mixtures were tested, with 36 compressive samples, 5 flexural strength samples, and 6 transport property samples per mixture.

3.1.Fresh Properties

Table 3.1. Workability results for alkali-activated fly ash mortars - Phase I

Workability (Slump Flow, cm)					
Solution-to-Binder	2.5 M NaOH	5 M NaOH	7.5 M NaOH	10 M NaOH	12.5 M NaOH
0.42	15.24	12.70	11.75	7.30	6.14
0.46	15.24	15.24	11.75	9.53	7.30
0.50	15.24	15.24	12.07	11.75	8.47

3.1.1. Workability

3.1.1.1. Effects of Solution-to-Binder Ratio on Workability

As depicted in Table 3.1 as well as Figure 3.1, workability increased with increased solution-to-binder ratio. Due to the limits of the test apparatus, workability values of 15.24 cm (6 in) shall not be used in terms of comparison. With that said, between 0.42 and 0.46 solution-to-binder ratio, there was, on average, approximately a 30% and 19% increase for the mixtures containing 10 and 12.5 M sodium hydroxide, respectively. A 2.7%, 23.5% and 16.0% increase was seen for the studied mortars with 7.5, 10, and 12.5 M NaOH between 0.46 and 0.50, respectively. Higher amounts of water were available with increased solution-to-binder ratio while the amount of available fly ash decreased, both of which led to reduction in binding reactivity of the matrix and higher amount of free liquid within the mixture. In the study done by Joseph and Mathew (2012), the compacting factor was used to determine workability versus slump flow as in this study, however, both describe workability. Ultimately, the study concluded that the compacting factor increased with increased alkali-to-fly ash ratio. A similar trend was also found in this study.

3.1.1.2. Effects of Activator Concentration on Workability

Referring to Table 3.1, workability decreased with increased activator concentration, regardless of solution-to-binder ratio. Again, due to the limitations of the test apparatus, only values less than 15.24 cm (6 in) will be compared. When molarity increased from 5 to 7.5 M NaOH, there was a 7.5% decrease for 0.42 solution-to-binder ratio. Upon further molarity increase to 10 M NaOH, there was a 38%, 19% and 2.6% decrease for 0.42, 0.46, and 0.50 solution-to-binder ratio, respectively. There was a 16%, 23% and 28% decrease for 0.42, 0.46 and 0.50 solution-to-binder ratio, respectively, once molarity increased to 12.5 M NaOH. On

average, for every 2.5 M increase in sodium hydroxide, the workability of the studied mortars decreased by 20%, 21%, and 15% for solution-to-binder ratios of 0.42, 0.46 and 0.50, respectively. For a given solution-to-binder ratio, increased activator concentration allowed for more of the alkaline solution to react upon contact with more fly ash, resulting in lower workability of the studied mortars.

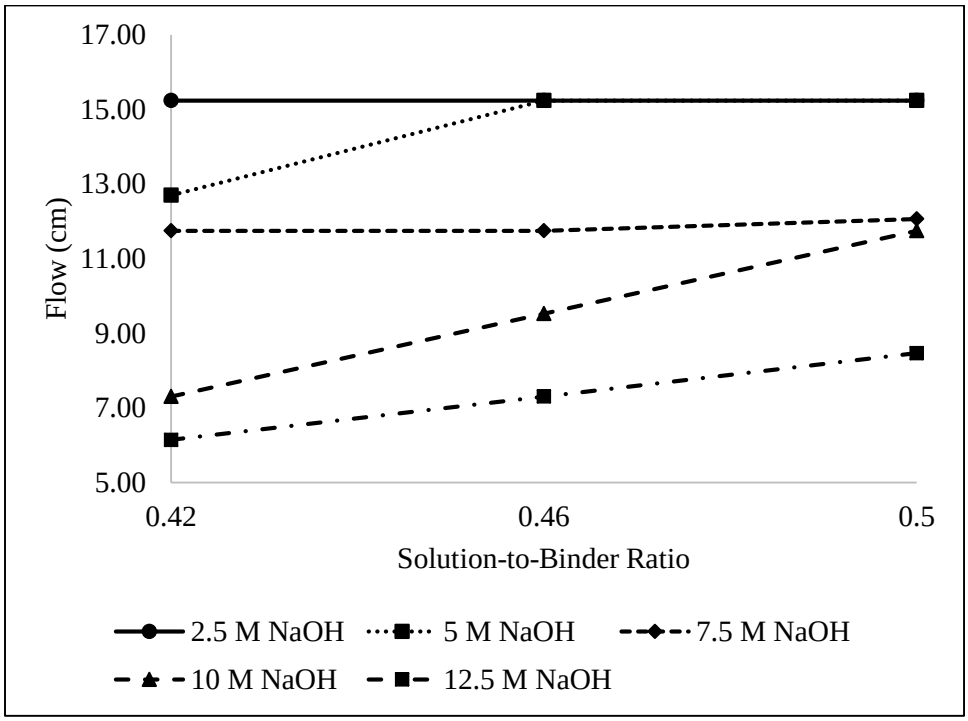

Figure 3.1. Workability as functions of solution-to-binder ratio for alkali-activated fly ash mortars - Phase I

3.1.2. Setting Times

3.1.2.1. Effects of Solution-to-Binder Ratio on Setting Times

As seen in Table 3.2, both initial and final setting times increased with increased solution-to-binder ratio for all selected activator concentration. Once solution-to-binder ratio increased from 0.42 to 0.46, initial setting time increased 26.5%, 12.2%, 23.4%, and 153.3% for 5, 7.5, 10, and 12.5 M NaOH, respectively; final setting time increased 5.2%, 20.5%, 38.3%, and

99.4% for the mortars containing 5, 7.5, 10, and 12.5 M NaOH, respectively. When solution-to-binder ratio increased from 0.46 to 0.50 solution-to-binder ratio, initial setting time increased 117.6%, 54.5%, 16.6%, and 42.7% for 5, 7.5, 10, and 12.5 M NaOH, respectively; final setting time increased 79.6%, 44.0%, 14.8%, and 24.2% for the mortars made with 5, 7.5, 10, and 12.5 M NaOH contained mortars, respectively. On average, initial setting time increased by 72%, 33%, 20%, and 98% with every 0.04 increase in solution to binder ratio for the mixtures containing 5, 7.5, 10, and 12.5 M NaOH, respectively. With every 0.04 incremental increase in solution-to-binder ratio, final setting time increased by approximately 42%, 32%, 27%, and 62% when 5, 7.5, 10, and 12.5 M NaOH, respectively, were used. Due to the similarity between both fresh properties investigated in this study, the two can be correlated with one another. With that said, similar explanations can be made for setting times as that made for workability. In order to maintain a constant mortar volume, an increase in solution-to-binder ratio resulted in a lower content of fly ash, as well as higher availability of free liquid, leading to reduced chemical reactivity and increased time for initial and final settings.

Table 3.2. Setting time results for alkali-activated fly ash mortars - Phase I

	Setting Time				
Property	Solution-to-Binder	5 M NaOH	7.5 M NaOH	10 M NaOH	12.5 M NaOH
Initial Setting (hour)	0.42	9.88	8.35	7.47	3.03
	0.46	12.50	9.37	9.22	7.68
	0.5	27.20	14.47	10.75	10.97
Final Setting (hour)	0.42	22.08	10.23	8.80	5.50
	0.46	23.23	12.33	12.17	10.97
	0.5	41.72	17.77	13.97	13.62

3.1.2.2. Effects of Activator Concentration on Setting Times

Depicted in Table 3.2 and as well as Figure 3.2 and 3.3, initial and final setting times decreased with increased activator concentration. When molarity increased from 5 to 7.5 M NaOH, initial setting time decreased approximately 16%, 25%, and 47% for 0.42, 0.46 and 0.50 solution-to-binder ratio, respectively; final setting time decreased nearly 54%, 47% and 57% for the same increases in solution-to-binder ratio. From 7.5 to 10 M NaOH, initial setting time decreased approximately 106%, 1.6% and 26% for 0.42, 0.46 and 0.50 solution-to-binder ratio, respectively, whereas final setting time decreased about 14%, 1.5% and 21% for the same increases in solution-to-binder ratio. With a 2.5 M NaOH increase in molarity to 12.5 M NaOH, initial setting time decreased approximately 59% and 17% for 0.42 and 0.46 solution-to-binder ratio, respectively, with minimal changes occurring for 0.50 solution-to-binder ratio while final setting time decreased 38%, 9.9% and 2.5% for the same increases in solution-to-binder ratio. On average, initial setting time decreased with every 2.5 M increase in sodium hydroxide by 60%, 15%, and 37% for 0.42, 0.46 and 0.50 solution-to-binder ratio, respectively, whereas final setting time decreased by 35%, 19% and 27%. Increased activator concentration allowed for more sodium hydroxide to react with fly ash, resulting in reduced workability and setting times. In a study by Lee and Lee (2013), similar setting time trends were reported.

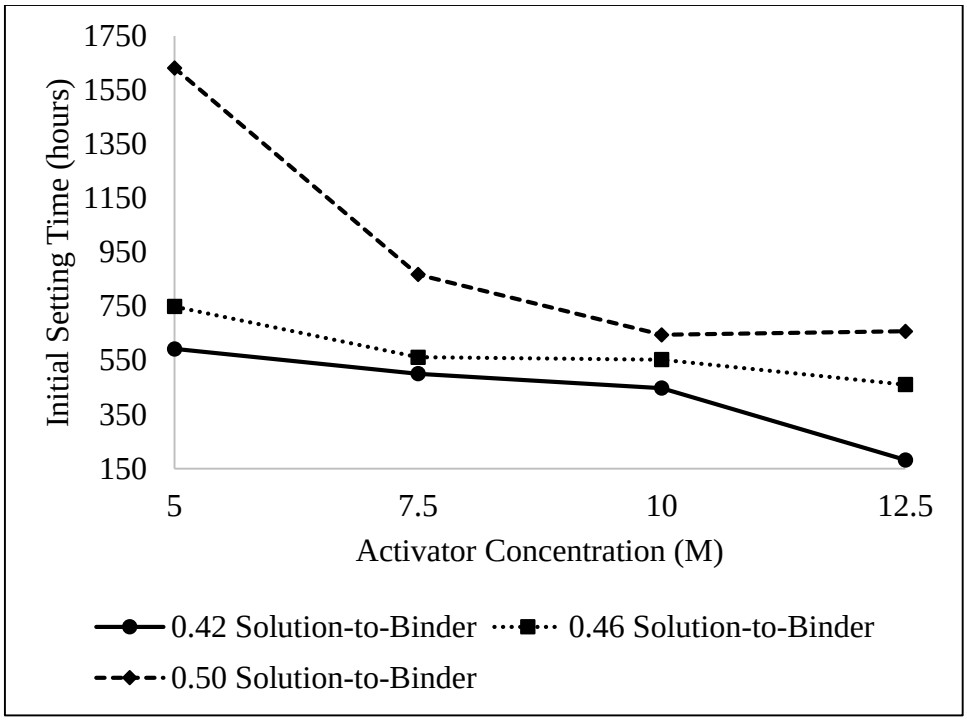

Figure 3.2. Initial Setting Time as functions of activator concentration for alkali-activated fly ash mortars - Phase I

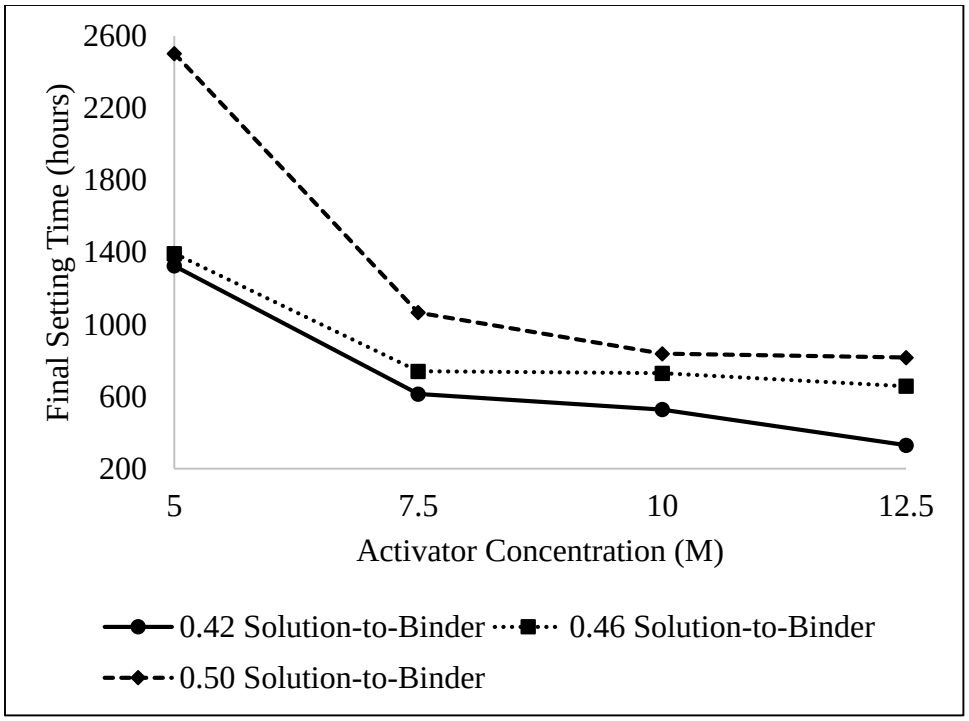

Figure 3.3. Final Setting Time as functions of activator concentration for alkali-activated fly ash mortars - Phase I

3.2.Mechanical Properties

3.2.1. Compressive Strength

Compressive strengths of the studied alkali-activated fly ash mortars, affected by curing age and condition, were shown in Table 3.3.

Table 3.3. Compressive strength (MPa) results for alkali-activated fly ash mortars - Phase I

Mixture Types		Air Curing			Moisture Exposed Curing			Sealed Curing		
Mix	NaOH Molarity (M)	1 Day	3 Day	7 Day	1 Day	3 Day	7 Day	1 Day	3 Day	7 Day
A-2.5	2.5	0.81	0.87	0.94	1.65	3.73	5.13	2.04	5.44	6.08
B-2.5	2.5	0.66	0.74	0.74	1.57	3.37	4.22	2.01	4.94	5.60
C-2.5	2.5	0.60	0.70	0.66	1.29	3.14	3.91	2.05	4.76	5.31
A-5	5	5.62	6.09	6.15	9.26	22.45	30.10	9.72	24.49	21.20
B-5	5	4.41	6.02	6.02	8.22	15.47	22.08	8.51	19.12	19.69
C-5	5	4.16	5.38	6.03	7.46	14.08	22.83	8.30	17.82	20.62
A-7.5	7.5	17.50	20.98	22.65	17.73	29.22	36.18	18.38	31.10	32.62
B-7.5	7.5	17.31	15.88	18.05	17.60	26.16	35.25	18.62	28.74	30.42
C-7.5	7.5	16.24	16.65	17.78	17.15	23.86	30.37	17.79	26.51	26.72
A-10	10	27.34	31.41	33.35	29.31	37.12	40.14	28.40	35.31	38.19
B-10	10	26.04	26.63	27.46	28.72	35.75	37.75	27.51	33.49	34.32
C-10	10	19.53	21.61	23.29	22.33	29.17	31.79	20.03	27.47	30.41
A-12.5	12.5	32.38	37.17	37.66	34.31	39.33	42.01	33.78	38.04	40.27
B-12.5	12.5	27.05	33.12	34.46	27.43	37.02	40.02	27.36	34.83	37.18
C-12.5	12.5	25.24	30.57	31.43	27.06	34.50	37.56	27.15	32.17	34.71

A=0.42 Solution-to-Binder Ratio, B=0.46 Solution-to-Binder Ratio, C=0.50 Solution-to-Binder Ratio

3.2.1.1. Effects of Curing Conditions on Compressive Strength

As stated in Chapter 2, three curing methods were utilized in this study; namely, air curing, moisture exposed curing, and sealed curing. For 2.5 M NaOH mixtures, regardless of age and solution-to-binder ratio, sealed curing produced the highest compressive strength, followed in descending order by moisture exposed and air curing conditions. Once curing condition changed from air curing to moisture exposed curing condition, 7-day compressive strength of mixtures containing 2.5 M NaOH increased by nearly 470%. Seven-day compressive strength for the mixtures containing 2.5 M NaOH increased by 29% when the curing condition changed from moisture exposed to sealed curing. Both 5 and 7.5 M NaOH showed sealed curing to produce the highest compressive strength, regardless of solution-to-binder ratio, up to three days; moisture exposed followed and lastly air curing had the lowest compressive strength. After seven days of curing, however, for 5 and 7.5 M NaOH, moisture exposed curing produced the highest compressive strength, followed by sealed and air curing. Between the two molarities up to three days of curing as well as between moisture exposed and sealed curing, the difference in compressive strength decreased with increased activator concentration. The difference in compressive strength between both curing conditions was approximately 16.2% 8.3% for 5 and 7.5 M NaOH, respectively, for all solution-to-binder ratios. Both 10 and 12.5 M NaOH showed compressive strength development to be greatest for moisture exposed curing, followed by sealed and air curing. On average, sealed-cured compressive strength was higher than that of air-cured samples by approximately 31% and 16% for the mixtures containing 10 and 12.5 M NaOH, respectively. Compressive strength increased about 18% for both 10 and 12.5 M NaOH when the curing condition changes from sealed to moisture exposed.

A possible explanation for the mentioned trend can be related to the amount of water used to make the needed alkaline solution. As depicted in Table 2.1, once concentration of the activator increased, the amount of water required to make the solution decreased. Consequently, there was less free water in the alkaline solution readily available to the mixture for those made with 7.5 M NaOH, serving as an explanation for the decreased difference between moisture exposed and sealed curing between 5 and 7.5 M NaOH. Ultimately, the mixture benefited from the moisture made available during curing, as seen when the activator concentration increased for both moisture exposed and sealed curing conditions.

Another explanation can be related to the past reported studies that have addressed carbonation issues that have occurred when lower humidity environments were used for curing (Criado et al., 2005; Criado et al., 2010; Criado et al., 2012; Kovalchuk et al., 2007). Mixtures cured at a lower relative humidity are at risk of forming alkaline bicarbonates. Alkaline bicarbonate hinders strength development, resulting in a lower degree of reactivity as well as a lower pH. Additionally, in the study by Criado et al. (2005), alkaline bicarbonates were more present with increased curing time. When relative humidity of at least 80% is present, the pores of the matrix of which are filled with water, have a better distribution of moisture, thus limiting the amount of carbon dioxide (CO_2) distribution in the matrix system. With that said, this can help provide an explanation for why moisture exposed curing samples out performed sealed curing samples over time. Over time, sealed curing consumed all of its water and allowed alkaline bicarbonates to form. This also served as an explanation for the minimal strength development in sealed curing samples from three to seven days. For air curing samples, minimal strength development occurred at all ages, irrespective of solution-to-binder ratio and activator

concentration. Due to the lack of moisture available to these samples, alkaline bicarbonates were allowed to form early on, which hindered the degree of reactivity of fly ash.

Table 3.4. pH values after 7 days of curing for alkali-activated fly ash mortars - Phase I (Approximate)

Mix	Solution-to-Binder	NaOH Molarity	Air Curing	Moisture Exposed Curing	Sealed Curing
A-2.5	0.42	2.5 M	9	11	9
B-2.5	0.46	2.5 M	9	11	9
C-2.5	0.50	2.5 M	9	11	9
A-5	0.42	5 M	9	11	9
B-5	0.46	5 M	9	10	9
C-5	0.50	5 M	10	11	9
A-7.5	0.42	7.5 M	9	11	10
B-7.5	0.46	7.5 M	10	12	12
C-7.5	0.50	7.5 M	10	11	10
A-10	0.42	10 M	10	12	10
B-10	0.46	10 M	10	12	11
C-10	0.50	10 M	10	12	11
A-12.5	0.42	12.5 M	13	13	12
B-12.5	0.46	12.5 M	10	12	11
C-12.5	0.50	12.5 M	13	13	12

A=0.42 Solution-to-Binder Ratio, B=0.46 Solution-to-Binder Ratio, C=0.50 Solution-to-Binder Ratio

In addition to strength, the pH was also measured at each age for all samples, as shown in Table 3.4. Regardless of activator concentration and solution-to-binder ratio, moisture exposed curing had the highest pH over time, followed by sealed and air curing. As stated, the presence of alkaline bicarbonates lowered the pH of the system. This theory was confirmed with the pH findings in this study as it also solidified the assumption for the presence of alkaline bicarbonates in the studied sealed and air curing mixtures.

3.2.1.2. Effects of Solution-to-Binder Ratio on Compressive Strength

As seen in Table 3.3, regardless of curing condition and activator concentration, compressive strength of the studied mortars decreased with increased solution-to-binder ratio. For 7-day air curing, an increase of solution-to-binder ratio from 0.42 to 0.46 decreased compressive strength by nearly 26%, 2%, 26%, 22%, and 9% for the mixtures made with 2.5, 5, 7.5, 10, and 12.5 M NaOH, respectively. Upon further increase from 0.46 to 0.50 solution-to-binder ratio, compressive strength decreased 12%, 0.2%, 1.5%, 18%, and 10% for the mixtures containing 2.5, 5, 7.5, 10, and 12.5 M NaOH, respectively. For 7-day moisture exposed curing, when solution-to-binder ratio increased from 0.42 to 0.46, compressive strength decreased 22%, 36%, 3%, 6%, and 5% for the cylinders having 2.5, 5, 7.5, 10, and 12.5 M NaOH, respectively. Upon further 0.04 increase in solution-to-binder ratio to 0.50, compressive strength decreased by 8%, 16%, 19%, and 7% for the same mixtures. 5 M NaOH had minimal change in compressive strength when solution-to-binder ratio of the studied mortars increased from 0.46 to 0.50. For every 0.04 increase in solution-to-binder ratio, the 7-day compressive strength decreased by nearly 9%. Similar to the discussion given previously for workability and setting times in sections 3.1.1.1 and 3.1.2.1, respectively, increased solution-to-binder ratio allowed for increased amount of alkaline solution as well as decreased amount of fly ash available to react with the alkaline solution due to maintaining the same mortar volume for all mixtures.

Another explanation for this trend may be related to the porosity of the system. With an increased amount of alkaline solution, porosity increases as well. Increased porosity can lead to decreased compressive strength due to more voids being present with increased porosity. While porosity of the trial mortars was not evaluated in this study, the results of absorption results obtained for the studied alkali-activated fly ash mortars, discussed in section 3.3.1.1, can serve to

explain the decreased compressive strength with an increase in solution-to-binder ratio of the studied mortars.

3.2.1.3. Effects of Activator Concentration on Compressive Strength

Referring to Table 3.3, regardless of curing condition and solution-to-binder ratio, compressive strength increased with increased activator concentration. For 7-day air curing, between 2.5 and 5 M NaOH, compressive strength increased 556%, 708% and 807% when solution-to-binder ratios of 0.42, 0.46, and 0.50, respectively, were used. Upon further increase from 5 to 7.5 M NaOH, compressive strength increase by 268%, 200% and 195% for the mixtures made with 0.42, 0.46 and 0.50 solution-to-binder ratios, respectively. When sodium hydroxide concentration increased from 7.5 to 10 M NaOH, compressive strength increased 47%, 52% and 31% for the same groups of solution-to-binder ratios. Further increase from 10 to 12.5 M NaOH allowed for compressive strength to increase by 13%, 26% and 35% for the mortars containing 0.42, 0.46 and 0.50 solution-to-binder ratios, respectively. For 7-day moisture exposed curing, compressive strength increased by 487%, 424% and 483% for the mortars made with 0.42, 0.46 and 0.50 solution-to-binder ratios, respectively, when sodium hydroxide increased from 2.5 to 5 M NaOH. Upon further increase from 5 to 7.5 M NaOH, compressive strength increased 20%, 60% and 33% for the same groups of solution-to-binder ratios. When sodium hydroxide concentration increased from 7.5 to 10 M NaOH, compressive strength increased 11%, 7% and 5% for 0.42, 0.46 and 0.50 solution-to-binder ratios, respectively. When increased further from 10 to 12.5 M NaOH, compressive strength increased 5%, 6% and 18% for the mortars containing 0.42, 0.46 and 0.50 solution-to-binder ratios, respectively. For 7-day sealed curing, compressive strength increased approximately 263% when sodium hydroxide concentration increased from 2.5 to 5 M. Upon further increase from 5 to 7.5 M NaOH,

compressive strength increased about 46%, regardless of solution-to-binder ratio. When increased from 7.5 to 10 M NaOH, compressive strength increased approximately 15% for all studied solution-to-binder ratios. Further increase of sodium hydroxide concentration from 10 to 12.5 M NaOH allowed for compressive strength to increase by 9%. Past studies (Arioz et al., 2012; Katz, 2012; Ravikumar et al., 2010; Ryu et al., 2013) have tested different activator concentrations and found similar results. In the study by Arioz et al. (2012), degree of reaction also increased with increased activator concentration; Katz (2012) also came to the same conclusion. With that said, a direct correlation can be made between the activator concentration and the degree of reaction. With increased activator concentration, more sodium hydroxide was made readily available for a given solution-to-binder ratio. Higher availability of sodium hydroxide allowed for steady formation of activated fly ash and N-A-S-H gel (geopolymer gel), resulting in continued strength gain of the studied mortars. The reduction in setting times with increased activator concentration, as discussed in section 3.1.2.2., also corroborates this explanation.

For the studied compressive strength properties, the standard deviations of the tested samples varied from 0.004 MPa to 3.6 MPa and coefficient of variations from 0.2% to 56.4%.

3.2.2. Flexural Strength

3.2.2.1. Effects of Solution-to-Binder Ratio on Flexural Strength

In reference to Figure 3.4, regardless of activator concentration, flexural strength decreased with increased solution-to-binder ratio. However, the gap amongst the flexural strength of the studied alkali-activated fly ash mortars became smaller with every 2.5 M increase in sodium hydroxide concentration. When the solution-to-binder ratio increased from 0.42 to 0.46, flexural strength decreased 12%, 10%, 9.3%, and 5.4% for the mixtures made with 5, 7.5,

10, and 12.5 M NaOH, respectively. With a further 0.04 increase in solution-to-binder ratio to 0.50, flexural strength decreased 50%, 40%, 32%, and 4.8% for 5, 7.5, 10, and 12.5 M NaOH, respectively. On average, flexural strength decreased approximately 31%, 25%, 21%, and 5.1% for 5, 7.5, 10, and 12.5 M NaOH, respectively, with every 0.04 increase in solution-to-binder ratio. Similar to the results obtained for compressive strength, with a higher solution-to-binder ratio, while more activator solution was present, less fly ash was readily available for reaction due to the constant mortar volume that was maintained for all mixtures; excess amount of water in the mixture hindered flexural strength development of the studied alkali-activated mortars.

3.2.2.2. Effects of Activator Concentration on Flexural Strength

As shown in Figure 3.5, regardless of solution-to-binder ratios, flexural strength of the studied mortars increases with increases in activator concentration. Between 5 to 7.5 M NaOH, flexural strength increased approximately 21%, 23% and 32% for 0.42, 0.46 and 0.50 solution-to-binder ratio, respectively. As the molarity of sodium hydroxide increased from 7.5 to 10 M, flexural strength increased 54%, 55% and 65% when 0.42, 0.46 and 0.50 solution-to-binder ratios, respectively, were used. With an increase in activator concentration from 10 to 12.5 M, flexural strength increased 1.8%, 5.5%, and 33% for the same groups of solution-to-binder ratios. On average, with every 2.5 M increase in sodium hydroxide concentration, flexural strength increased 26%, 28%, and 43% for the mortars containing 0.42, 0.46 and 0.50 solution-to-binder ratio, respectively. As discussed first in Section 3.2.1.3., increased activator concentration allowed for more sodium hydroxide to become available to react with fly ash to form the main reaction product, N-A-S-H gel, thus allowing for increased flexural strength results.

The standard deviations for the evaluated flexural strength properties ranged from 0.3 MPa to 1.5 MPa and coefficient of variations ranged from 4.4% and 23.3%.

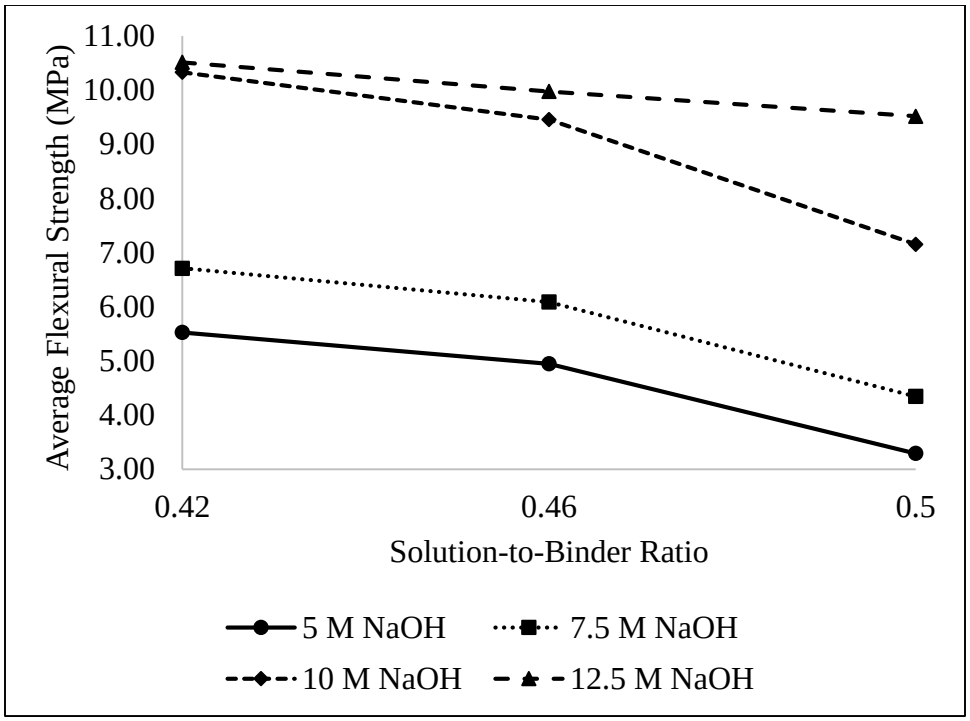

Figure 3.4. Flexural strength as functions of solution-to-binder ratio for alkali-activated fly ash mortars - Phase I

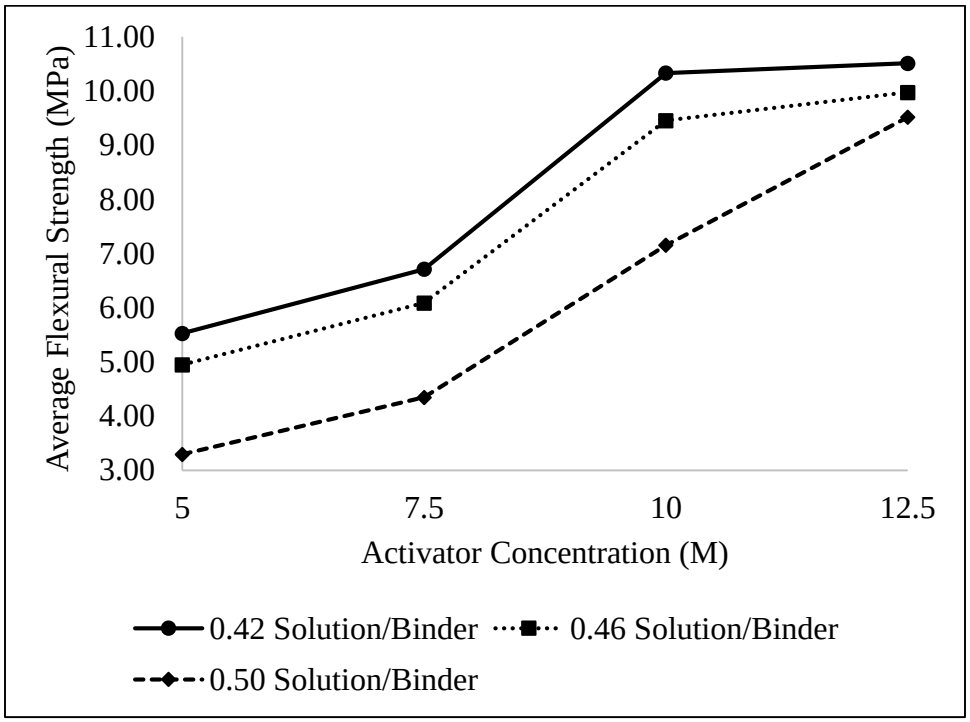

Figure 3.5. Flexural strength as functions of activator concentration for alkali-activated fly ash mortars - Phase I

3.2.3. Modulus of Elasticity

3.2.3.1. Effects of Solution-to-Binder Ratio on Modulus of Elasticity

Irrespective of the amount of activator concentration, modulus of elasticity decreased with increased solution-to-binder ratio. The results are shown in Figure 3.6. Once the solution-to-binder ratio increased from 0.42 and 0.46, modulus of elasticity decreased about 19%, 25%, 23%, and 9% for the mortars containing 5, 7.5, 10, and 12.5 M NaOH, respectively. As the solution-to-binder ratio increased from 0.46 to 0.50, modulus of elasticity decreased approximately 26%, 14%, 16%, and 6.5% for the mixtures made with 5, 7.5, 10, and 12.5 M NaOH, respectively. Overall, with every 0.04 increase in solution-to-binder ratio, modulus of

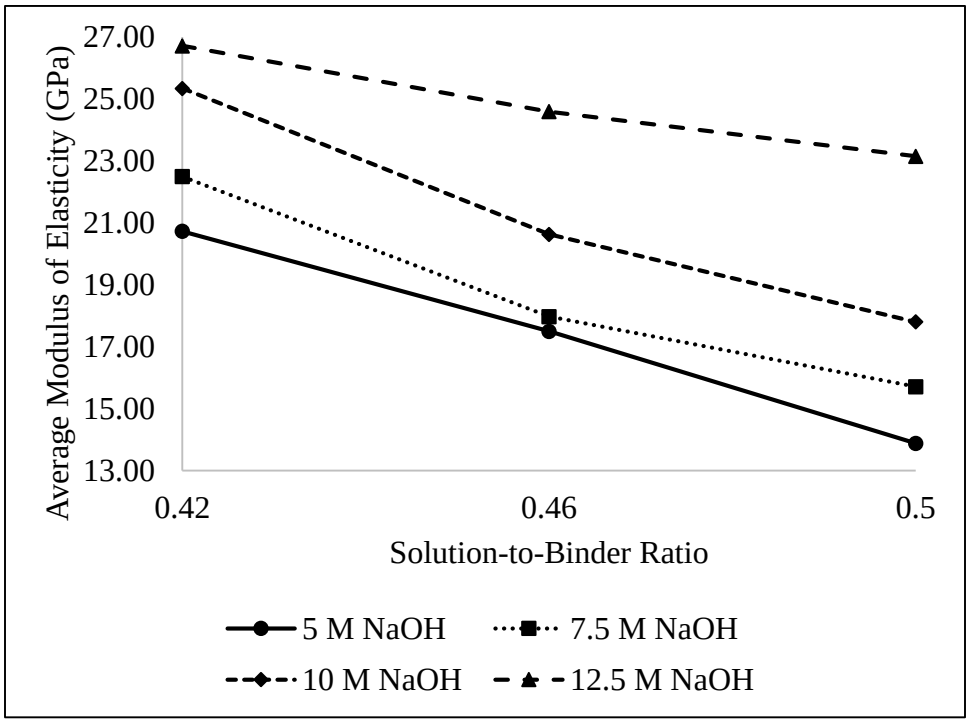

Figure 3.6. Modulus of Elasticity as functions of solution-to-binder ratio of alkali-activated fly ash mortars - Phase I

elasticity decreased averagely by 23%, 20%, 20%, and 8% when 5, 7.5, 10, and 12.5 M NaOH, respectively, were used. An increase in solution-to-binder ratio allowed for more free liquid in the mixture, adversely affecting both strength as well as modulus of elasticity.

3.2.3.2. Effects of Activator Concentration on Modulus of Elasticity

As shown in Figure 3.7, irrespective of the utilized solution-to-binder ratio, modulus of elasticity of the studied alkali-activated mortars increased with increased activator concentration. With an increased in sodium hydroxide concentration from 5 to 7.5 M NaOH, modulus of elasticity increased approximately 8.5%, 2.7% and 13% for 0.42, 0.46, and 0.50 solution-to-binder ratios, respectively. When molarity of sodium hydroxide increased 2.5 to 10 M NaOH, modulus of elasticity increased approximately 14%. Upon another 2.5 increase in molarity from

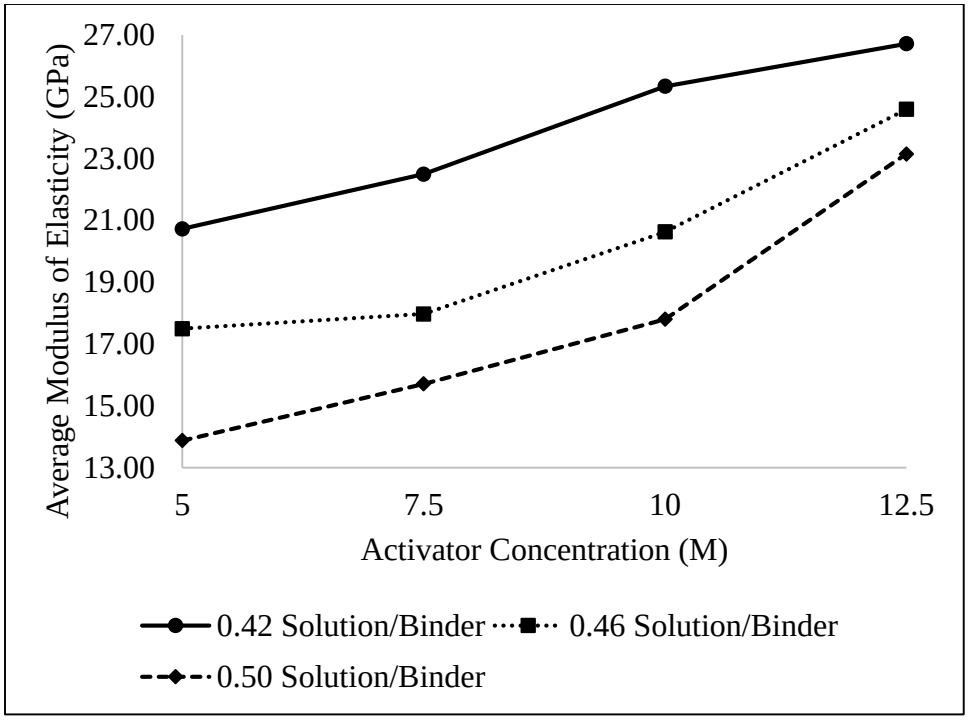

Figure 3.7. Modulus of Elasticity as functions of activator concentration for alkali-activated fly ash mortars - Phase I

10 to 12.5 M NaOH, modulus of elasticity increased about 5.4%, 19% and 30% for 0.42, 0.46 and 0.50 solution-to-binder ratio, respectively. As was the case for the both compressive and flexural strength results discussed in section 3.2.1.3 and 3.2.2.2., higher activator concentration allowed for more fly ash to react. The increased chemical reactivity led to higher strength as well as increased modulus of elasticity.

For the modulus of elasticity results obtained, the standard deviations ranged from 0.09 MPa to 2.3 MPa and coefficient of variations of 0.6% and 9.7%.

3.2.4. Mechanical Property Comparisons

Table 3.5 below shows the comparisons between flexural and compressive strength, as well as modulus of elasticity and compressive strength. Seven-day sealed compressive strength results were used for comparisons in order to be consistent with both flexural and modulus of elasticity results. The discussions of both comparisons related to the effects of solution-to-binder ratio and activator concentration are to follow.

3.2.4.1. Flexural vs. Compressive Strength

As shown in Table 3.5, the ratios between the flexural and compressive strength of the tested alkali-activated mortars were calculated. For up to 10 M NaOH, the ratio decreased with increased solution-to-binder ratio while it remained fairly uniform for 12.5 M NaOH. Minimal increase in the flexural-to-compressive ratio was seen with respect to activator concentration. On average, the flexural-to-compressive ratio was remained approximately at .0.24.

Table 3.5: Mechanical Property Comparisons – Phase I

Mix	7-Day Compressive Strength (MPa)	7-Day Flexural Strength (MPa)	7-Day Modulus of Elasticity (MPa)	Flexural/ Compressive Ratio	Modulus of Elasticity/ Compressive Ratio
A-5	21.20	5.53	20727.36	0.26	977.88
B-5	19.69	4.95	17495.45	0.25	888.40
C-5	20.62	3.30	13875.70	0.16	672.88
A-7.5	32.62	6.71	22494.15	0.21	689.50
B-7.5	30.42	6.09	17969.46	0.20	590.72
C-7.5	26.72	4.35	15707.12	0.16	587.94
A-10	38.19	10.33	25338.23	0.27	663.42
B-10	34.32	9.46	20626.82	0.28	600.96
C-10	30.41	7.16	17797.09	0.24	585.27
A-12.5	40.27	10.52	26717.18	0.26	663.53
B-12.5	37.18	9.98	24593.35	0.27	661.45
C-12.5	34.71	9.52	23146.99	0.27	666.95

A=0.42 Solution-to-Binder Ratio, B=0.46 Solution-to-Binder Ratio, C=0.50 Solution-to-Binder Ratio

3.2.4.2. Modulus of Elasticity vs. Compressive Strength

As depicted in Table 3.5, the modulus of elasticity-to-compressive strength ratio decreased with increased solution-to-binder ratio for up to 10 M NaOH, whereas it displayed minimal changes when 12.5 M NaOH was used. In general, modulus of elasticity-to-compressive strength ratio changed more rapidly for the mixtures containing a lower concentration of sodium hydroxide. When increased from 0.42 to 0.46 solution-to-binder ratio, modulus of elasticity-to-compressive strength ratio decreased 9%, 14%, 9%, and 0.3% for the mortars made with 5, 7.5, 10, and 12.5 M NaOH, respectively. Upon further increase from 0.46 to 0.50 solution-to-binder ratio, modulus of elasticity-to-compressive strength ratio decreased 24%, 0.5% and 3% for 5, 7.5 and 10 M NaOH, respectively, whereas 12.5 M NaOH had an increase of less than 1%. On average, modulus of elasticity-to-compressive strength ratio decreased 17%, 7% and 6% for 5,

7.5 and 10 M NaOH, respectively, whereas only negligible increase of approximately 0.25% was seen for the mortars made with 12.5 M NaOH.

Modulus of elasticity-to-compressive strength ratio decreased with increased activator concentration, however, the difference was much higher for the mixtures containing lower activator concentration. When sodium hydroxide increased from 5 to 7.5 M NaOH, modulus of elasticity-to-compressive strength ratio decreased 29%, 34%, and 13% for 0.42, 0.46 and 0.50 solution-to-binder ratios, respectively. Upon further increase from 7.5 to 10 M NaOH, modulus of elasticity-to-compressive strength ratio decreased 4% for 0.42 solution-to-binder ratio while on average less than 1% difference was seen for the mortars made with 0.46 and 0.50 solution-to-binder ratios. Overall, modulus of elasticity-to-compressive strength ratio decreased 11% and 7% for 0.42 and 0.46 solution-to-binder ratio, respectively, and remained fairly unchanged for the mortars made with 0.50 solution-to-binder ratio.

3.3.Transport Properties

3.3.1. Absorption

3.3.1.1. Effects of Solution-to-Binder Ratio on Absorption

Absorption results are presented in Figure 3.8. Absorption was found to increase with increased solution-to-binder ratio for all activator concentrations used in this study. When solution-to-binder ratio increased from 0.42 to 0.46, minimal increase in absorption occurred for all activator concentrations. Upon further increase from 0.46 to 0.50 solution-to-binder ratio, absorption increased approximately 8.3%, 12%, 21%, and 20% for the mortars made with 5, 7.5, 10, and 12.5 M NaOH, respectively. Overall, from 0.42 to 0.50 solution-to-binder ratio, absorption increased approximately 17% irrespective of sodium hydroxide concentration. Although no other studies have investigated absorption as functions of solution-to-binder ratio

for alkali-activated fly ash, previous studies investigating the porosity as functions of solution-to-binder ratio can be used to discuss the results obtained in this study. Ravikumar et al. (2010) discussed the relationship between porosity and solution-to-binder ratio for which porosity increased with increased solution-to-binder ratio, resulting in accelerated rate of fluid penetration into the matrix, as evident by the increased absorption results of the studied alkali-activated fly ash mortars.

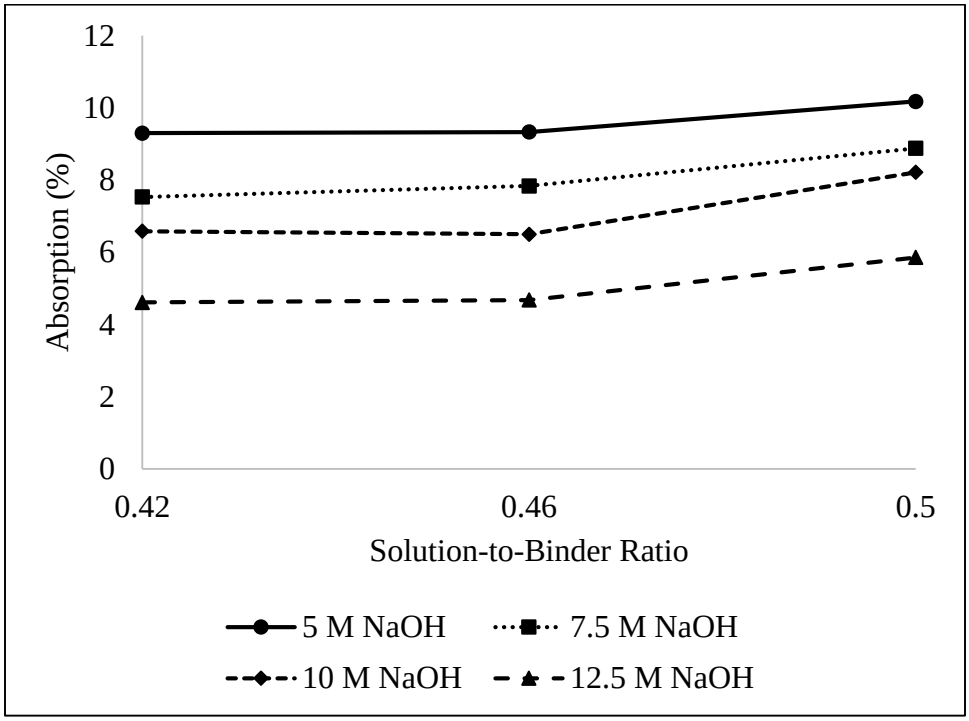

Figure 3.8. Absorption results as functions of solution-to-binder ratio for alkali-activated fly ash mortars - Phase I

3.3.1.2. Effects of Activator Concentration on Absorption

Absorption decreased with increased activator concentration, as shown in both Figure 3.8 and 3.9. When sodium hydroxide molarity of the studied mortars increased from 5 to 7.5 M NaOH, absorption decreased approximately 16%. An increase in NaOH from 7.5 to 10 M decreased absorption by nearly 35%, 17% and 7.5% for when solution-to-binder ratios of 0.42,

0.46 and 0.50, respectively, were used. Upon further increase in sodium hydroxide concentration from 10 to 12.5 M NaOH, absorption, on average, decreased 29% for all the studied solution-to-binder ratios. This finding can be attributed to the increased amount of reaction production formed with increased activator concentration which allowed for decreased void content and absorption of the studied alkali-activated fly ash mortars.

For the absorption results obtained for the tested alkali-activated mortars, standard deviation values varied between 0.005% and 0.4% and coefficient of variations of 0.06% and 6.1%.

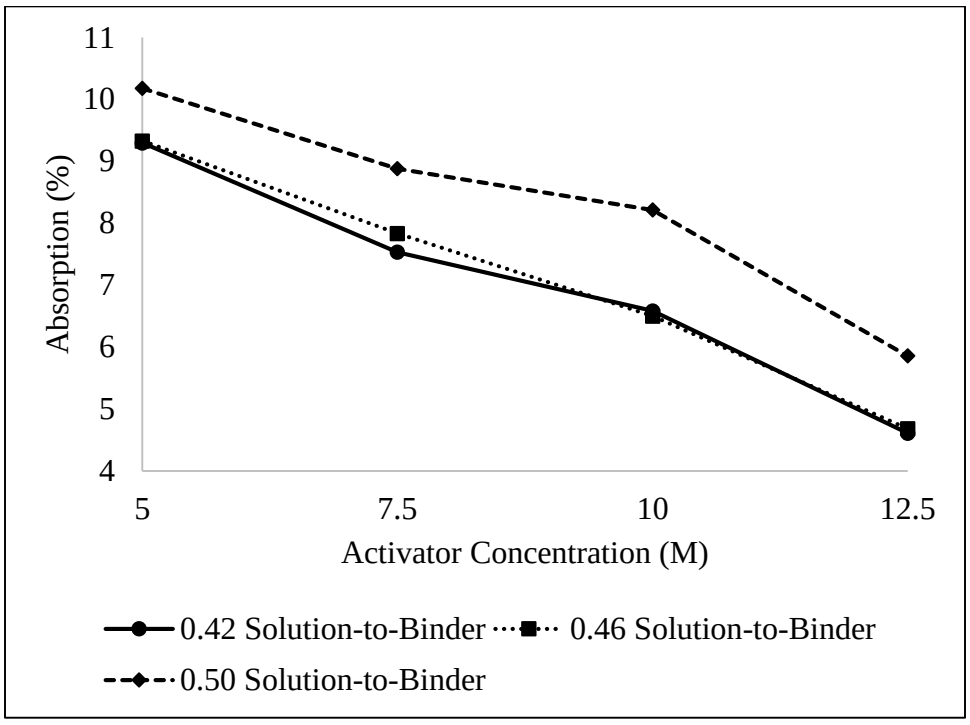

Figure 3.9. Absorption results as functions of activator concentration for alkali-activated fly ash mortars - Phase I

3.3.2. Density

3.3.2.1. Effects of Solution-to-Binder Ratio on Density

Although minimal, density decreased with increased solution-to-binder ratio, as seen in Figure 3.10. Between 0.42 and 0.50 solution-to-binder ratio, density decreased by an average of 3% for all activator concentrations. Increased porosity, which also allowed for higher absorption, resulted in the formation of a less dense matrix.

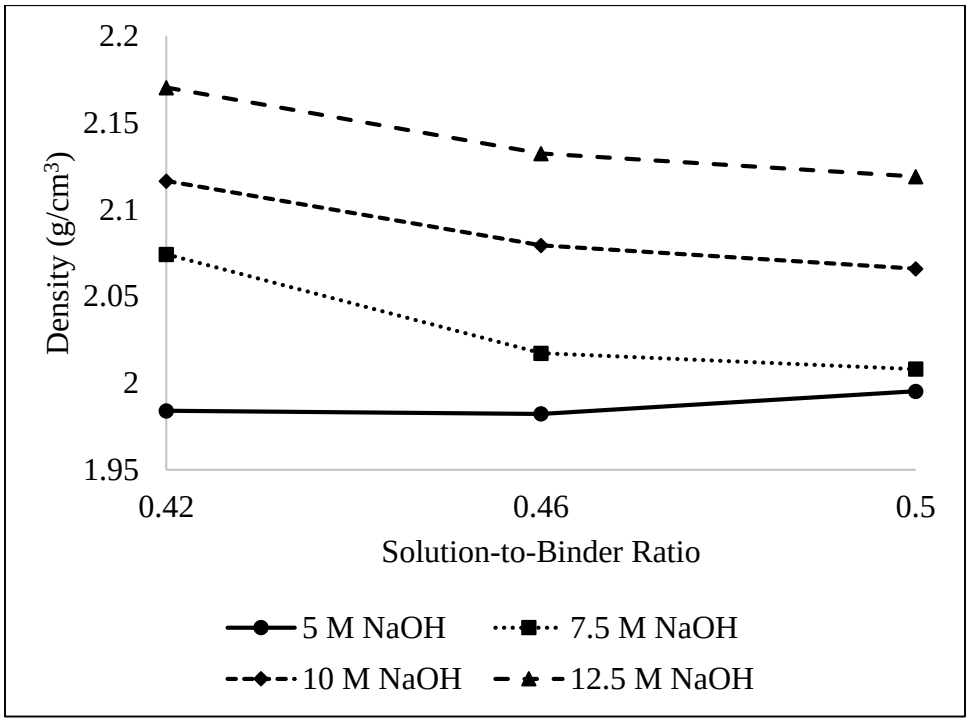

Figure 3.10. Density as functions of solution-to-binder ratio for alkali-activated fly ash mortars - Phase I

3.3.2.2. Effects of Activator Concentration on Density

Density as functions of activator concentration is shown in Figure 3.11. Density increased marginally with increased activator concentration for all solution-to-binder ratios. On average, an increase of NaOH from 7.5 to 10 M resulted in an increase of density by about 2.7%. Upon further increase in sodium hydroxide concentration from 10 to 12.5 M NaOH, density increased

averagely by 2.5%. Increased reaction product due to increases in activator concentration produced fewer voids which allowed for a denser mortar structure.

Standard deviation values ranged between 0.004 g/cm^3 and 0.02 g/cm^3 and coefficient of variations between 0.2% and 1.1% for the obtained density results of the evaluated alkali-activated fly ash mortars.

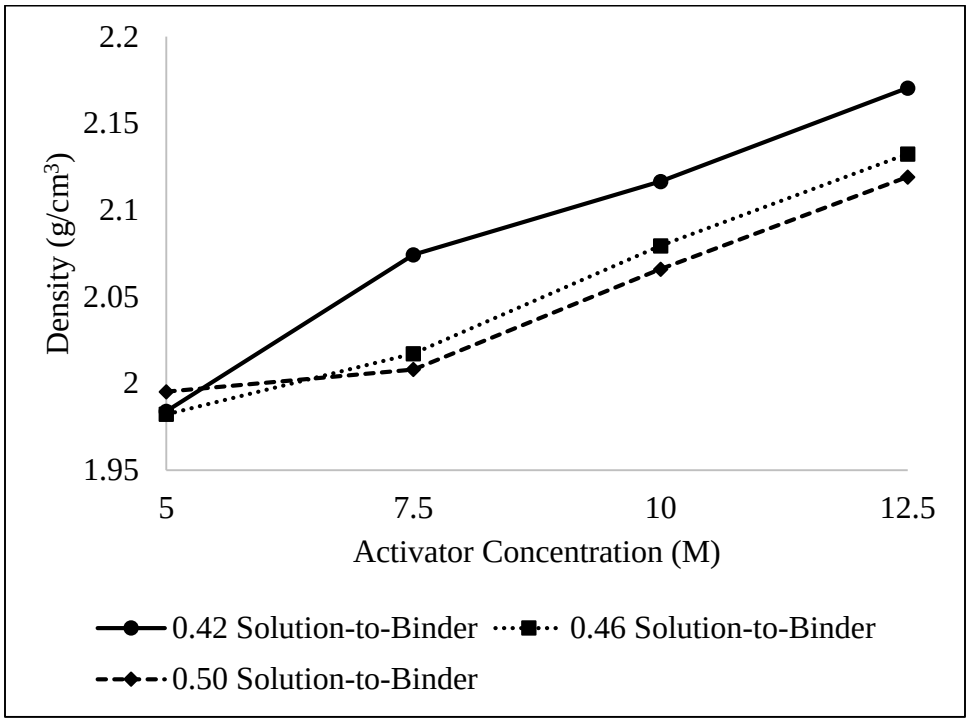

Figure 3.11. Density as functions of activator concentration for alkali-activated fly ash mortars - Phase I

3.3.3. Rapid Chloride Migration

3.3.3.1. Effects of Solution-to-Binder Ratio on Chloride Migration

The results of rapid chloride migration of the studied mortars as functions of solution-to-binder ratio are shown in Figure 3.12. Chloride depth increased with increased in solution-to-binder ratio for all activator concentrations used in this study. Overall, chloride depth increased nearly 12%. Similar to the absorption results, discussed in Section 3.3.1.1., increases in solution-

to-binder ratio allowed for higher porosity and penetration of chloride ions into the studied mortars.

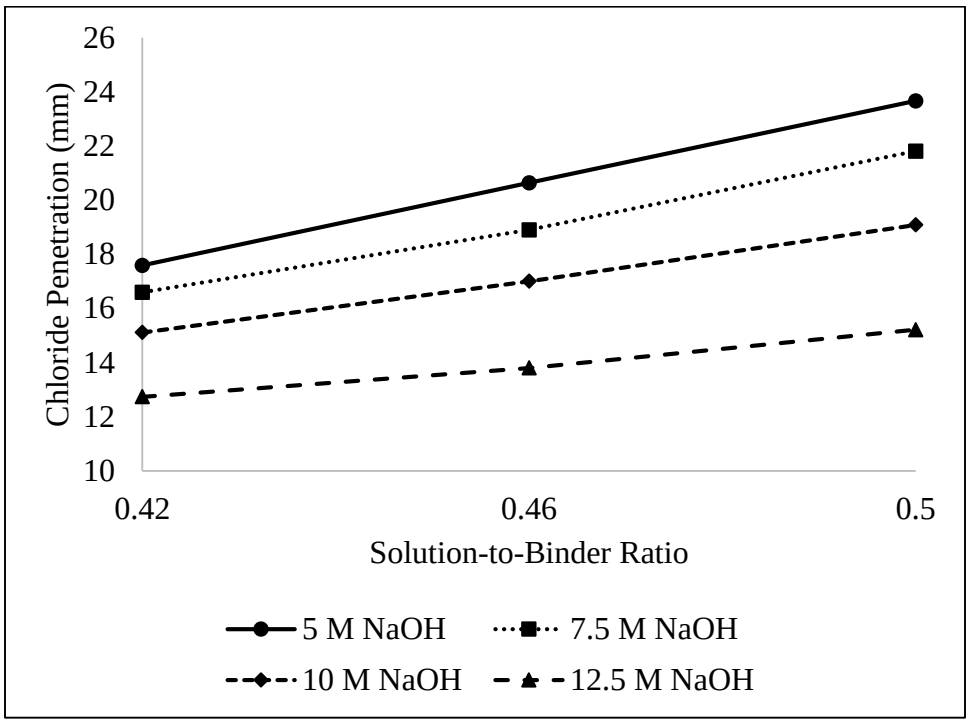

Figure 3.12. Chloride migration as functions of solution-to-binder ratio for alkali-activated fly ash mortars - Phase I

3.3.3.2. Effects of Activator Concentration on Chloride Migration

Figure 3.13 displays the chloride depth results as a function of activator concentration. Irrespective of solution-to-binder ratio, chloride depth decreased with increased activator concentration. When sodium hydroxide concentration increased from 5 and 7.5 M NaOH, chloride penetration depth decreased by an average of 7.3%. Upon further sodium hydroxide concentration to10 M NaOH, chloride depth decreased by about 10.7%. As molarity of sodium hydroxide concentration increased from 10 and 12.5 M NaOH, chloride penetration depth decreased by an average of approximately 18.3%. Increased activator concentration allowed for

increased degree of reactivity, resulting in lower porosity and decreased penetration of chloride ions into the mortar sample.

For the rapid chloride migration results obtained for the tested alkali-activated mortars, standard deviation values differed from 0.7 mm and 1.2 mm and coefficient of variations from 0.04% and 0.07%.

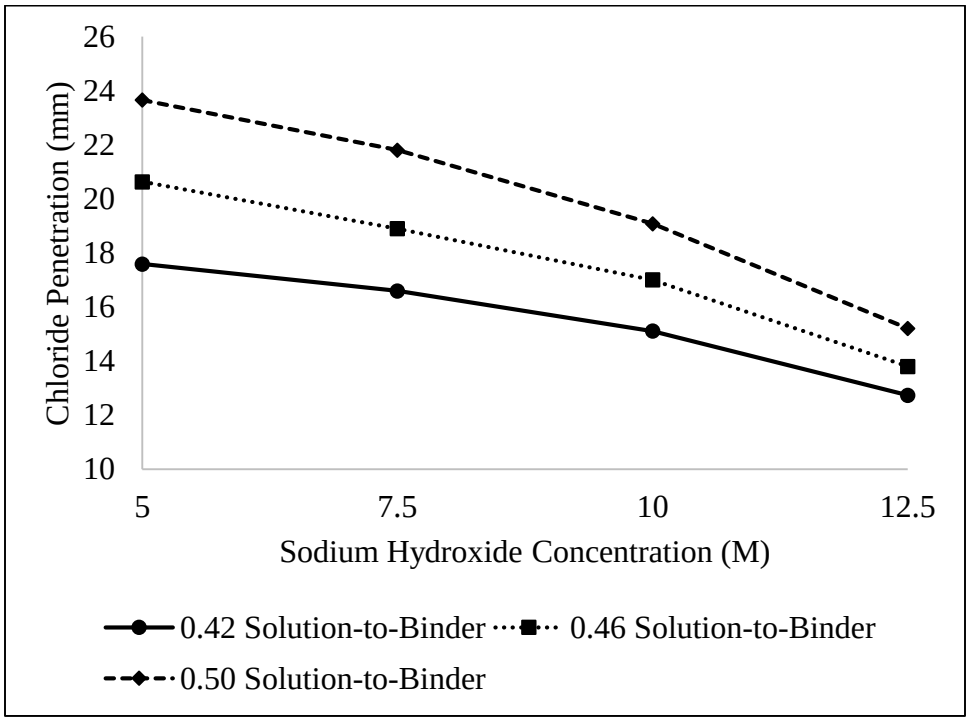

Figure 3.13. Chloride migration in as functions of activator concentration for alkali-activated fly ash mortars - Phase I

3.4.Conclusions

This chapter studied the fresh, mechanical and transport properties of alkali-activated fly ash mortars when sodium hydroxide was used as the sole activator. The influence of curing condition and age, activator concentration, and solution-to-binder ratio on these properties were examined. Based on the results of this study, the following conclusions can be drawn.

1. Both workability and setting times increased with increased solution-to-binder ratio. The opposite trend was obtained with increased activator concentration.
2. The most efficient curing condition to produce optimum mechanical properties of the studied alkali-activated fly ash mortars was found to be dependent on the activator concentration. For samples containing 2.5 M NaOH, regardless of curing age, the best curing condition was found to be sealed curing, followed by moisture exposed and air curing. For 5 and 7.5 M NaOH samples, the best curing condition was sealed curing followed by moisture exposed and air curing up to 3 days of curing. Afterward, moisture exposed curing produced the highest compressive strength, followed by sealed and air curing. For 10 and 12.5 M NaOH samples, moisture exposed curing had the highest compressive strength for all ages, followed by sealed and air curing. Compressive strength of the studied mortars decreased and increased with increased solution-to-binder ratio and activator concentration, respectively. Similar results were found for both flexural strength and modulus of elasticity of the studied alkali-activated fly ash mortars.
3. Chloride penetration depth increased and decreased with increased solution-to-binder ratio and activator concentration, respectively. Similar results were found for absorption. Density decreased and increased with increased solution-to-binder ratio and activator concentration, respectively.

CHAPTER 4

PHASE II-PART I: EFFECTS OF ACTIVATOR CONCENTRATION AND SODIUM SILICATE-TO-TOTAL SOLUTION RATIO ON ALKALI-ACTIVATED FLY ASH MORTARS

Phase II of this thesis focused on the influence of the combined sodium silicate and sodium hydroxide solutions on fresh, mechanical, transport, and durability properties of alkali-activated fly ash mortars. Similar to the phase I, workability was the fresh property tested. Mechanical properties included compressive and flexural strength, as well as modulus of elasticity. Rapid chloride migration, absorption, density, and void content were the transport properties tested. Durability properties included resistance to sulfate attack in terms of loss in compressive strength and length change, resistance to sulfuric acid attack in terms of loss in mass loss and compressive strength, freeze-thaw resistance in terms of mass loss, and abrasion resistance in terms of depth of wear.

4.1. Fresh Properties

4.1.1. Workability

Table 4.1. Workability results for alkali-activated fly ash mortars - Phase II-Part I

	Workability (cm)			
Sodium Silicate-to-Total Solution	5 M NaOH	7.5 M NaOH	10 M NaOH	12.5 M NaOH
0.20	15.24	11.27	8.89	6.35
0.40	12.54	8.89	6.56	3.81
0.60	8.73	6.99	5.08	---

--- = Not Available

4.1.1.1. Effects of Activator Concentration on Workability

In reference to Table 4.1 and Figure 4.1, irrespective of sodium silicate-to-total solution ratio, workability decreased with increased sodium hydroxide concentration. When increased from 5 to 7.5 M NaOH, workability decreased approximately 25% regardless of sodium silicate-to-total solution ratio. When sodium hydroxide molarity increased from 7.5 to 10 M NaOH, workability also decreased by an average of nearly 25%. Upon further sodium hydroxide concentration increase to 12.5 M NaOH, workability decreased by nearly 35% for both 0.20 and 0.40 sodium silicate-to-total solution ratio. The results obtained mirrored those found in phase I of this study (see Chapter 3 and section 3.1.1.2). Increased sodium hydroxide concentration allowed for increased degree of reactivity and reduction in workability of alkali-activated mortars. In addition, an increase in sodium hydroxide concentration lowered the initial water content used in the matrix. This could also contributed to the decreased workability when sodium hydroxide concentration increased of the tested alkali-activated mortars.

4.1.1.2. Effects of Sodium Silicate-to-Total Solution Ratio on Workability

As shown in Table 4.1 and Figure 4.2, workability decreased with increased sodium silicate-to-total solution ratio. When sodium silicate-to-total solution ratio increased from 0.20 to 0.40, workability decreased approximately 18%, 21%, 26%, and 40% for 5, 7.5, 10, and 12.5 M NaOH, respectively. Upon further increase from 0.40 to 0.60 sodium silicate-to-total solution ratio, workability decreased 30%, 21% and 23% for 5, 7.5 and 10 M NaOH, respectively. Panias et al. (2007) concluded that increased sodium silicate, leading to increased SiO_2/Na_2O ratio, can limit mixture workability. Similarly in this study, workability expressed in slump flow reduced significantly at high SiO_2/Na_2O ratios and casting became extremely difficult due to lower water content present in the sodium hydroxide solution.

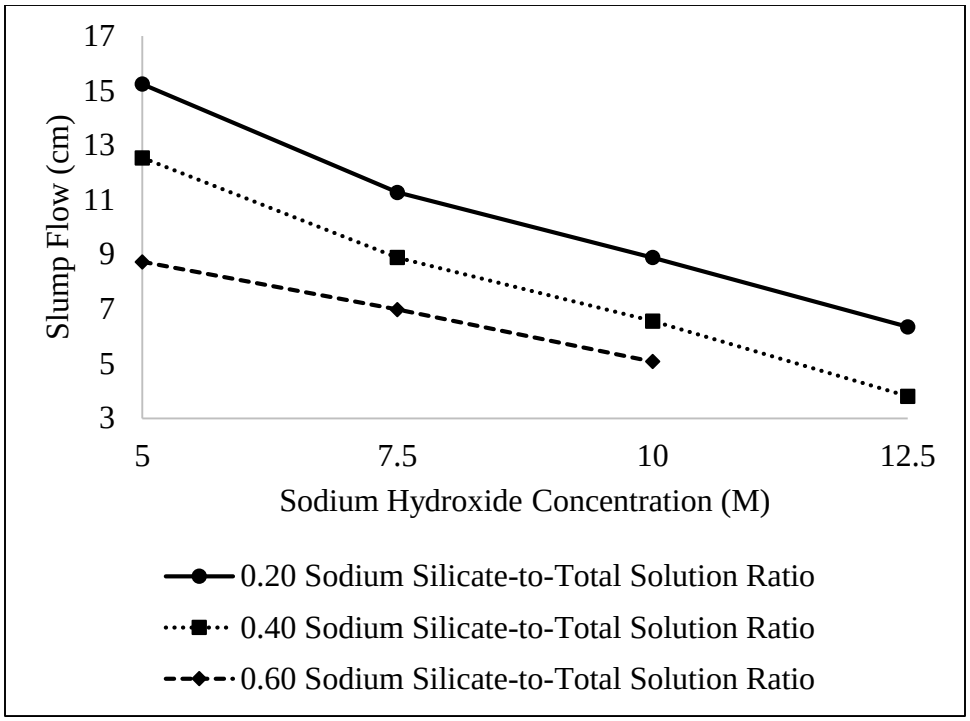

Figure 4.1. Workability as functions of sodium hydroxide concentration for alkali-activated fly ash mortars - Phase II-Part I

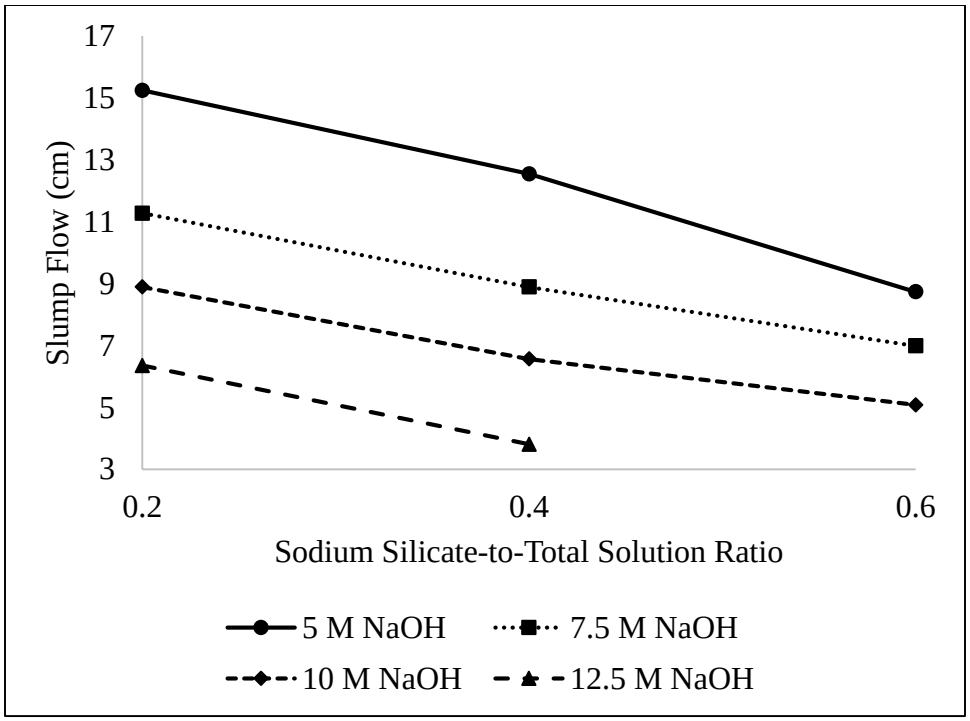

Figure 4.2. Workability as functions of sodium silicate-to-total solution ratio for alkali-activated fly ash mortars - Phase II-Part I

4.2. Mechanical Properties

4.2.1. Compressive Strength

Compressive strength results obtained for alkali-activated fly ash mortars are shown in Table 4.2.

4.2.1.1. Effects of Activator Concentration on Compressive Strength

In reference to Table 4.2 and Figure 4.3, compressive strength increased with increased sodium hydroxide concentration for all studied sodium silicate-to-total solution ratios, with the exception of the mixture containing 0.60 sodium silicate-to-total solution ratio. When sodium hydroxide increased from 5 to 7.5 M NaOH, 7-day compressive strength increased 242%, 27% and 30% for the mortars containing 0.20, 0.40, and 0.60 sodium silicate-to-total solution ratio, respectively. Upon further 2.5 M NaOH increase from 7.5 to 10 M NaOH, 7-day compressive strength increased 77% and 17% for the mortars containing 0.20 and 0.40 sodium silicate-to-total solution ratio, respectively. With further increase from 10 to 12.5 M NaOH, 7-day cured compressive strength increased 19% and 32% when 0.20 and 0.40 sodium silicate-to-total solution ratio, respectively, were used. Overall, with every 0.20 sodium silicate-to-total solution ratio increase, 7-day compressive strength increased approximately 100%, 47% and 26% for every 2.5 M NaOH increase. The trend in strength development for this phase was similar to that found in phase I, as well as those reported by other researchers (Arioz et al., 2012; Katz, 2012; Ravikumar et al., 2010; Ryu et al., 2013). With increase in sodium hydroxide concentration, higher amounts of N-A-S-H gel were produced, resulting in higher strength for the studied alkali-activated fly ash mortars.

Table 4.2. Compressive strength results for alkali-activated fly ash mortars - Phase II-Part I

Compressive Strength (MPa)					
Mix	Sodium Silicate-to-Total Solution	NaOH Concentration	1 Day	3 Days	7 Days
D-5	0.20	5 M	5.88	11.87	12.60
E-5	0.40	5 M	30.78	43.21	44.40
F-5	0.60	5 M	44.02	57.79	58.19
D-7.5	0.20	7.5 M	27.49	39.03	43.09
E-7.5	0.40	7.5 M	42.16	52.98	56.23
F-7.5	0.60	7.5 M	65.45	74.15	75.53
D-10	0.20	10 M	62.94	75.67	76.20
E-10	0.40	10 M	51.82	64.93	65.93
F-10	0.60	10 M	46.97	59.41	60.64
D-12.5	0.20	12.5 M	76.50	87.89	90.38
E12.5	0.40	12.5 M	75.65	83.67	87.12

D=0.20 Sodium Silicate-to-Total Solution Ratio, E=0.40 Sodium Silicate-to-Total Solution Ratio, F=0.60 Sodium Silicate-to-Total Solution Ratio

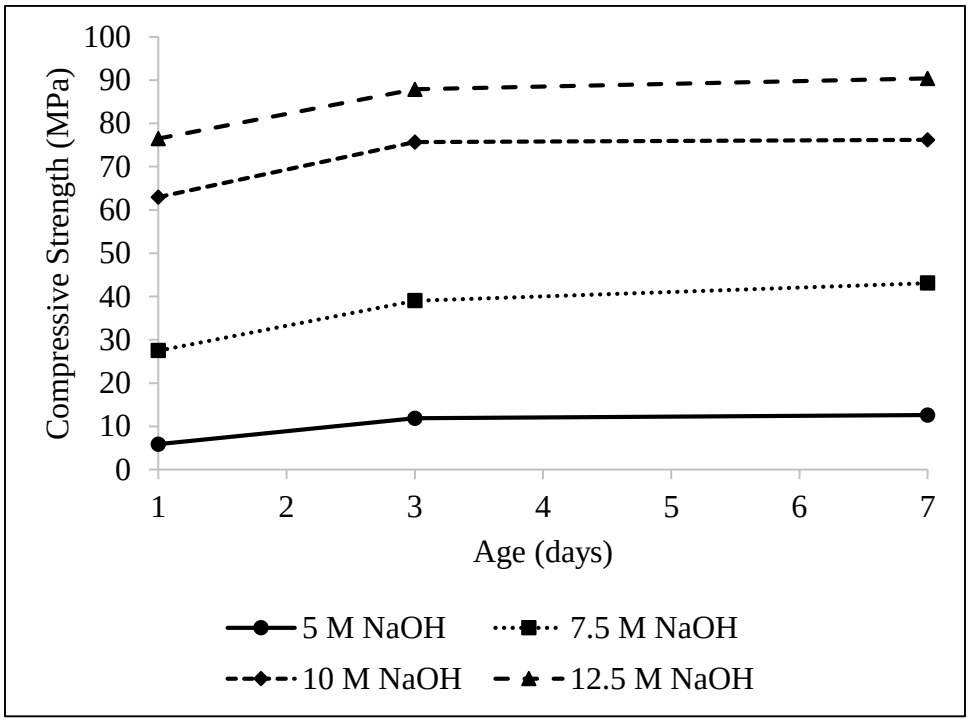

Figure 4.3. Compressive Strength as functions of sodium hydroxide concentration for alkali-activated fly ash mortars - Phase II-Part I, 0.20 sodium silicate-to-total solution ratio

4.2.1.2. Effects of Sodium Silicate-to-Total Solution Ratio on Compressive Strength

Compressive strength increased with increased sodium silicate-to-total solution ratio for 5 and 7.5 M NaOH, while the contrary was found for 10 and 12.5 M NaOH, as seen in Table 4.2 and Figures 4.4 and 4.5. With increased sodium silicate-to-total solution ratio from 0.20 to 0.40 sodium silicate-to-total solution ratio, compressive strength after 7 days of curing increased 252% and 31% for 5 and 7.5 M NaOH, respectively. On the other hand, 7-day compressive strength decreased 13% and 4% for the mortars activated with 10 and 12.5 M NaOH, respectively. Upon further increase from 0.40 to 0.60 sodium silicate-to-total solution ratio, 7-day compressive strength increased 31% and 34% for the fly ash mortars made with 5 and 7.5 M NaOH, respectively; whereas the same marginally decreased by 2% for 10 M NaOH. Overall, for every 2.5 M NaOH up to 7.5 M NaOH, 7-day compressive strength increased approximately 88% for every 0.20 sodium silicate-to-total solution ratio increase. For increased sodium hydroxide concentration from 10 to 12.5 M NaOH, compressive strength decreased about 9% for every 0.20 sodium silicate-to-total solution ratio increase up to 0.40. Although more compact structures are formed with more Si ions in corresponding gels due to the presence of silicate ions, there is a limit associated with this phenomenon. At higher concentrations of sodium hydroxide, such as 10 and 12.5 M NaOH as used in this study, there is an insufficient amount of sodium hydroxide available to hydrate fly ash adequately, resulting in higher amounts of non-reacted fly ash particles and ultimately lower compressive strength (Joseph and Mathew, 2012; Panias et al., 2007). In a study conducted by Joseph and Mathew (2012) specifically, the insufficient amounts of sodium hydroxide was found to hinder on the dissolution process within the entire geopolymerization process, otherwise known as the reaction product formation process. Although sodium silicate showed higher compressive strength results in comparison to using

sodium hydroxide solely, the pH of sodium silicate is lower and with higher contents, there is a higher $[SiO(OH)_2]^{2-}$ content. A higher $[SiO(OH)_2]^{2-}$ content hinders on the condensation process of the reaction product formation (Fernandez-Jimenez et al., 2007). In conjunction with the results found in this study, it can be said that for higher sodium hydroxide concentration, increased sodium silicate-to-total solution ratio allowed for higher $[SiO(OH)_2]^{2-}$ content that prevented steady formation of reaction product and lowered compressive strength of the studied alkali-activated fly ash mortars.

For the evaluated compressive strength properties, the standard deviation and coefficient of variation values varied from 0.8 MPa to 6.0 MPa and 0.1% and 14.2%, respectively.

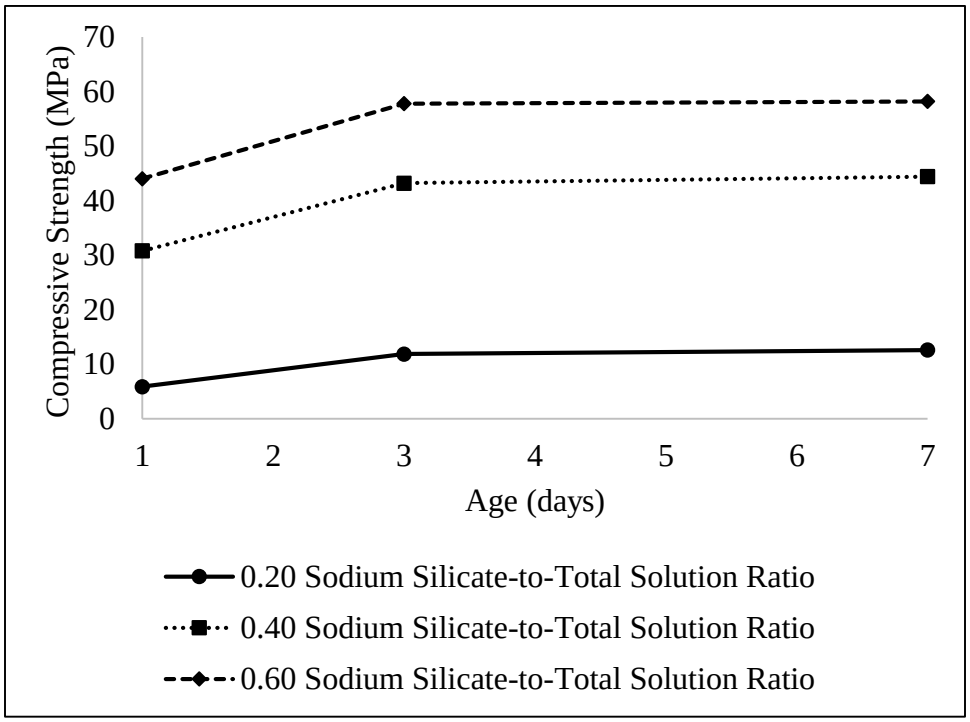

Figure 4.4. Compressive strength as functions of sodium silicate-to-total solution ratio for alkali-activated fly ash mortars - Phase II-Part I, 5 M NaOH

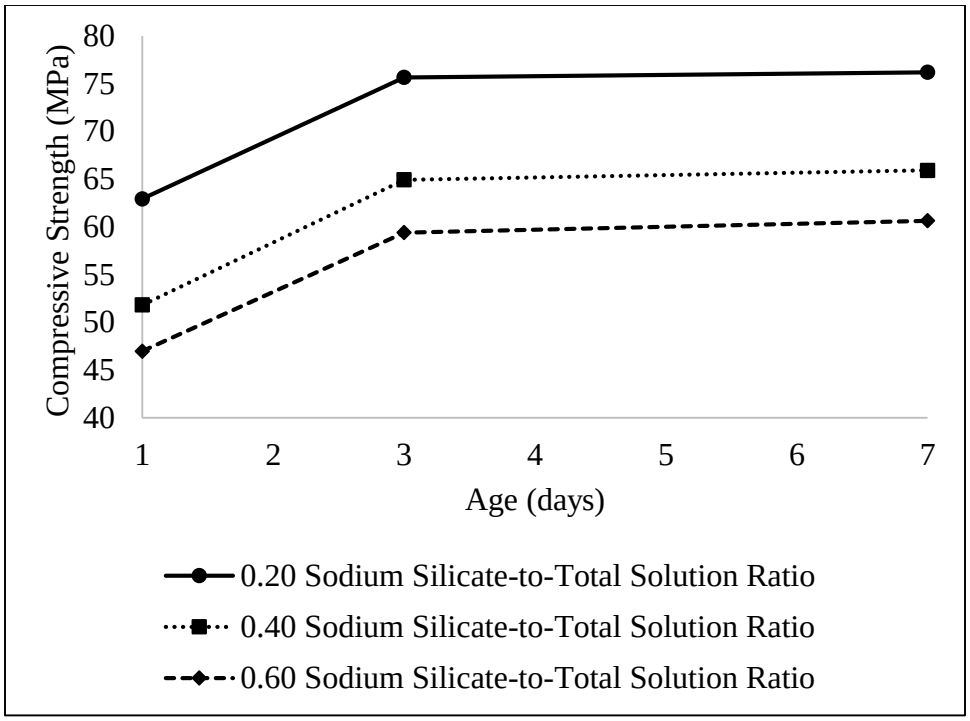

Figure 4.5. Compressive strength as functions of sodium silicate-to-total solution ratio for alkali-activated fly ash mortars - Phase II-Part I, 10 M NaOH

4.2.2. Flexural Strength

The 7-day flexural strength results obtained for the tested alkali-activated fly ash mortars are displayed in Table 4.3.

Table 4.3. Flexural strength results for alkali-activated fly ash mortars - Phase II-Part I

Average Flexural Strength (MPa)				
Sodium Silicate-to-Total Solution	5 M NaOH	7.5 M NaOH	10 M NaOH	12.5 M NaOH
0.20	2.98	3.89	9.40	10.75
0.40	4.66	5.83	6.91	8.65
0.60	5.72	6.36	6.75	---

--- = Not Available

4.2.2.1. Effects of Activator Concentration on Flexural Strength

In reference to Table 4.3, flexural strength increased with increased sodium hydroxide concentration, regardless of sodium silicate-to-total solution ratio. When sodium hydroxide concentration increased from 5 to 7.5 M NaOH, flexural strength increased 31%, 25% and 11% for the mortars containing 0.20, 0.40 and 0.60 sodium silicate-to-total solution ratio, respectively. Upon further increase in molarity of sodium hydroxide up to 10 M NaOH, flexural strength increased 142%, 18% and 6% for the matrices made with 0.20, 0.40 and 0.60 sodium silicate-to-total solution ratio, respectively. Once molarity increased from 10 to 12.5 M NaOH, flexural strength increased 14% and 25% for the fly ash mortars activated with 0.20 and 0.40 sodium silicate-to-total solution ratio, respectively. Higher strength was developed with increased production of N-A-S-H gel over the same time frame as compared to the samples with lower sodium hydroxide concentration.

4.2.2.2. Effects of Sodium Silicate-to-Total Solution Ratio on Flexural Strength

Similar to the findings reported for compressive strength in section 4.2.1.2., flexural strength increased with increased sodium silicate-to-total solution ratio for 5 and 7.5 M NaOH and decreased with increased sodium silicate-to-total solution ratio for 10 and 12.5 M NaOH. The results are documented in Figure 4.6. When sodium silicate-to-total solution ratio was increased from 0.20 to 0.40, flexural strength increased by an average of 53.5% for 5 and 7.5 M NaOH and decreased approximately 24% for 10 and 12.5 M NaOH. When sodium silicate-to-total solution ratio increased from 0.40 to 0.60, flexural strength increased 23% and 9% for 5 and 7.5 M NaOH, respectively; whereas it decreased 2.3% for 10 M NaOH. Similar to the earlier findings reported for compressive strength of alkali-activated fly ash mortars, sodium silicate is influential in improving strength up to an upper limit of 7.5 M NaOH. With an increase in

SiO_2/Na_2O ratio, the amount of Na_2O of the system was relatively low, allowing for the pH of the mortars to decrease. The decreased pH adversely affected the chemical reaction between the activator and fly ash, ultimately resulting in decreased strength properties.

Standard deviation and coefficient of variation values for the obtained flexural strength results differed from 0.03 MPa to 0.5 MPa and 0.2% to 8.0%.

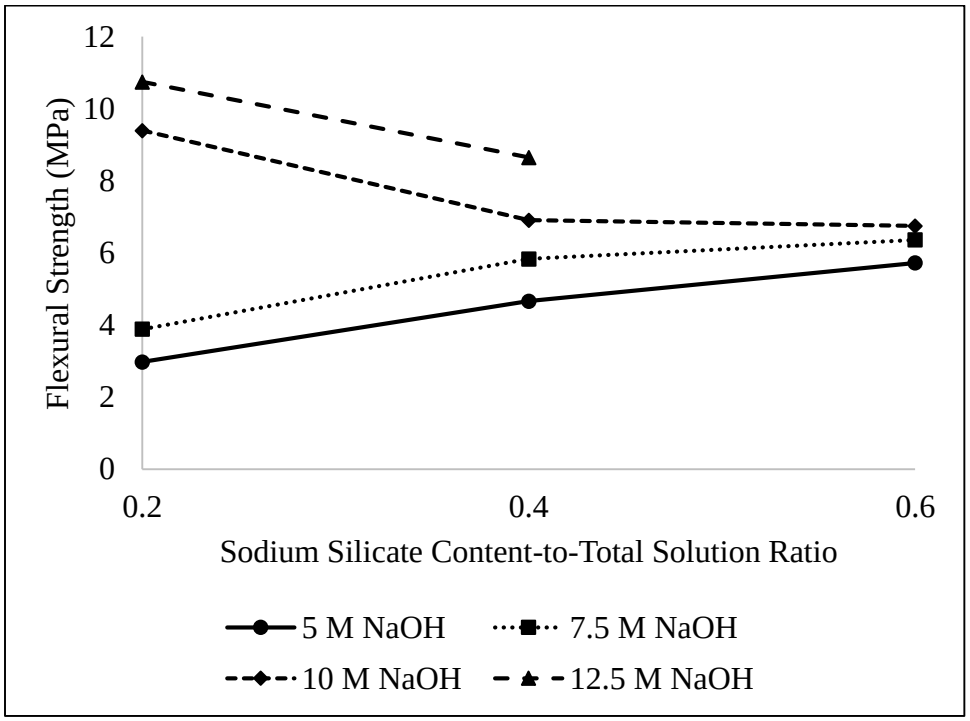

Figure 4.6. Flexural strength as functions of sodium silicate-to-total solution ratio on alkali-activated fly ash mortars - Phase II-Part I

4.2.3. Modulus of Elasticity

Modulus of elasticity of the tested alkali-activated fly ash mortars can be found in Table 4.4.

Table 4.4. Modulus of elasticity for alkali-activated fly ash mortars - Phase II-Part I

Modulus of Elasticity (GPa)				
Sodium Silicate-to-Total Solution	5 M NaOH	7.5 M NaOH	10 M NaOH	12.5 M NaOH
0.20	14.49	46.62	67.62	77.50
0.40	35.14	59.43	62.55	74.06
0.60	56.51	58.76	61.93	---

--- = Not Available

4.2.3.1. Effects of Activator Concentration on Modulus of Elasticity

Irrespective of sodium silicate-to-total solution ratio, the modulus of elasticity of the studied mortars increased with an increase in sodium hydroxide concentration, as seen in Table 4.4. When molarity of sodium hydroxide increased from 5 to 7.5 M NaOH, modulus of elasticity increased 222%, 69% and 4% for the mortars made with 0.20, 0.40 and 0.60 sodium silicate-to-total solution ratio, respectively. Upon further increase in sodium hydroxide concentration from 7.5 to 10 M NaOH, modulus of elasticity increased 45%, 5% and 5.5% for 0.20, 0.40 and 0.60 sodium silicate-to-total solution ratio, respectively. On average, modulus of elasticity increased 16.5% when sodium hydroxide molarity increased from 10 to 12.5 M for the tested sodium silicate-to-total solution ratios. Similar to the trends seen for compressive and flexural strengths, increased sodium hydroxide concentration allowed for more reaction product, N-A-S-H gel, and higher strength development (Ryu et al., 2013). With increased strength, modulus of elasticity was also expected to increase, which was confirmed by the results of this study.

4.2.3.2. Effects of Sodium Silicate-to-Total Solution Ratio on Modulus of Elasticity

Modulus of elasticity for the tested mortar samples increased with increased sodium silicate-to-total solution ratio for 5 and 7.5 M NaOH, while the opposite was found when 10 and 12.5 M NaOH were used, as seen in Table 4.4 and Figure 4.7. These results mimic those found

for compressive and flexural strengths. When increased from 0.20 and 0.40 sodium silicate-to-total solution ratio, modulus of elasticity increased 142% and 28% for 5 and 7.5 M NaOH, respectively; there was a 7.5% and 4% decrease for 10 and 12.5 M NaOH, respectively. When sodium silicate-to-total solution ratio increased from 0.40 to 0.60, modulus of elasticity increased 60.8% for 5 M NaOH; modulus of elasticity did not change for 7.5 and 10 M NaOH, with their negligible differences being nearly 1%. Increased sodium silicate-to-total solution ratio caused the SiO_2/Na_2O ratio to rise and Na_2O to drop in favor of SiO_2. With decreased amounts of Na_2O, the pH of the system also decreased (a similar study by Fernandez-Jimenez and Palomo (2005)). Lower pH decreased mechanical strength, as confirmed by the results in this study. Moreover, values found in this thesis were found to be similar to those reported in a study conducted by Joseph and Mathew (2012).

The standard deviation and coefficient of variation values obtained for the modulus of elasticity results presented for the evaluated alkali-activated fly ash mortars ranged from 0.03 MPa to 19.9 MPa and 0.04% to 62.3%, respectively.

4.2.4. Mechanical Property Comparisons

Table 4.5 below displays 7-day compressive and flexural strengths, and 7-day modulus of elasticity obtained for the studied alkali-activated fly ash mortars. These final values were compared against one another and their results are also in Table 4.5. With the exception of the matrix containing 5 M NaOH and 0.20 sodium silicate-to-total solution ratio, all flexural-to-compressive strength ratios stayed in a relatively narrow range with the change in sodium hydroxide concentration and sodium-silicate-to-total solution ratio. Modulus of elasticity-to-compressive strength ratios varied from almost 800 to approximately 1150 for all of the tested alkali-activated fly ash mortars.

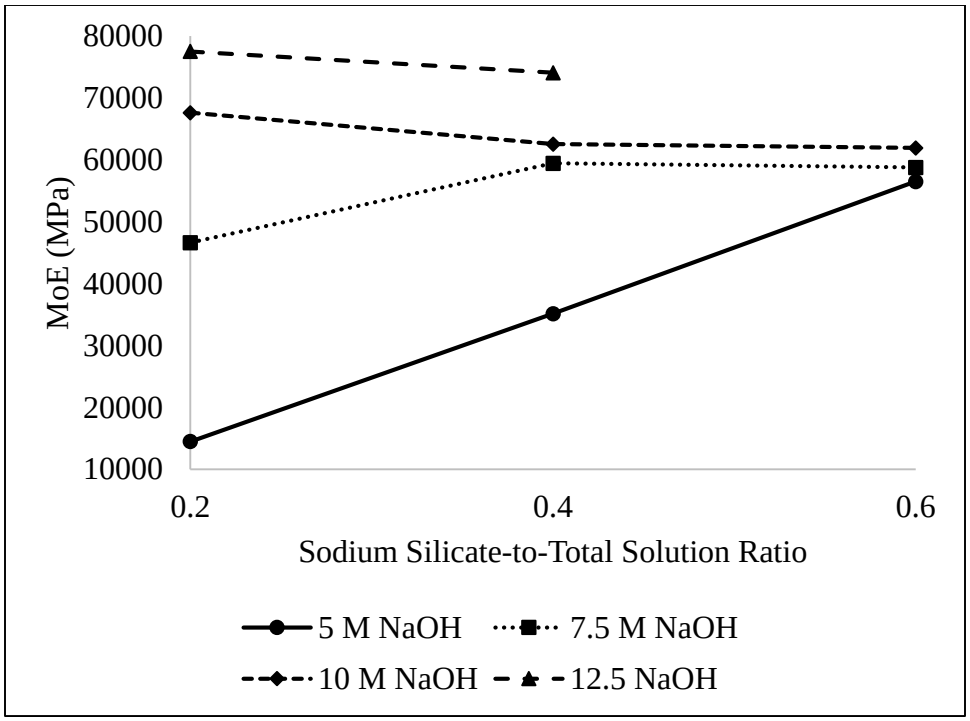

Figure 4.7. Modulus of elasticity as functions of sodium silicate-to-total solution ratio for alkali-activated fly ash mortars - Phase II-Part I

Table 4.5. Mechanical Property Comparisons - Phase II-Part I

Mix	7-Day Compressive Strength (MPa)	7-Day Flexural Strength (MPa)	7-Day Modulus of Elasticity (GPa)	Flexural vs. Compressive Strength	Modulus of Elasticity vs. Compressive
D-5	12.60	2.98	14.49	0.24	1150.16
E-5	44.40	4.66	35.14	0.11	791.40
F-5	58.19	5.72	56.51	0.10	971.14
D-7.5	43.09	3.89	46.62	0.09	1081.87
E-7.5	56.23	5.84	59.43	0.10	1056.93
F-7.5	75.53	6.36	58.76	0.08	778.03
D-10	76.20	9.40	67.62	0.12	887.40
E-10	65.93	6.91	62.55	0.10	948.78
F-10	60.64	6.75	61.93	0.11	1021.24
D-12.5	90.38	10.75	77.50	0.12	857.47
E-12.5	87.12	8.65	74.06	0.10	850.15

D=0.20 Sodium Silicate-to-Total Solution Ratio, E=0.40 Sodium Silicate-to-Total Solution Ratio, F=0.60 Sodium Silicate-to-Total Solution Ratio

4.3. Transport Properties

4.3.1. Water Absorption

A standardized testing method used to determine water absorption, as discussed in Chapter 2, allowed for the determination of absorption, density and void content. The results are presented in Table 4.6. In the following subsections, the results for each parameter are discussed.

4.3.1.1. Absorption

Table 4.6. Absorption results for alkali-activated fly ash mortars - Phase II-Part I

Absorption (%)				
Sodium Silicate-to-Total Solution	5 M NaOH	7.5 M NaOH	10 M NaOH	12.5 M NaOH
0.20	7.857	7.061	3.603	3.009
0.40	7.539	6.739	4.851	3.109
0.60	6.823	6.000	4.322	---

--- = Not Available

4.3.1.1.1. Effects of Activator Concentration on Absorption

In reference to Table 4.6, absorption decreased with increased sodium hydroxide concentration for all sodium silicate-to-total solution ratios. Absorption decreased by an average of 11% when sodium hydroxide concentration increased from 5 to 7.5 M NaOH. When sodium hydroxide increased from 7.5 to 10 M NaOH, absorption decreased 49% when 0.20 sodium silicate-to-total solution ratio was used and 28% when 0.40 or 0.60 sodium silicate-to-total solution ratio was used in the studied mortars. Upon further increase from 10 to 12.5 M NaOH, absorption decreased 17% and 36% for the mortars containing 0.20 and 0.40 sodium silicate-to-total solution ratio, respectively. The results were opposite to those found for all mechanical properties. As discussed for compressive strength, reaction product formation increased with increased concentration of sodium hydroxide. With increased reaction product formation,

absorption was expected to decrease, as confirmed by the results obtained for the studied alkali-activated fly ash mortars.

4.3.1.1.2. Effects of Sodium Silicate-to-Total Solution Ratio on Absorption

Absorption decreased with increased sodium silicate-to-total solution ratio for 5 and 7.5 M NaOH while the opposite was found when 10 and 12.5 M NaOH were utilized, as seen in Table 4.6. When sodium silicate-to-total solution ratio increased by 0.20 increments up to 0.60, absorption decreased, on average, by approximately 5% and 10% for the first and second increment for both 5 and 7.5 M NaOH. When increased from 0.20 to 0.40 sodium silicate-to-total solution ratio, absorption increased 34.7% and 3.3% for 10 and 12.5 M NaOH, respectively. As mentioned in the previous section, the results obtained for absorption were contrary to those obtained for all mechanical properties. In reference to section 4.2.1.2., a more compact structure was formed with the presence of silicate ions from sodium silicate, however, the increase was limited. With higher sodium hydroxide concentration accompanying higher sodium silicate-to-total solution ratio, there was an insufficient amount of sodium hydroxide capable of activating fly ash effectively, thus resulting in a higher amount of unreacted fly ash and hindering the geopolymerization process. With a higher amount of unreacted fly ash, a less compact structure is formed, resulting in higher absorption capabilities, as evident by the results obtained for the studied alkali-activated fly ash mortars.

Absorption values determined for the studied alkali-activated fly ash mortars had standard deviation values ranging from 0.001% to 1.92% and coefficient of variation values from 0.01% and 24.4%.

4.3.1.2. Dry Bulk Density

Table 4.7. Dry Bulk Density results for alkali-activated fly ash mortars - Phase II-Part I

Density (g/cm^3)				
Sodium Silicate-to-Total Solution	5 M NaOH	7.5 M NaOH	10 M NaOH	12.5 M NaOH
0.20	1.660	1.756	2.121	2.124
0.40	1.754	1.998	2.085	2.114
0.60	1.748	2.021	2.113	---

--- = Not Available

4.3.1.2.1. Effects of Activator Concentration on Dry Bulk Density

As displayed in Table 4.7, dry bulk density increased with increased sodium hydroxide concentration, for all studied sodium silicate-to-total solution ratios. When sodium hydroxide molarity increased from 5 to 7.5 M NaOH, density increased 6%, 14% and 16% for the studied mortars made with 0.20, 0.40 and 0.60 sodium silicate-to-total solution ratio, respectively. Upon further 2.5 increase in molarity to 10 M NaOH, density increased 21%, 4% and 5% when 0.20, 0.40 and 0.60 sodium silicate-to-total solution ratio, respectively, were used. Density increased only approximately 1% when sodium hydroxide molarity increased from 10 to 12.5, independent of sodium silicate-to-total solution ratio. As reported in previous sections, increased sodium hydroxide concentration led to increased amounts of reaction product formed. Increased reaction product allowed for density to also increase.

4.3.1.2.2. Effects of Sodium Silicate-to-Total Solution Ratio on Density

Density increased with increased sodium silicate-to-total solution ratio for 5 and 7.5 M NaOH while the contrary was found for 10 and 12.5 M NaOH, as seen in Table 4.7. Density increased more significantly when increased from 0.20 to 0.40 sodium silicate-to-total solution ratio, while minimal change was seen when more than 0.40 sodium silicate-to-total solution ratio

was used. From 0.20 to 0.40 sodium silicate-to-total solution ratio, density increased 6% and 14% for 5 and 7.5 M NaOH, respectively. For the same interval, density decreased approximately 1.5% for both 10 and 12.5 M NaOH. On average, density changed less than 1% when increased from 0.40 to 0.60 sodium silicate-to-total solution ratio for all sodium hydroxide concentrations. As stated in section 4.3.1.2.1., increased reaction product formation was accompanied by increased density. This finding was consistent with those obtained for strength and absorption of the studied alkali-activated fly ash mortars.

For the tested alkali-activated fly ash mortars, the standard deviation values calculated for the obtained density values varied between 0.001 g/cm^3 and 0.324 g/cm^3 and coefficient of variation values between 0.05% and 19.5%.

4.3.1.3. Void Content

4.3.1.3.1. Effects of Activator Concentration on Void Content

As shown in Figure 4.8, regardless of sodium silicate-to-total solution ratio, void content decreased with increased sodium hydroxide concentration. From 5 to 7.5 M NaOH, void content decreased about 2% for the matrices containing 0.20 and 0.40 sodium silicate-to-total solution ratio and 6% for 0.60 sodium silicate-to-total solution ratio. Once sodium hydroxide increased from 7.5 to 10 M NaOH, void content decreased 48% and 16% for 0.20 and 0.60 sodium silicate-to-total solution ratio, respectively. Upon further increased molarity to 12.5 M NaOH, void content decreased 8% and 51% when 0.20 and 0.40 sodium silicate-to-total solution ratio, respectively, were used. By taking in consideration the absorption results presented in section 4.3.1.1.1., the two properties shall have similar results. With increased sodium hydroxide concentration, reaction product formation increased and a more compact and dense structure was

formed. A more compact and dense structure minimized the ability for liquids to penetrate the matrix, as confirmed by the void content results obtained in this study.

4.3.1.3.2. Effects of Sodium Silicate-to-Total Solution Ratio on Void Content

In reference to Figure 4.9, void content decreased with increased sodium silicate-to-total solution ratio for 5 and 7.5 M NaOH, while the contrary occurred when 10 and 12.5 M NaOH were used. Void content decreased by an average of 16% for both mortars incorporating 5 and 7.5 M NaOH when sodium silicate-to-total solution ratio increased from 0.20 to 0.40. For the mortars containing 12.5 M NaOH, void content increased approximately 3%. When sodium silicate-to-total solution ratio increased from 0.40 to 0.60, void content decreased approximately 13% for both mortars made with 5 and 7.5 M NaOH. Void content increased 17% from 0.20 to 0.60 sodium silicate-to-total solution ratio for 10 M NaOH mortars. For the alkali-activated mortars having 5 and 7.5 M NaOH, reaction product increased with increased sodium silicate-to-total solution ratio, allowing for total void content to decrease. When 10 and 12.5 M NaOH were used, reaction product decreased with increased sodium silicate-to-total solution ratio, resulting in increased total void content. These results and conclusions replicate those obtained for absorption in section 4.3.1.1.2. Although increased amount of sodium silicate aided in the formation of reaction product, higher concentrations of sodium hydroxide limited these increases and ultimately hindered the full potential for reaction product formation to achieve.

The standard deviation and coefficient of variation values determined for the void content results presented ranged between 0.01% and 2.2% and 0.07% and 16%, respectively.

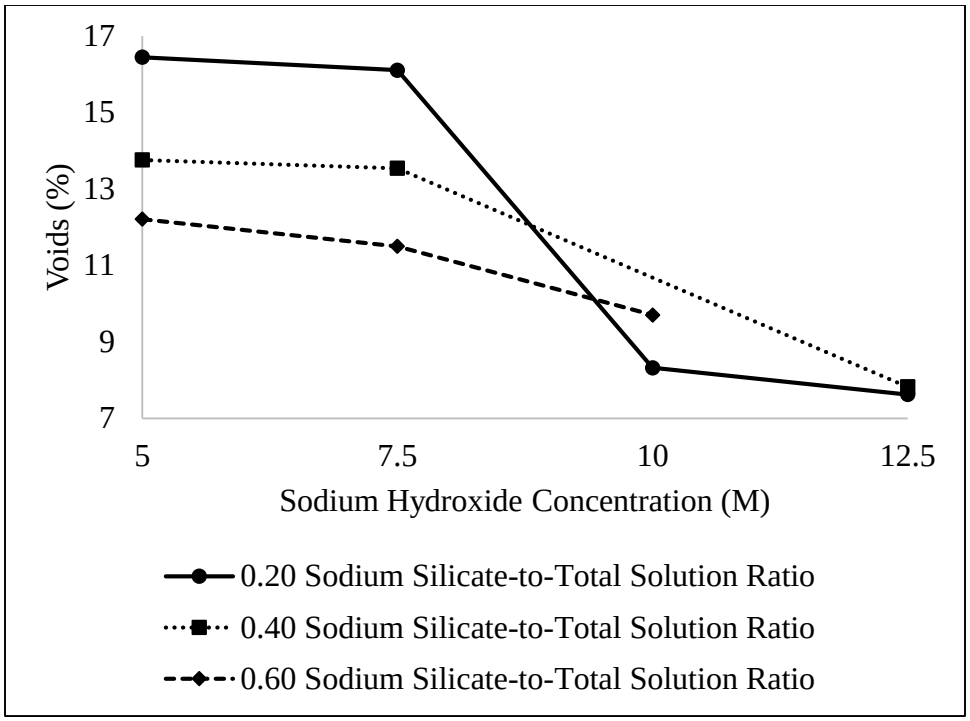

Figure 4.8. Void content as functions of sodium hydroxide concentration for alkali-activated fly ash mortars - Phase II-Part I

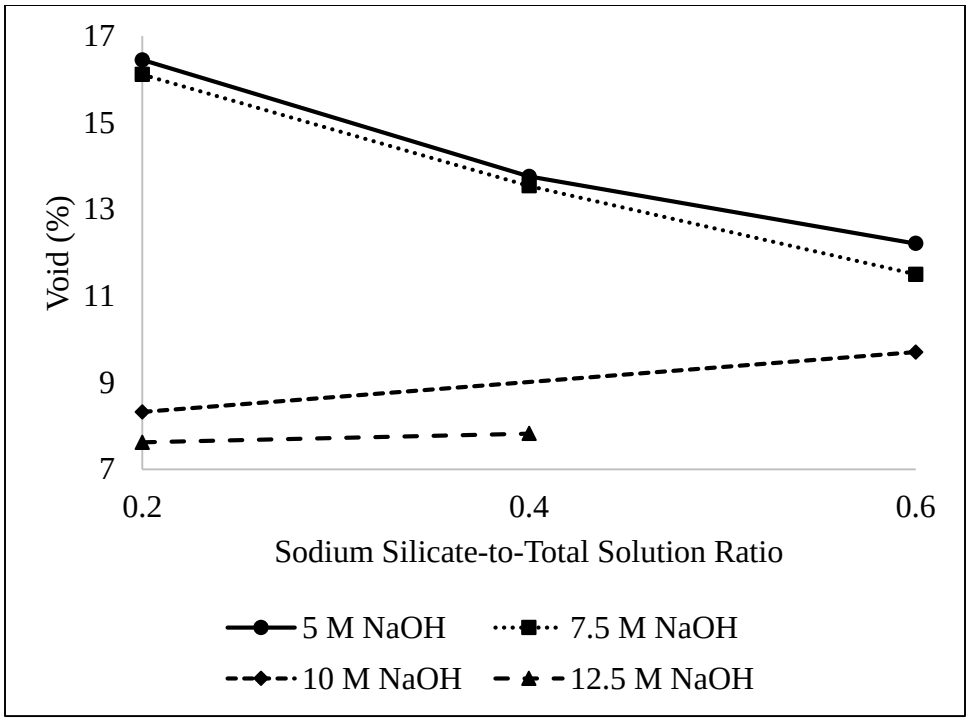

Figure 4.9. Void content as functions of sodium silicate-to-total solution ratio for alkali-activated fly ash mortars - Phase II-Part I

4.3.2. Rapid Chloride Migration

Results obtained for rapid chloride migration results of the tested alkali-activated mortars are displayed in Table 4.8.

Table 4.8. Chloride migration results for alkali-activated fly ash mortars - Phase II-Part I

Average Chloride Depth (mm)				
Sodium Silicate-to-Total Solution	5 M NaOH	7.5 M NaOH	10 M NaOH	12.5 M NaOH
0.20	33.68	25.67	9.20	7.60
0.40	28.51	22.32	10.612	9.24
0.60	23.97	20.12	13.64	---

--- = Not Available

4.3.2.1. Effects of Activator Concentration on Chloride Migration

As shown in Table 4.8 and Figure 4.10, chloride penetration depth decreased with increased sodium hydroxide concentration, for all studied sodium silicate-to-total solution ratios. When mortars contained NaOH from 5 to 7.5 M, chloride depth decreased approximately 21%, for all sodium silicate-to-total solution ratios. Upon further sodium hydroxide molarity increase from 7.5 to 10 M NaOH, chloride depth decreased 64%, 52% and 32% for the mortars made with 0.20, 0.40 and 0.60 sodium silicate-to-total solution ratio, respectively. Once sodium hydroxide concentration increased by 2.5 to 12.5 M NaOH, chloride depth decreased averagely by 11.5% when 0.20 or 0.40 sodium silicate-to-total solution ratio was used. The absorption and void content results reported in sections 4.3.1.1.1. and 4.3.1.3.1., respectively, are used to explain these findings. Increased sodium hydroxide concentration allowed for increased geopolmerization process, which led to increased reaction product formation, resulting in decreased absorption and void content. As such, harsh mediums were not allowed to enter the

matrix and, thus, the depth of penetrated chloride decreased with an increase in sodium hydroxide concentration.

4.3.2.2. Effects of Sodium Silicate-to-Total Solution Ratio on Chloride Migration

Chloride depths as functions of sodium silicate-to-total solution ratio of the studied alkali-activated mortars are shown in Figure 4.11. Penetration of chloride decreased with increased sodium silicate-to-total solution ratio for the mortars containing 5 and 7.5 M NaOH, whereas the contrary was found for the companion mixtures having 10 and 12.5 M NaOH. With every 0.20 increase in sodium silicate-to-total solution ratio up to 0.60, chloride depth decreased by an average of 15.5% and 11.5% for the mortars made with 5 and 7.5 M NaOH, respectively. When sodium silicate-to-total solution ratio increased from 0.20 to 0.40, chloride depth increased 15% and 22% for the mortars having 10 and 12.5 M NaOH, respectively. Chloride depth further decreased by 29% for the 10 M NaOH mortars when increased from 0.40 to 0.60 sodium silicate-to-total solution ratio. These results mirror those obtained for absorption and void content reported in sections 4.3.1.1.2. and 4.3.1.3.2., respectively. Although increased sodium silicate-to-total solution ratio allowed for a higher geopolymerization rate, the processes suffered at higher sodium hydroxide concentrations.

For the rapid chloride migration results presented for the evaluated alkali-activated mortars, standard deviation values varied between 0.7 mm and 2.4 mm and coefficient of variation values between 0.2% and 10.2%.

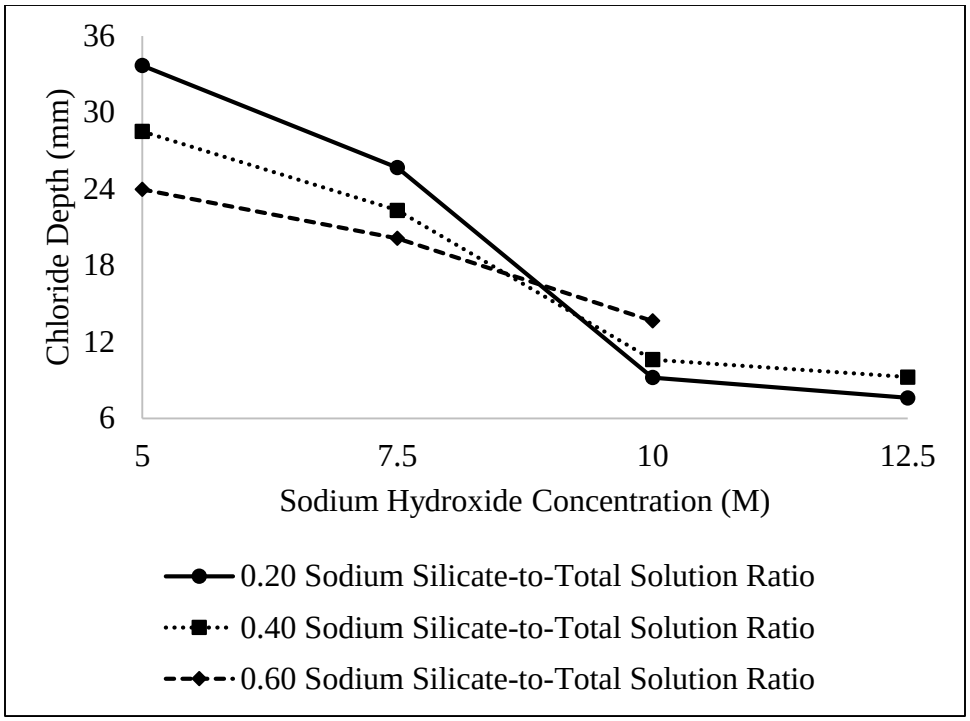

Figure 4.10. Chloride depth as functions of sodium hydroxide concentration for alkali-activated fly ash mortars - Phase II-Part I

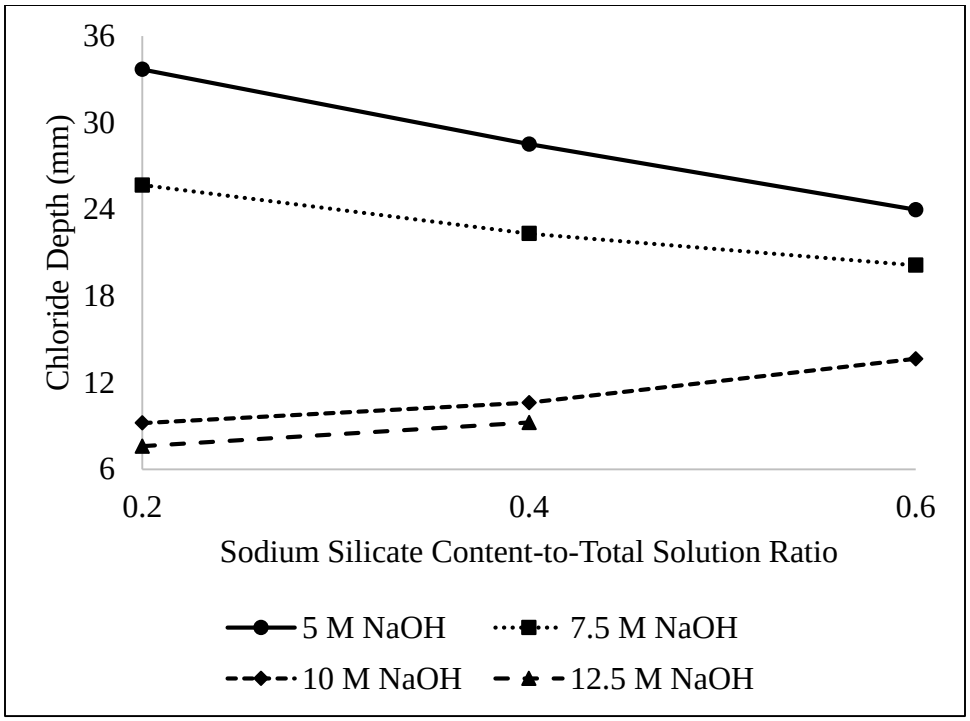

Figure 4.11. Chloride depth as functions of sodium silicate-to-total solution ratio for alkali-activated fly ash mortars - Phase II-Part I

4.4. Durability Properties

Four types of physical and chemical durability properties were evaluated; namely resistance to acid, freezing and thawing, external sulfate attack, and wear. Acid resistance was evaluated through strength and mass loss measurements. Freezing and thawing resistance was determined through mass loss measurements. Strength loss and length expansion measurements were used to study resistance to external sulfate attack. Resistance for abrasion was evaluated through depth of wear measurements.

4.4.1. Resistance to Acid Attack

As stated, acid resistance was determined by strength and mass loss measurements. The following subsection discusses the results for both measurements as function of activator concentration and sodium silicate content.

4.4.1.1. Acid-Induced Mass Loss

Table 4.9 reports on the total mass loss measured of samples immersed in sulfuric acid solution for 8 weeks.

Table 4.9. Acid-induced total mass loss for alkali-activated fly ash mortars - Phase II-Part I

Total Acid Mass Loss (%)		
NaOH Concentration	Sodium Silicate-to-Total Solution	Total Mass Loss
5 M	0.20	2.61
5 M	0.60	0.13
7.5 M	0.20	0.68
7.5 M	0.60	0.18
10 M	0.20	0.40
10 M	0.60	1.00
12.5 M	0.20	0.47

4.4.1.1.1. Effects of Activator Concentration on Acid-Induced Mass Loss

Table 4.9 displays the overall mass loss for the samples immersed in sulfuric acid for up to 8 weeks. Mass loss decreased with increased sodium hydroxide concentration, although total mass loss was minimal for all treated samples. Decreased mass loss can be correlated to the void content of the studied mortars. As discussed in section 4.3.2.3.1., void content decreased with increased sodium hydroxide concentration, due to increased degree of chemical reactivity. Using the void content as an explanation for increased mass loss with lower sodium hydroxide concentrations, increased void content led to increased permeability and acid was able to penetrate the matrix faster than those with lower void content. With a higher void content, acid was allowed to moderately cause loss in mass of the studied alkali-activated fly ash mortars.

4.4.1.1.2. Effects of Sodium Silicate-to-Total Solution Ratio on Acid-Induced Mass Loss

As seen in Table 4.9, measured mass loss of samples immersed in sulfuric acid decreased with increased sodium silicate-to-total solution ratio for the mortars made with 5 and 7.5 M NaOH. An opposite trend was found when 10 and 12.5 M NaOH were used. These results correlated well with not only the strength trends established previously, but also with the results reported for absorption and void content. For the mortars made with 5 and 7.5 M NaOH, void content decreased with increased sodium silicate-to-total solution ratio, similar to the results for the acid-induced mass loss shown in Table 4.9. For the mortars made with 10 and 12.5 M NaOH, void content increased with increased sodium silicate-to-total solution ratio, again mimicking the results for mass loss as shown in Table 4.9. Increased void content allowed for ease in acid penetration and subsequent loss in mass as compared to the samples with a lower void content.

For the total mass loss results presented for resistance to acid attack of the tested alkali-activated fly ash mortars, standard deviation values ranged from 0.06% and 0.08% and coefficient of variation values from 2.6% and 52%.

4.4.1.2. Strength Loss due to Acid Attack

Table 4.10 displays the strength results obtained of samples immersed in sulfuric acid solution for up to 8 weeks.

4.4.1.2.1. Effects of Activator Concentration on Strength Loss Measurements

As seen in Table 4.10, strength loss was rather minimal for all tested mortars, with the average strength loss of approximately 7%. In general, alkali-activated fly ash binders have excellent resistance against acid and other harmful mediums as compared to OPC, mainly due to its insufficient amount of calcium oxide (Pacheco-Torgal et al., 2012; Rangan, 2010; Thokchom et al., 2009). Durability issues in OPC have been found to be caused by its calcium content (Fernandez-Jimenez et al., 2007; Rangan, 2010). Class F fly ash, as used for this study, had less than 10% calcium content and allowed for excellent performance while immersed in sulfuric acid solution. With minimal strength loss, accompanied with minimal mass loss discussed in section 4.4.1.1., strength was expected to stay consistent to the original trends established in previous sections.

4.4.1.2.2. Effects of Sodium Silicate-to-Total Solution Ratio on Strength Loss Measurements

As stated in section 4.4.1.2.1., strength loss over time due to sulfuric acid immersion was minimal throughout, with an average strength loss of 7% for all evaluated mortars. Similar to what was discussed previously, minimal strength loss occurred. Overall, strength trends stayed as

those presented in section 4.2.1.2. As discussed in section 4.4.1.2.2., Class F fly ash has a calcium content less than 10% which allowed for its excellent resistance to acid attack of the tested alkali-activated mortars.

Standard deviation and coefficient of variation values calculated for compressive strength loss due to acid attack varied from 0.7 MPa and 4.2 MPa and 0.06% and 36%, respectively.

Table 4.10. Acid strength loss measurements for alkali-activated fly ash mortars - Phase II-Part I

Compressive Strength (MPa)						
Sodium Silicate-to-Total Solution	NaOH Concentration	Time in Acid				
		0 week	1 week	2 weeks	4 weeks	8 weeks
0.20	5 M	10.71	9.97	10.70	10.37	10.60
0.40	5 M	33.30	32.90	34.83	31.81	33.77
0.60	5 M	43.64	43.58	43.04	43.10	42.62
0.20	7.5 M	38.78	38.28	37.86	31.62	30.36
0.40	7.5 M	50.61	48.06	47.90	44.00	40.80
0.60	7.5 M	60.43	57.65	56.23	55.31	54.76
0.20	10 M	72.39	69.56	69.78	71.57	73.61
0.40	10 M	62.63	61.66	57.67	57.09	56.37
0.60	10 M	60.64	61.55	59.78	59.00	58.47
0.20	12.5 M	87.68	86.60	85.02	82.32	80.06
0.40	12.5 M	87.12	85.01	84.07	80.56	95.01

4.4.2. Resistance to External Sulfate Attack

Two evaluation methods were utilized to examine the sulfate resistance of the studied alkali-activated fly ash mortars, namely strength loss and linear expansion. The discussion of the results for each method as functions of sodium hydroxide concentration and sodium silicate-to-total solution ratio are given in the next two subsections.

4.4.2.1. Length Change Measurements

4.4.2.1.1. Effects of Activator Concentration on Sulfate-Induced Length Change

Overall, minimal length expansion occurred while immersed in sodium sulfate solution for up to 15 weeks. The results are shown in Figure 4.12. Alkali-activated fly ash mortars made with 5 M NaOH had a higher length expansion than those batched with 10 M NaOH. This difference in length change between the two mortar types was higher in early age and gradually narrowed as the immersion age progressed. This behavior can be related to the void content, which was higher for the mortars made with 5 M NaOH for which allowed for sulfate to penetrate into its matrix. Overall, for the studied mortars, the maximum length change due to external sulfate attack was minimal. Once again, this can be attributed to the low calcium oxide found in Class F fly ash. Without a sufficient amount of calcium oxide, sodium sulfate cannot form $Ca(OH)_2$, which has been found to be responsible for expansion and ultimately the deterioration of OPC (Fernandez-Jimenez et al., 2007; Rangan, 2010). With such a small length expansion found for the tested prisms, it can be concluded that alkali-activated fly ash mortars have excellent sulfate resistance.

4.4.2.1.2. Effects of Sodium Silicate-to-Total Solution on Sulfate-Induced Length Change

As stated in section 4.4.2.1.1., minimal length change occurred when samples were immersed in sodium sulfate solution for up to 15 weeks, seen in Figure 4.13. Length expansion decreased with increased sodium silicate-to-total solution ratio for the mortars activated with 10 M NaOH. Length expansion between 0.20 and 0.60 sodium silicate-to-total solution ratio was about 0.0015%, although the difference is negligible. Overall, length expansion was found to be minimal due to the small amount of calcium oxide available in Class F fly ash.

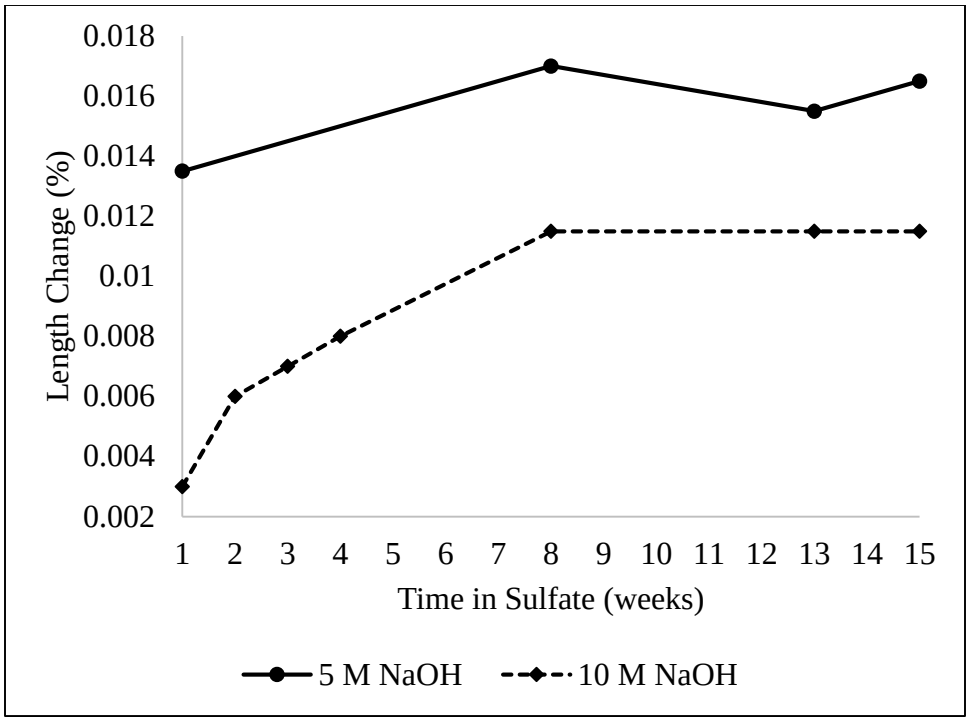

Figure 4.12. Sulfate-induced length change for 0.60 sodium silicate-to-total solution ratio samples for alkali-activated fly ash mortars - Phase II-Part I

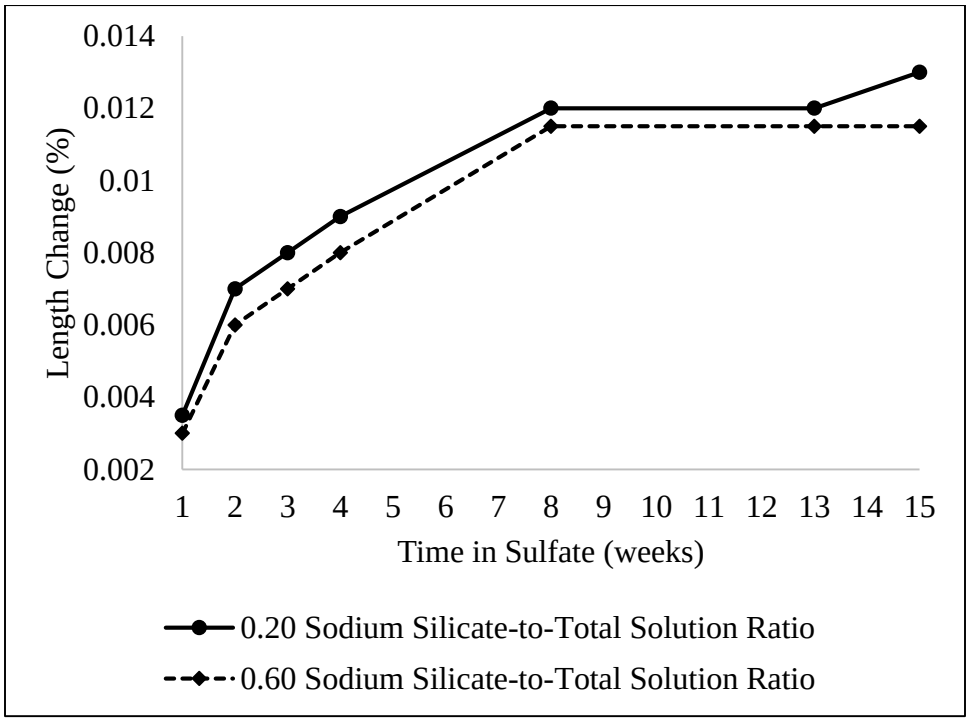

Figure 4.13. Sulfate-induced length change for 10 M NaOH samples for alkali-activated fly ash mortars - Phase II-Part I

Sulfate-induced length expansion values of the evaluated alkali-activated mortars had standard deviation calculations between 0.0002% and 0.002% and coefficient of variation calculations between 4.3% and 14.2%.

4.4.2.2. Strength Loss due to Sulfate Attack

Compressive strength of alkali-activated mortars immersed in sodium sulfate solution for up to 8 weeks are displayed in Table 4.11.

Table 4.11. Sulfate strength loss measurements for alkali-activated fly ash mortars - Phase II-Part I

Compressive Strength (MPa)						
Sodium Silicate-to-Total Solution	NaOH Concentration	Time in Sulfate				
		0 week	1 week	2 weeks	4 weeks	8 weeks
0.20	5 M	10.08	9.42	8.29	7.81	7.72
0.40	5 M	39.97	39.66	37.58	34.25	34.10
0.60	5 M	52.37	50.81	49.77	46.57	46.41
0.20	7.5 M	32.32	31.40	31.23	30.90	30.46
0.40	7.5 M	44.99	44.09	42.50	39.85	43.13
0.60	7.5 M	52.87	52.58	51.41	50.51	49.49
0.20	10 M	76.20	75.77	72.59	73.54	80.81
0.40	10 M	62.63	62.52	61.97	60.06	58.58
0.60	10 M	60.64	60.79	58.55	59.57	62.14
0.20	12.5 M	87.68	86.56	81.72	80.90	77.50
0.40	12.5 M	82.76	82.31	81.75	80.93	88.27

4.4.2.2.1. Effects of Activator Concentration on Strength Loss due to Sulfate Attack

Table 4.11 displays the compressive strength results of the evaluated mortars immersed in sodium sulfate for up to 8 weeks. In general, total strength loss decreased with increased sodium hydroxide concentration. On average, total compressive strength loss was 16%, 5% and 2% when 5, 7.5 and 12.5 M NaOH, respectively, were used. Due to the low calcium oxide

content in the fly ash used in this study, there wasn't enough calcium hydroxide formed to react with sodium sulfate to cause expansion and to lower the pH of the system for deterioration.

4.4.2.2.2. Effects of Sodium Silicate-to-Total Solution Ratio on Strength Loss due to Sulfate Attack

In reference to Table 4.11, compressive strength loss of mortars immersed in sodium sulfate decreased with increased sodium silicate-to-total solution ratio for the fly ash mortars activated by 5 and 7.5 M NaOH, while strength loss increased with increased sodium silicate-to-total solution ratio for the matrices made with 10 and 12.5 M NaOH. Averagely, sulfate-induced strength loss was approximately 6%. As explained was explained in section 4.4.2.2.1., insufficient amount of calcium oxide in Class F fly ash was responsible for the excellent performance of the studied mortars when immersed in sodium sulfate solution.

For the compressive strength loss due to external sulfate attack values obtained for the tested alkali-activated fly ash mortars, standard deviation ranged from 0.3 MPa to 5.1 MPa and coefficient of variation from 0.01% and 21%.

4.4.3. Resistance to Freezing and Thawing (F-T)

4.4.3.1. F-T Mass Loss

Table 4.12 displays the cumulative mass loss of the alkali-activated fly ash mortars measured during freeze-thaw resistance testing. Mass loss was evaluated as a percentage of the initial mass of samples. Discussion of the results as functions of activator concentration and sodium silicate-to-total solution ratio are given below.

Table 4.12. Freeze-thaw induced mass loss - Phase II-Part I

Freeze-Thaw Mass Loss Measurements (% total mass loss)							
Mix	Sodium Silicate-to-Total Solution	NaOH Concentration	10 Cycles	20 Cycles	30 Cycles	40 Cycles	50 Cycles
D-5	0.20	5 M	8.46	58.68	70.10	100	100
E-5	0.40	5 M	8.63	35.43	57.18	71.18	82.98
F-5	0.60	5 M	3.15	20.79	39.70	50.95	58.99
D-10	0.20	10 M	0.68	5.29	8.98	11.64	15.15
E-10	0.40	10 M	0.36	4.45	9.13	13.39	16.95
F-10	0.60	10 M	0.33	4.58	12.34	22.56	31.00

D=0.20 Sodium Silicate-to-Total Solution Ratio, E=0.40 Sodium Silicate-to-Total Solution Ratio, F=0.60 Sodium Silicate-to-Total Solution Ratio

4.4.3.1.1. Effects of Activator Concentration on F-T Induced Mass Loss

As seen in Table 4.12, mass loss, measured every 10 freezing and thawing cycles, decreased with increased activator concentration. The results obtained in this study can be attributed to the absorption and total void content of the evaluated alkali-activated fly ash mortars. When sodium hydroxide concentration increased, chemical reaction product increased, leading to a better bond and a more compact structure. Both absorption and total void content decreased, as documented in sections 4.3.1.1.1 and 4.3.1.3.1, respectively, allowing for lower penetration of water to expand during freezing.

4.4.3.1.2. Effects of Sodium Silicate-to-Total Solution Ratio on F-T Induced Mass Loss

Total mass loss occurred during freeze-thaw resistance testing results are shown in Table 4.12. For matrices containing 5 and 10 M NaOH, mass losses were found to have an opposite trend to that displayed by the compressive strength of companion mortars. When 5 M NaOH was

used, mass loss decreased with increased sodium silicate-to-total solution ratio. Mass loss for the mixtures containing 10 M NaOH increased with increased sodium silicate-to-total solution ratio. The trends found for both 5 and 10 M NaOH matrices follow the trends found for absorption and total void content, as shown in sections 4.3.1.1.2 and 4.3.1.3.2, respectively. With increased sodium silicate-to-total solution ratio, matrices containing 5 M NaOH, for example, experienced increased strength and decreased absorption and void content, due to an increase in chemical reaction products. The increased formation in reaction products resulted in a more compact structure which was able to withstand deterioration caused by freezing of penetrated water during the freeze-thaw regime. An opposite explanation applies to the matrices containing 10 M NaOH.

Standard deviation and coefficient of variation values for the total mass loss due to freezing and thawing varied between 0.4% and 11.3% and 1.0% and 44.2%, respectively.

4.4.4. Resistance to Wear

Table 4.13 displays the results obtained from abrasion (wear) resistance testing of the studied alkali-activated fly ash mortars. The discussions of the results are given in the two following subsections.

Table 4.13. Abrasion resistance for alkali-activated mortars - Phase II-Part I

Abrasion Depth (mm)				
Sodium Silicate-to-Total Solution Ratio	5 M NaOH	7.5 M NaOH	10 M NaOH	12.5 M NaOH
0.20	2.51	1.90	0.93	0.84
0.40	1.50	1.14	1.12	0.96
0.60	1.01	0.97	1.17	---

--- = Not Available

4.4.4.1. Effects of Activator Concentration on Abrasion Resistance Results

As shown in Table 4.13, abrasion depth decreased with increased activator concentration with the exception of the matrix containing 10 M NaOH and 60% sodium silicate content. When sodium hydroxide concentration increased from 5 to 7.5 M, abrasion depth decreased approximately 24%, 24% and 4% for the mortars having 0.20, 0.40 and 0.60 sodium silicate-to-total solution ratio, respectively. Upon further increase from 7.5 M to 10 M NaOH, abrasion depth decreased about 51% and 2% for the fly ash mortars containing 0.20 and 0.40 sodium silicate-to-total solution ratio, respectively. Another 2.5 M NaOH increase from 10 to 12.5 M NaOH caused abrasion depth to decrease by approximately 10% and 14% for the mortars made with 0.20 and 0.40 sodium silicate-to-total solution ratio, respectively. Overall, with every 2.5 M NaOH, abrasion depth decreased by nearly 28%, 13% and 4% when 0.20, 0.40 and 0.60 sodium silicate-to-total solution ratio, respectively, were made. The results obtained for abrasion resistance were found to be inversely related to those obtained for strength properties. Increased sodium hydroxide concentration, for a given sodium silicate content, allowed for higher reaction product, N-A-S-H or geopolymer gel formation, resulting in a stronger matrix, which contributed to improved abrasion resistance.

4.4.4.2. Effects of Sodium Silicate-to-Total Solution Ratio on Abrasion Resistance Results

Increased sodium silicate-to-total solution ratio allowed for abrasion depth to decrease for 5 and 7.5 M NaOH and to increase for 10 and 12.5 M NaOH, as seen in Table 4.13. When increased from 0.20 to 0.40 sodium silicate-to-total solution ratio, abrasion depth decreased approximately 40% when both 5 or 7.5 M NaOH was used. Abrasion depth increased nearly 20% and 14% for the mortars made with 10 and 12.5 M NaOH, respectively. Upon further

increase in sodium silicate-to-total solution ratio from 0.40 to 0.60, abrasion depth decreased by about 33% and 15% for the fly ash mortars activated by 5 and 7.5 M NaOH, respectively. Abrasion depth increased by approximately 5% when 10 M NaOH was used. Overall, with every 20% increase in sodium silicate-to-total solution ratio, abrasion depth decreased by approximately 37% and 28% for the mortars having an alkaline solution of 5 and 7.5 M NaOH, respectively. Abrasion depth increased by nearly 13% for when 10 or 12.5 M NaOH was used. For 5 and 7.5 M NaOH matrices, increased sodium silicate-to-total solution ratio allowed for increased reaction product formation, whereas for 10 and 12.5 M NaOH, increased sodium silicate-to-total solution ratio experienced decreased reaction product formation. The amount of reaction product formed has been found to be responsible for a stronger matrix and improved resistance to abrasive reactions.

The wear depth values determined for the evaluated alkali-activated mortars had standard deviation values between 0.06 mm and 0.4 mm and coefficient of variation values between 2.3% and 18.6%.

4.5. Conclusions

Phase II-Part I of this study evaluated the fresh, mechanical, transport, and durability properties of fly ash mortars activated with both sodium hydroxide and sodium silicate. Sodium hydroxide concentrations and sodium silicate-to-total solution ratio were varied to the influence on properties of alkali-activated fly ash mortars. For the results obtained, the following conclusions can be drawn.

1. Workability decreased with both increased sodium hydroxide concentration and sodium silicate-to-total solution ratio.

2. Compressive strength increased with increased sodium hydroxide concentration. For the mortars containing 5 and 7.5 M NaOH, compressive strength increased with an increase in sodium silicate-to-total solution ratio. Compressive strength of the cylinders made with 10 and 12.5 M sodium hydroxide decreased with increases in sodium silicate-to-total solution ratio. Similar trends were found for flexural strength and modulus of elasticity.
3. The penetrated depth of chloride decreased with increases in sodium hydroxide concentration of the studied fly ash mortars. When 5 or 7.5 M NaOH was used, chloride penetration depth decreased with an increase in sodium silicate-to-total solution ratio, whereas it increased with increased sodium silicate-to-total solution ratio for the mortars containing 10 and 12.5 M NaOH. Absorption and void content also had similar results while density showed an opposite trend.
4. Although minimal, mass loss while immersed in sulfuric acid solution decreased with increased sodium hydroxide concentration. Acid-induced mass loss also decreased with increased sodium silicate-to-total solution ratio for 5 and 7.5 M NaOH whereas the contrary occurred for 10 and 12.5 M NaOH. Acid-induced strength loss was mostly modest, with an average strength loss of 7% for the evaluated mortars. Minimal length change occurred while immersed in sodium sulfate solution as the length expansion decreased with increased sodium silicate-to-total solution ratio. Compressive strength loss was minimal for mortars immersed in a sodium sulfate solution. Mass loss caused by freeze-thaw cycles decreased with increased sodium hydroxide concentration. For the studied mortars containing 5 and 10 M NaOH, freeze-thaw mass losses were found to mirror the trends established for void content. Abrasion depth was found to decrease with increased sodium hydroxide concentration. As sodium silicate-to-total solution ratio

increased, abrasion depth decreased for the mortars activated by 5 and 7.5 M NaOH, whereas it increased when 10 and 12.5 M NaOH were used to activate fly ash mortars.

CHAPTER 5

PHASE II-PART II: FEASABILITY OF ALKALI-ACTIVATED FLY ASH MORTAR CURED AT AMBIENT TEMPERATURE

In continuation from phase II, the feasibility of curing alkali-activated fly ash mortar at ambient temperature was investigated using 10 M NaOH and 0.20, 0.40 and 0.60 sodium silicate-to-total solution ratio. Mechanical, transport, and durability properties were evaluated.

5.1. Mechanical Properties

5.1.1. Compressive Strength

The results for compressive strength are shown in Figure 5.1. Although 0.40 sodium silicate-to-total solution ratio produced the highest compressive strength up to 14 days, mortars containing 0.20 sodium silicate-to-total solution ratio produced the highest compressive strength after 28 days of curing, followed by the mortars made with 0.40 and 0.60 sodium silicate-to-total solution ratio. The 28-day compressive strength decreased 16% and 21% when sodium silicate-to-total solution ratio increased from 0.20 to 0.40 and from 0.40 to 0.60, respectively. Overall, the 28-day compressive strength decreased approximately 19% with every 0.20 increase in sodium silicate-to-total solution ratio. This finding could be related to limited amount of sodium hydroxide to complete the dissolution step of the geopolymerization process. In general, sodium silicate has a lower pH as compared to sodium hydroxide, therefore with increased sodium silicate-to-total solution ratio, pH was expected to decrease. Lower pH led to a lower concentration of $[Al(OH)_4]^-$, responsible for the rate of condensation, the next step in the geopolymerization process (Sagoe-Crentsil and Weng, 2007), specifically, the rate of

condensation between aluminate and silicate species resulted in a solid-state geopolymer structure, the reaction product N-A-S-H gel. A relatively high pH is needed in order to severe the glassy chain found on the surface of fly ash in order to begin the reaction between Si and Al atoms found within fly ash (Ryu et al., 2013). With decreased pH of the system, the reaction process between Si and Al atoms decreased, which led to decreased strength, as well as total degree of reactivity of the tested alkali-activated fly ash mortars.

For the compressive strength values determined for the evaluated alkali-activated mortars, standard deviation values ranged from 1.1 MPa and 1.6 MPa and coefficient of variation values from 1.8% and 8.2%.

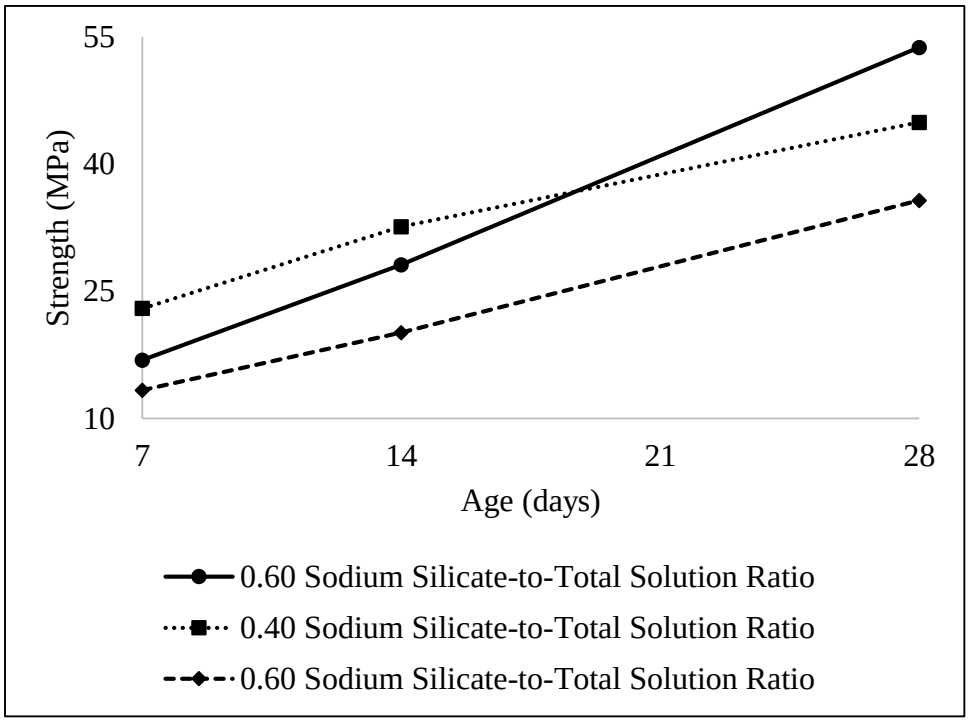

Figure 5.1. Compressive strength results for alkali-activated fly ash mortars - Phase II-Part II

5.1.2. Flexural Strength

The results for flexural strength are shown in Figure 5.2. Alkali-activated mixtures containing 0.20 sodium silicate-to-total solution ratio had the highest flexural strength after 28 days of curing, followed by the mortars containing 0.40 and 0.60 sodium silicate-to-total solution ratios. When sodium silicate-to-total solution ratio increased from 0.20 to 0.40, flexural strength decreased 19.2%. Flexural strength decreased 6.3% once sodium silicate-to-total solution ratio increased from 0.40 to 0.60. As explained for the compressive strength results in section 5.1.1., increased sodium silicate-to-total solution ratio reduced the pH of the system. The decreased pH allowed for a decrease in the reaction process between aluminate and silicate species, resulting in a lower degree of reactivity and reduced flexural strength.

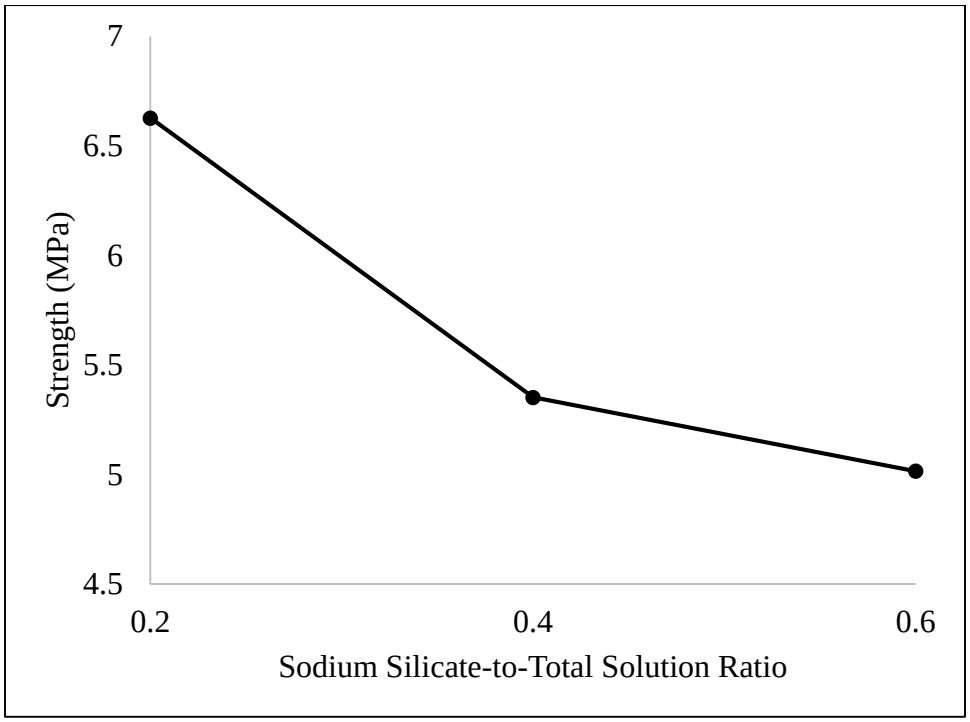

Figure 5.2. Flexural strength results for alkali-activated fly ash mortars - Phase II-Part II

The standard deviation and coefficient of variation values calculated for the obtained flexural strength results differed from 0.1 MPa to 0.4 MPa and 2.3% to 7.2%, respectively.

5.1.3. Modulus of Elasticity

Figure 5.3 displays modulus of elasticity of the studied mortars decreased with an increase in sodium silicate-to-total solution ratio. Overall, modulus of elasticity decreased by an average of 14%. The finding was consistent with the general expectation that modulus of elasticity reduces with lower strength. Due to this direct relationship between strength and stiffness, similar explanation given for compressive strength also holds true for the modulus of elasticity of the studied alkali-activated fly ash mortars.

For the modulus of elasticity values presented, standard of deviation was found to be between 0.2 MPa and 2.4 MPa and coefficient of variation between 0.5% and 64.5%.

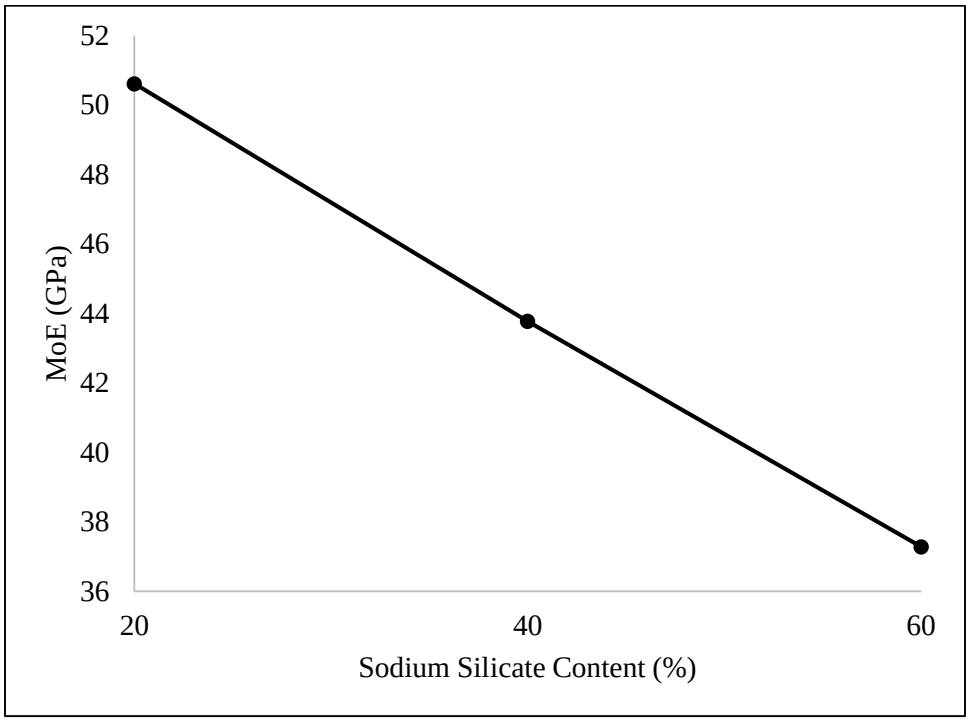

Figure 5.3. Modulus of elasticity for alkali-activated fly ash mortars - Phase II-Part II

5.1.4. Mechanical Property Comparisons

Table 5.1 documents the comparisons between all mechanical properties were made, namely flexural strength vs. compressive strength and modulus of elasticity vs. compressive strength. The flexural-to-compressive strength ratios increased from 0.12 to 0.14 when the sodium silicate-to-total solution ratio increased from 0.20 to 0.60. A similar trend was also found for modulus of elasticity-to-compressive strength. It increased with increased sodium silicate-to-total solution ratio. When increased from 0.20 and 0.40 sodium silicate-to-total solution ratio, modulus of elasticity vs. compressive strength ratio increased by 3.5%. With further increase in sodium silicate-to-total solution ratio to 0.60, modulus of elasticity vs. compressive strength ratio increased 7.2%. On average, modulus of elasticity vs. compressive strength ratio increased by 5.3% for every 0.20 increase in sodium silicate-to-total solution ratio.

Table 5.1. Mechanical Property Comparisons - Phase II-Part II

Mix	28-Day Compressive Strength (MPa)	28-Day Flexural Strength (MPa)	28-Day Modulus of Elasticity (MPa)	Flexural vs. Compressive	Modulus of Elasticity vs. Compressive
D-MC-10	53.76	6.63	50609.62	0.12	941.32
E-MC-10	44.94	5.35	43772.34	0.12	973.98
F-MC-10	35.72	5.02	37282.16	0.14	1043.66

D=0.20 Sodium Silicate-to-Total Solution Ratio, E=0.40 Sodium Silicate-to-Total Solution Ratio, F=0.60 Sodium Silicate-to-Total Solution Ratio

MC= Moist Cured

5.2. Transport Properties

5.2.1. Water Absorption

5.2.1.1. Absorption

Figure 5.4 displays both absorption after immersion and absorption after immersion and boiling. In general, both absorption types increased similarly with increases in sodium silicate-to-total solution ratio. When increased from 0.20 to 0.40 sodium silicate-to-total solution ratio, absorption increased by an average of 21%. Upon further increase from 0.40 to 0.60 sodium silicate-to-total solution ratio, absorption increased an averagely by 8%. With increased sodium silicate-to-total solution ratio, the degree of reaction decreased due to decreased rate of the geopolymerization process, as first discussed in Chapter 4 as well as section 5.1.1. With a lower degree of chemical reactivity, a less compact structure was formed, allowing for higher

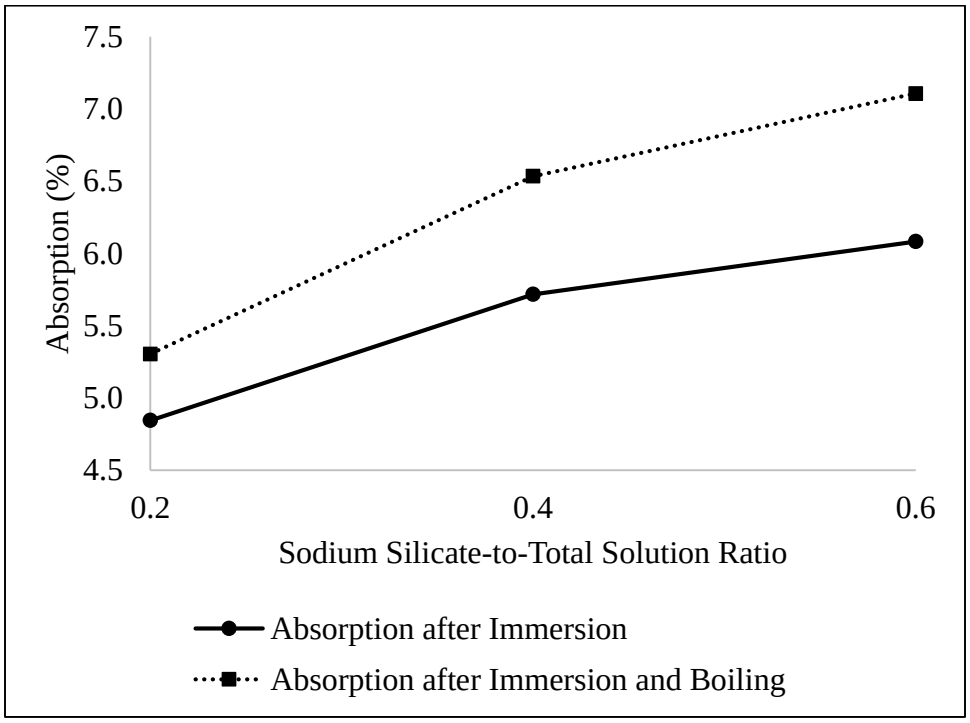

Figure 5.4. Absorption for alkali-activated fly ash mortars - Phase II-Part II

absorptions for the studied alkali-activated fly ash mortars.

Absorption values presented for the evaluated alkali-activated fly ash mortars had standard deviation values between 0.2% and 0.7% and coefficient of variation values between 2.9% and 10.0%.

5.2.1.2. Density

Table 5.2. Density for alkali-activated fly ash mortars - Phase II-Part II

Sodium Silicate-to-Total Solution	Dry Bulk Density (kg/m^3)	Bulk Density after Immersion (kg/m^3)	Bulk Density after Immersion and Boiling (kg/m^3)	Apparent Density (kg/m^3)
0.20	2.122	2.224	2.240	2.397
0.40	2.062	2.185	2.202	2.399
0.60	2.043	2.167	2.188	2.402

In Table 5.2, values of different densities, namely dry bulk density, bulk density after immersion, bulk density after immersion and boiling, and apparent density are displayed. Dry bulk density decreased with increased sodium silicate-to-total solution ratio. Although the differences between all values were minimal, an average of 2% decrease was found regardless of sodium silicate-to-total solution ratio. Both bulk density after immersion and bulk density after immersion and boiling had similar trends. Both densities decreased with increased sodium silicate-to-total solution ratio, although the decrease was rather marginal. When increased from 0.20 to 0.40 sodium silicate-to-total solution ratio, both densities decreased an average of 2%. Once sodium silicate-to-total solution ratio increased from 0.40 to 0.60, both densities decreased less than 1%. While these changes are minimal, decrease in density can be explained. As discussed throughout this study, degree of chemical reaction was related to the rate of the

geopolymerization process. Samples with 0.20 sodium silicate-to-total solution ratio had higher strength and also a higher rate of geopolymerization, resulting in a minor increase in density.

Apparent density increased with increased sodium silicate-to-total solution ratio, contrary to the trends established for all bulk densities mentioned previously. Although minimal, apparent density increased only 0.1%. When measuring apparent density, dry bulk density and void content are taken into account. With that said, a lower dry bulk density was expected to have a higher apparent density as compared to the samples with higher bulk density. Also, a higher void content was expected to have a higher apparent density. Void content is discussed in the following section. By comparing the dry bulk density and void content results, mortars containing 0.20 sodium silicate-to-total solution ratio had the highest dry bulk density and lowest void content; therefore, it had the lowest apparent density. Fly ash mortars activated with 0.60 sodium silicate-to-total solution ratio had the highest void content, lowest dry bulk density and highest apparent density.

For the density values found for the studied alkali-activated mortars, standard deviation values ranged from 0.002 g/cm^3 to 0.05 g/cm^3 and coefficient of variation values from 0.07% and 1.9%.

5.2.1.3. Void Content

Void content increased with increases in sodium silicate-to-total solution ratio, as documented in Figure 5.5. When increased from 0.20 to 0.40 sodium silicate-to-total solution ratio, void content increased 11%. Upon further increase from 0.40 to 0.60 sodium silicate-to-total solution ratio, void content increased 16%. As explained in previous sections, increased sodium silicate-to-total solution ratio accompanied with a decreased rate of geopolymerization,

as well as chemical reactivity. As void content and compressive strength are inversely related, mortars made with 0.20 sodium silicate-to-total solution ratio had the highest compressive strength. A similar pattern was also obtained for the mortars containing 0.40 and 0.60 sodium silicate-to-total solution ratios.

Standard deviation and coefficient of variation values obtained for the void content results presented differed between 0.4 and 0.5 and 2.8% and 4.7%, respectively.

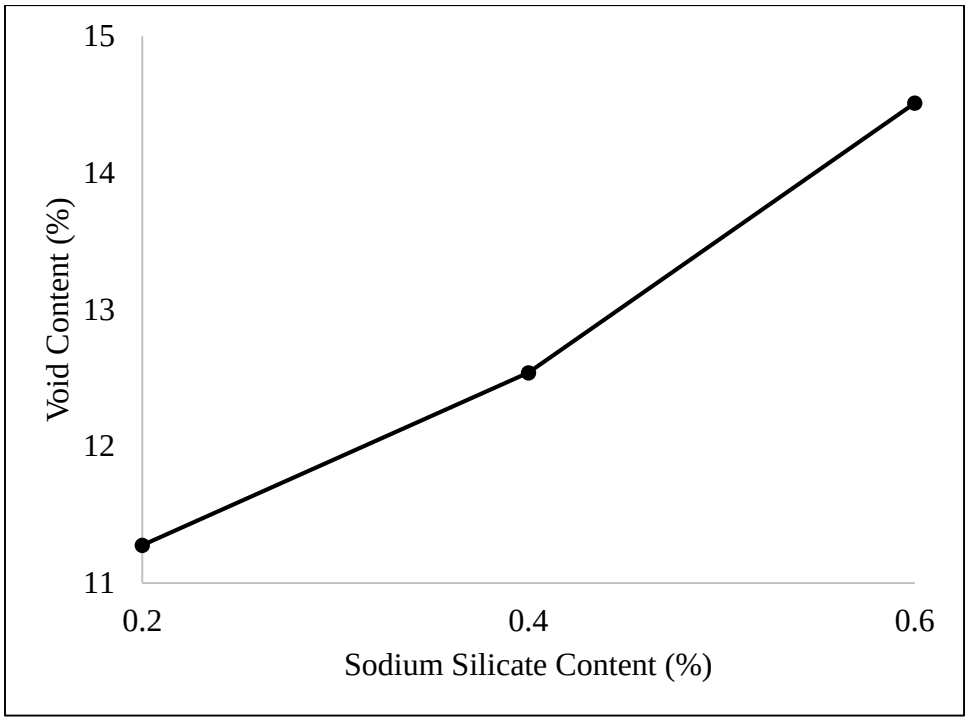

Figure 5.5. Void content for alkali-activated fly ash mortars - Phase II-Part II

5.2.2. Rapid Chloride Migration

Chloride depth increased with increased sodium silicate-to-total solution ratio as depicted in Figure 5.6. Chloride depth increased 13% when sodium silicate-to-total solution ratio increased from 0.20 to 0.40. Upon further 0.20 increase to 0.60 sodium silicate-to-total solution

ratio, chloride depth increased 41%. As discussed in the previous sections, higher degree of chemical reactivity led to a lower void content and reduced chloride depth penetration.

For the rapid chloride migration results presented for the studied alkali-activated fly ash mortars, standard deviation ranged between 0.5 mm and 3.2 mm and coefficient of variation between 4.0% and 18.4%.

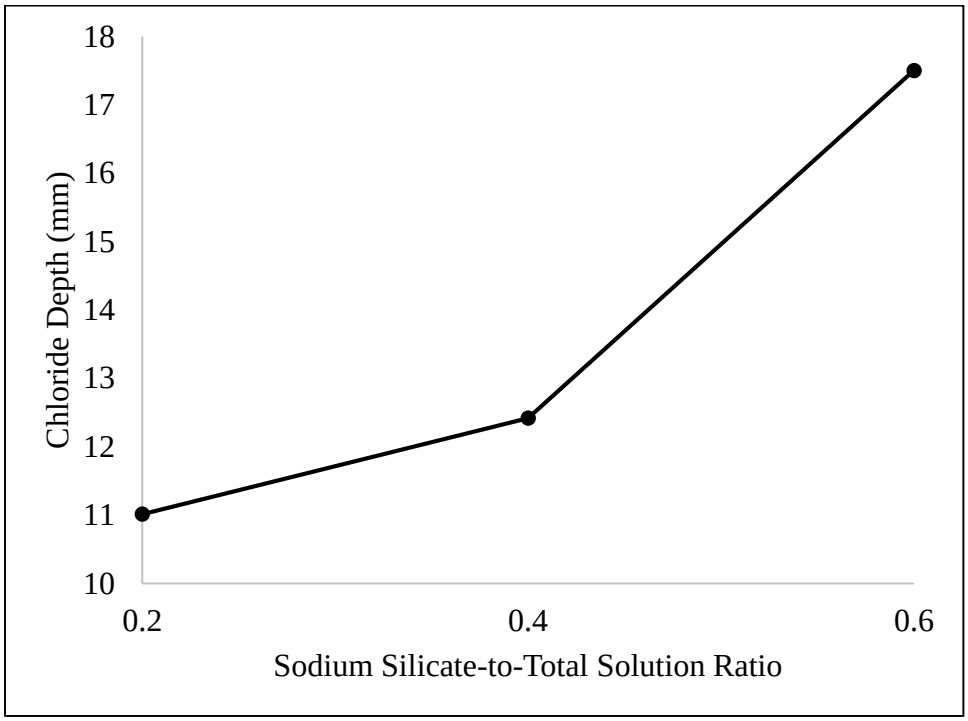

Figure 5.6. Chloride migration for alkali-activated fly ash mortars - Phase II-Part II

5.3. Durability Properties

As discussed in Chapter 4, durability-related properties evaluated for the studied alkali-activated fly ash mortars were resistance to sulfuric acid, external sulfate attack, and wear. Mass loss and loss in strength were evaluated under acid attack regimens. Loss in strength was used to

evaluate resistance to external sulfate attack. Wear depth was evaluated to determine abrasion resistance for the studied alkali-activated fly ash mortars.

5.3.1. Resistance to Acid Attack

5.3.1.1. Sulfuric Acid Induced Mass Loss

As shown in Figure 5.7, mass loss of the samples immersed in a sulfuric acid solution increased with increased sodium silicate-to-total solution ratio. Although some deterioration was seen on the surface, the total mass loss was minimal with maximum mass loss of about 3%. Minimal mass loss when immersed in sulfuric acid solution was attributed to the lack of calcium in the fly ash used, as discussed in the previous chapter. Without an ample amount of calcium, sulfuric acid did not have a medium to react with and, therefore, had minimal effect on the tested alkali-activated mortars.

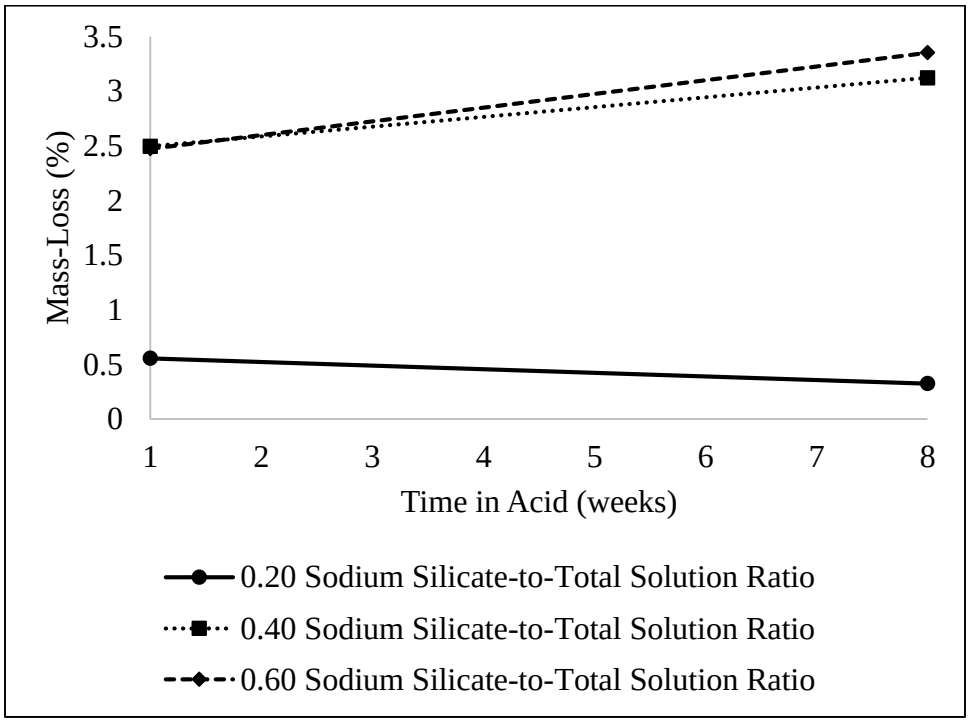

Figure 5.7. Acid resistance in terms of mass loss for alkali-activated fly ash mortars - Phase II-Part II

For the acid-induced total mass loss obtained for the evaluated alkali-activated fly ash mortars, standard deviation values varied between 0.04% and 0.2% and coefficient of variation values between 1.2% and 17.8%.

5.3.1.2. Strength Loss Measurements

In reference to Figure 5.8, compressive strength continued to increase while immersed in a sulfuric acid solution for up to 8 weeks. The excellent resistance when immersed in sulfuric acid solution is attributed to the fly ash used in this study, namely its lack of calcium in comparison to Ordinary Portland Cement (OPC). OPC's calcium content has been proven to be the main cause of its issues in terms of durability (Fernandez-Jimenez et al., 2007; Rangan, 2010). Class F fly ash has a calcium content of lower than 10%, much less than that found in

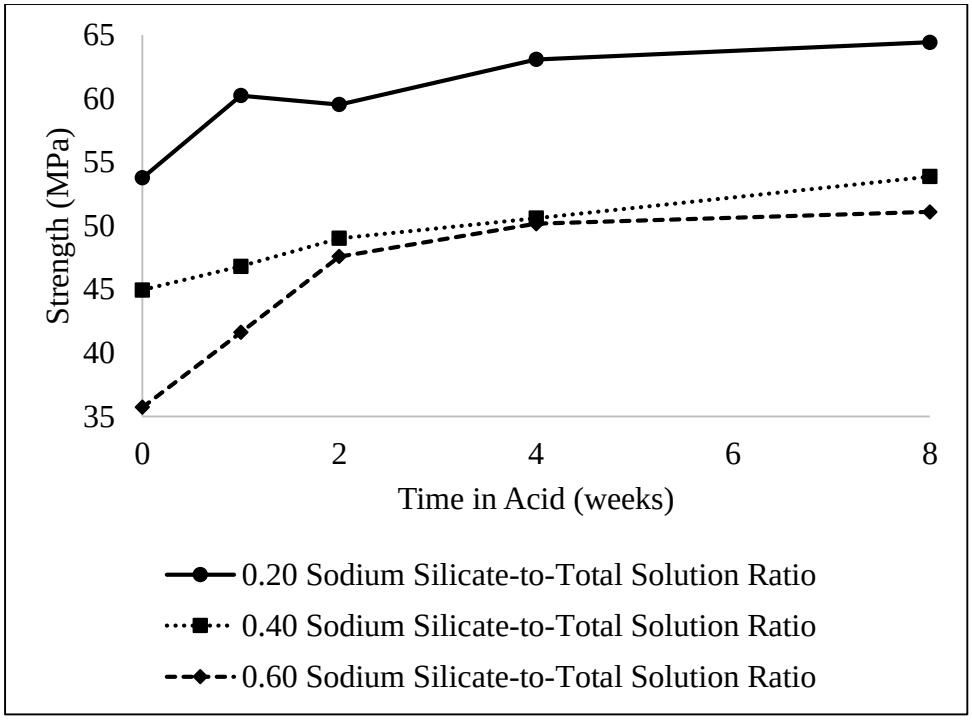

Figure 5.8. Acid resistance in terms of strength for alkali-activated fly ash mortars - Phase II-Part II

OPC. Therefore, sulfuric acid solution did not have much effect when samples were immersed in sulfuric acid solution. The moist environment assisted in improving compressive strength, overtaking any strength reduction due to acid attack.

Standard deviation and coefficient of variation values obtained for acid-induced compressive strength results differed from 1.1 MPa to 3.1 MPa and 0.2% and 12.9%, respectively.

5.3.2. Sulfate Resistance

Similar to the results obtained under exposed to sulfuric acid, compressive strength increased when immersed in a sodium sulfate solution for up to 8 weeks while maintaining the compressive strength trend established previously (see Figure 5.9). In the case of utilizing OPC as the main concrete binder, the durability issues for OPC are related to the calcium content of OPC. In OPC, sodium sulfate reacts with the C_3A of OPC resulting in ettringite and/or gypsum compound, known to cause expansion and loss in strength, lower the pH of the system and, ultimately, its deterioration (Fernandez-Jimenez et al., 2007; Rangan, 2010). When used as the main binder in alkali-activated mortars immersed in sodium sulfate solution, there was not much calcium available in Class F fly ash to react with sodium sulfate, to form ettringite compound, responsible for expansion. Due to the lack of reaction with sodium sulfate, the geoplymerization rate is allowed to continue over time, resulting in continued gain in strength for the studied alkali-activated fly ash mortars.

For the sulfate-induced compressive strength values obtained for the studied alkali-activated fly ash mortars, standard deviation values varied between 2.0 MPa and 3.9 MPa and coefficient of variation values between 2.3% and 9.0%.

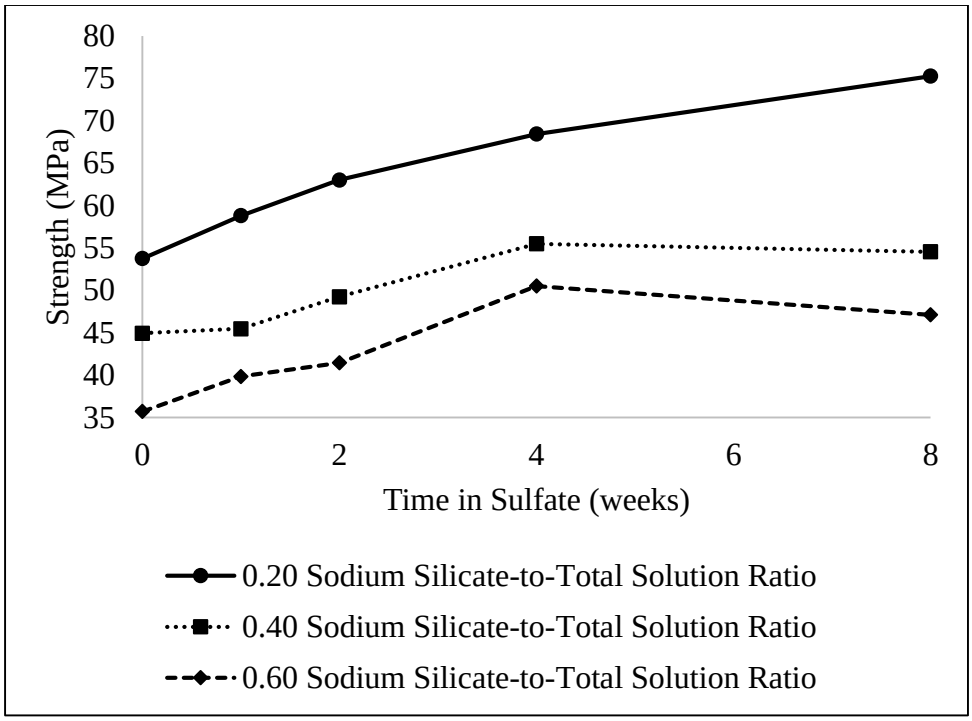

Figure 5.9. Sulfate resistance in terms of strength for alkali-activated fly ash mortars - Phase II-Part II

5.3.3. Abrasion Resistance

Table 5.3 displays the abrasion depth results obtained for the evaluated alkali-activated fly ash mortars. As seen, abrasion depth increased with increased sodium silicate-to-total solution ratio. From 0.20 to 0.40 sodium silicate-to-total solution ratio, abrasion depth increased approximately 6%. Once increased to 0.60 sodium silicate-to-total solution ratio, abrasion depth increased almost 60%. Overall, with every 0.20 increase in sodium silicate-to-total solution ratio, abrasion depth increased approximately 33%. The results presented here can be related to those obtained for mechanical strength in section 5.1. Strength decreased with increased sodium silicate-to-total solution ratio, in other words, matrix containing 0.20 sodium silicate-to-total solution ratio produced the highest strength while the matrix containing 0.60 sodium silicate-to-total solution ratio displayed the lowest strength results. With that said, it was expected that

matrices containing 0.20 sodium silicate-to-total solution ratio would display better abrasion resistance while mortars containing 0.60 sodium silicate-to-total solution ratio would perform the worst against abrasive action. This expectation was confirmed by the results produced by the studied alkali-activated fly ash mortars.

Standard deviation and coefficient of variation results determined for resistance to wear results differed between 0.003 mm and 0.09 mm and 0.1% and 5.9%, respectively.

Table 5.3. Abrasion depth (mm) for alkali-activated fly ash mortars - Phase II-Part II

Sodium Silicate-to-Total Solution	Abrasion Depth (mm)
0.20	1.38
0.40	1.46
0.60	2.32

5.4. Comparison between Elevated and Room Temperature Curing Conditions

Parts I and II of phase II studied similar matrices, with part I incorporated elevated oven temperature curing conditions, whereas part II utilized room temperature moist curing conditions. With that said, the results obtained in part I (Chapter 4) of this study were compared against the results reported in this chapter to determine the differences and, ultimately, the feasibility of implementing room temperature curing conditions. Specifically, matrices containing 10 M NaOH were utilized for this comparison.

5.4.1. Mechanical Properties

As discussed previously, compressive and flexural strength were tested as well as modulus of elasticity. In order to make a fair comparison between the two types of curing conditions, 7-day results were used for oven-cured samples and 28-day results were used for

room temperature cured samples. Table 5.4 displays the results obtained for matrices containing 10 M NaOH for both curing types.

Table 5.4. Mechanical properties comparisons for oven dried and room temperature moist cured samples - Phase II-Part II

Curing Type	Sodium Silicate-to-Total Solution	Compressive Strength (MPa)			7 Day Flexural Strength (MPa)	7 Day Modulus of Elasticity (GPa)
		1 Day	3 Day	7 Day		
Oven Curing	0.20	62.94	75.67	76.20	9.40	67.62
	0.40	51.82	64.93	65.93	6.91	62.55
	0.60	46.97	59.41	60.64	6.75	61.93
		Compressive Strength (MPa)			28 Day Flexural Strength (MPa)	28 Day Modulus of Elasticity (GPa)
		7 Day	14 Day	28 Day		
Room Temperature Moist Curing	0.20	16.90	28.14	53.76	6.63	50.61
	0.40	22.98	32.64	44.94	5.35	43.77
	0.60	13.34	20.14	35.72	5.02	37.28

As shown in Table 5.4, oven curing condition matrices had a greater compressive strength developed after 7 days than the mortars producing 28-day compressive strength under room temperature moist curing conditions. 7-day oven-cured compressive strength was higher than 28-day moist-cured compressive strength by 42%, 47% and 70% for the fly ash mortars made with 0.20, 0.40 and 0.60 sodium silicate-to-total solution ratio, respectively.

Comparison for flexural strength development between oven dried and room temperature moist curing conditions are also shown in Table 5.4. Oven curing conditions allowed for higher flexural strength development than room temperature moist curing conditions, similar to the trend found for compressive strength. There was a 42%, 29% and 35% difference in flexural strength between the two curing conditions for the mortars containing 0.20, 0.40 and 0.60 sodium silicate-to-total solution ratio, respectively.

Comparisons for modulus of elasticity between the two curing conditions are displayed in Table 5.4. Oven curing conditions allowed for higher modulus of elasticity development in comparison to room temperature moist curing conditions. Between 7-day oven and 28-day room temperature moist curing, there was a 34%, 43% and 66% difference for the fly ash mortars activated with 0.20, 0.40 and 0.60 sodium silicate-to-total solution ratio, respectively. The addition of heat during the curing process allowed for the rate of the dissolution stage of the geopolymerization process to increase, which led to increased formation of reaction product and improved strength development (Sagoe-Crentsil and Weng, 2007).

5.4.2. Transport Properties

Similar to mechanical properties, transport properties comparison utilized final curing durations, 7 and 28 days for oven dried and room temperature moist curing conditions, respectively. Rapid chloride migration, absorption, density, and void content were the tested transport properties, their results are displayed in Table 5.5.

Table 5.5. Transport properties comparison for oven and room temperature moist curing - Phase II-Part II

Curing Type	Sodium Silicate-to-Total Solution	Absorption after Immersion (%)	Dry Bulk Density (kg/m^3)	Void Content (%)	Chloride Depth (mm)
7-Day Oven Dry Curing	0.20	3.60	2.12	8.32	9.20
	0.40	4.85	2.09	15.90	10.61
	0.60	4.32	2.11	9.70	13.64
28-Day Room Temperature Moist Curing	0.20	4.84	2.12	11.28	11.02
	0.40	5.72	2.06	12.54	12.42
	0.60	6.08	2.04	14.51	17.51

Absorption was lower when oven curing conditions was used as compared to room temperature moist curing conditions. There was an average 27.5% difference in absorption values between the two curing conditions for all sodium silicate-to-total solution ratios.

Dry bulk density, as shown in Table 5.5, was higher when 7-day oven curing conditions were used as compared to that obtained for the 28-day room temperature moist curing conditions. There was a minimal difference between the two curing methods for the mortars made with 0.20 sodium silicate-to-total solution ratio, whereas a 3.4% difference was found for the mortars containing for 0.60 sodium silicate-to-total solution ratio.

Void content was also lower for oven curing, as seen in Table 5.5. Between the two curing types, there was a 26% and 33% difference for the mortars activated with 0.20 and 0.60 sodium silicate-to-total solution ratio, respectively.

Oven curing conditions had a lower chloride depth penetration as compared to that displayed by the moist-cured mortars, as shown in Table 5.5. One average, there was an 18% difference between the two curing conditions.

5.4.3. Durability Properties

Acid, sulfate and abrasion resistance were tested for durability properties. Acid-induced mass loss and wear depth results are shown in Table 5.6. Table 5.7 displays the strength loss due to acid attack and Table 5.8 shows the strength loss due to external sulfate attack.

As seen in Table 5.6, minimal mass loss was measured when samples were immersed in sulfuric acid for up to eight weeks. When comparing the two curing types, oven curing conditions experienced lesser mass loss. Due to the increased reaction product formed with elevated curing temperature, the bonding strength was also expected to be greater (Sagoe-

Crentsil and Weng, 2007). With increased bonding strength, mass loss was expected to be lower for elevated curing temperatures versus room temperature moist curing.

Although oven curing conditions caused slight strength loss and room temperature moist curing conditions had an increase in strength, oven curing conditions had the highest strength overall for all sodium silicate-to-total solution ratios, as seen in Table 5.7. As discussed in section 5.3.1.1., lack of calcium found in class F fly ash allowed for better durability than OPC (Fernandez-Jimenez et al., 2007; Rangan, 2010). With that said, the compressive strength results found previously were expected to stay the same for over-dried samples. As for room temperature moist curing mortar samples, continued exposure to a moist environment allowed for an increase in strength in the absence of acid induced attack.

For resistance to external sulfate attack, only strength loss measurements were conducted for room temperature moist curing conditions. With that said, Table 5.8 shows the comparison of strength loss measurements for both curing condition types. Similar to the results found for acid resistance, oven curing conditions had minimal strength loss over time while room temperature moist curing conditions had an increase in strength over time.

Table 5.6. Durability properties comparison for oven and room temperature moist curing - Phase II-Part II

Curing Type	Sodium Silicate-to-Total Solution	Acid-Induced Mass Loss (%)	Wear Depth (mm)
7-Day Oven Curing	0.20	0.40	0.93
	0.40	1.38	1.12
	0.60	0.99	1.17
28-Day Room Temperature Curing	0.20	0.33	1.38
	0.40	3.12	1.46
	0.60	3.87	2.32

Table 5.7. Acid-induced strength loss comparison for oven and room moist temperature curing - Phase II-Part II

Curing Type	Sodium Silicate-to-Total Solution	Acid-Induced Strength Loss (MPa)					
		7 Days	28 Days	1 Week	2 Weeks	4 Weeks	8 Weeks
7-Day Oven Curing	0.20	72.39		69.56	69.78	71.57	73.61
	0.40	62.63		61.66	57.67	57.09	56.37
	0.60	60.64		61.55	59.78	59.00	58.47
28-Day Room Temperature Moist Curing	0.20		53.76	60.23	59.52	63.07	64.43
	0.40		44.94	46.81	48.28	50.21	53.87
	0.60		35.72	41.61	47.58	50.15	51.09

Table 5.8. Strength loss due to external sulfate attack comparison for oven and room temperature moist curing - Phase II-Part II

Curing Type	Sodium Silicate-to-Total Solution	Strength Loss due to Sulfate Attack (MPa)					
		7 Days	28 Days	1 Week	2 Weeks	4 Weeks	8 Weeks
7-Day Oven Curing	0.20	76.20		75.77	72.59	73.54	80.81
	0.40	62.63		62.52	61.97	60.06	58.58
	0.60	60.64		60.79	58.55	59.57	62.14
28-Day Room Temperature Moist Curing	0.20		53.76	58.81	63.02	68.45	75.27
	0.40		44.94	45.48	49.25	55.50	54.55
	0.60		35.72	39.85	41.46	50.51	47.11

Table 5.6 also shows the 7-day oven-cured matrices had a lower wear depth as compared to those obtained for the 28-day room temperature moist-cured mortars. Similar to the rest of the comparisons, oven curing allowed for further reaction product formation, thus leading to a denser, stronger and more durable product.

5.5. Conclusions

Phase II-Part II focused on investigating the feasibility of moist-cured alkali-activated fly ash mortars at room temperature, similar to how OPC concrete is cured. Mechanical, transport and durability properties were evaluated. The following conclusions could be made:

1. Compressive and flexural strengths, and modulus of elasticity decreased with increased sodium silicate-to-total solution ratio.
2. Chloride migration, absorption, apparent density, and void content values increased with increased sodium silicate-to-total solution ratio. Dry bulk density, on the other hand, decreased with increased sodium silicate-to-total solution ratio.
3. Resistance to acid and sulfate resistance were found to be excellent with strength increasing over time rather than deteriorating. Minimal mass loss was measured for samples immersed in sulfuric acid solution. Resistance to abrasion results indicated that with increased sodium silicate-to-total solution ratio, depth of wear also increased.
4. When compared to the results obtained for oven curing conditions, moist curing underperformed for all properties evaluated.

CHAPTER 6

CONCLUSIONS AND RECCOMMENDATIONS

The study on the properties of alkali-activated fly ash mortars was divided into two phases. Phase I dealt with the influence of the curing condition, age, activator concentration, and solution-to-binder ratio on the fresh, mechanical and transport properties of alkali-activated fly ash mortars using sodium hydroxide as the sole alkaline activator. Phase II studied the influence of combined sodium hydroxide and sodium silicate, as a dual activator, on the fresh, mechanical, transport, and durability properties of alkali-activated fly ash mortars. Additionally, the mechanical, transport and durability properties of alkali-activated fly ash mortars moist-cured at ambient temperature were also investigated.

6.1. Phase I Results of Alkali-Activated Mortars utilizing Sodium Hydroxide as the Sole Alkaline Activator

Phase I of this study investigated the influence of curing condition, age, activator concentration, and solution-to-binder ratio on alkali-activated fly ash mortars using sodium hydroxide as the alkaline activator. The conclusions for Phase I are given in the subsections to follow.

6.1.1. Fresh Properties

The workability and setting times were the tested fresh properties of alkali-activated fly ash mortars. Overall, workability and setting times increased with increased solution-to-binder ratio, regardless of sodium hydroxide concentration, due to the higher amounts of water available with increased solution-to-binder ratio. In regards to increased sodium hydroxide concentration,

workability and setting times decreased. Increased sodium hydroxide concentration allowed for more activator solution to react upon contact with more fly ash.

6.1.2. Mechanical Properties

The evaluated mechanical properties were compressive and flexural strengths, as well as modulus of elasticity. Influence of curing conditions; namely air, moisture exposed and sealed oven curing; on these load dependent properties were also studied. The effects of different curing conditions were found to be dependent on the concentration of sodium hydroxide in the alkaline solution. For the matrices containing 2.5 M NaOH, sealed curing produced the highest compressive strength followed by moisture exposed and then air oven curing. For the studied matrices containing 5 and 7.5 M NaOH, sealed oven curing produced highest compressive strength followed by moisture exposed and air oven curing up to 3 days. Moisture exposed oven curing produced the highest compressive strength results for the mortars containing 5 and 7.5 M NaOH after 7 days of curing, followed by sealed and air oven curing. Moisture exposed oven curing also produced the highest compressive strength results for the fly ash mortars activated with 10 and 12.5 M NaOH, followed by sealed and air oven curing. Compressive strength was found to decrease and increase with increased solution-to-binder ratio and activator concentration, respectively. Flexural strength and modulus of elasticity were found to have the same trends.

6.1.3. Transport Properties

The evaluated transport properties were absorption, density and rapid chloride migration. Absorption was found to increase and decrease with increased solution-to-binder ratio and activator concentration, respectively. Rapid chloride migration results were also found to have

the same trend as absorption. Density decreased and increased with increased solution-to-binder ratio and activator concentration, respectively.

The alkali-activated mortars containing 12.5 M NaOH and 0.42 solution-to-binder ratio was found to offer the highest strength and stiffness, and lowest transport properties. However, they displayed the lowest flow ability and setting times.

6.2. Phase II Results of Alkali-Activated Fly Ash Mortars utilizing Sodium Hydroxide and Sodium Silicate as a Dual Alkaline Activator

The phase II of this study evaluated the properties of fly ash mortars activated using sodium hydroxide and sodium silicate. Fresh, mechanical, transport, and durability properties were evaluated. This phase of the study was divided into two parts, namely part I and II. Part I utilized sealed oven curing conditions while part II utilized moist curing conditions at ambient temperature.

6.2.1. Part I of Phase II

Part I of Phase II of this study evaluated the influence of sodium hydroxide concentration and sodium silicate-to-total solution ratio on fresh, mechanical, transport, and durability properties of the studied alkali-activated fly ash mortars.

6.2.1.1. Fresh Properties

Workability of the studied alkali-activated fly ash mortars decreased with increases in sodium hydroxide concentration and sodium silicate-to-total solution ratio. Increased sodium hydroxide concentration allowed for increased degree of reactivity, whereas increases in sodium

silicate-to-total solution ratio increased the total SiO_2/Na_2O ratio, causing workability to decrease.

6.2.1.2. Mechanical Properties (Load-Dependent Properties)

The evaluated mechanical properties for the studied alkali-activated fly ash mortars were compressive and flexural strength, as well as modulus of elasticity. Compressive strength was found to increase with increased sodium hydroxide concentration, irrespective of sodium silicate-to-total solution ratio. When sodium silicate-to-total solution ratio increased, however, compressive strength results were found to be dependent on the concentration of sodium hydroxide. For the fly ash mortars made with 5 and 7.5 M NaOH, compressive strength increased with increased sodium silicate-to-total solution ratio, whereas compressive strength decreased for the mortars containing 10 and 12.5 M NaOH. Flexural strength and modulus of elasticity results were also found to have a similar behavior to that displayed by the compressive strength.

6.2.1.3. Transport Properties

The evaluated transport properties were absorption, density, void content, and rapid chloride migration. Absorption was found to decrease with increased sodium hydroxide concentration. When sodium silicate-to-total solution ratio increased, absorption results were found to be dependent on the sodium hydroxide concentration. For the mortars containing 5 and 7.5 M NaOH, absorption decreased with increases in sodium silicate-to-total solution ratio, while absorption increased when 10 and 12.5 M NaOH were used. Apparent density, void content and rapid chloride migration results also followed a similar trend displayed by absorption results.

6.2.1.4. Durability Properties

Durability properties of the studied alkali-activated fly ash mortars involved resistance to sulfuric acid attack, sodium sulfate attack, freezing and thawing, and wear. Losses in mass and strength were used to evaluate resistance to acid attack. Length expansion and strength loss were investigated to determine the extent of resistance to sulfate attack. Mass loss was used to ascertain the resistance to freezing and thawing. Depth of wear was measured for resistance to abrasion.

Mass loss due to acid attack was found to decrease with increased sodium hydroxide concentration. Similar to the load-dependent properties, the influence of increased sodium silicate-to-total solution ratio on mass loss was found to be dependent on sodium hydroxide concentration. For the fly ash mortars made with 5 and 7.5 M NaOH, the total mass loss decreased with increased sodium silicate-to-total solution ratio. When alkali-activated fly ash mortars contained 10 and 12.5 M NaOH, the total mass loss was found to increase with increased sodium silicate-to-total solution ratio. Acid-induced strength loss was mostly modest, with an average strength loss of 7% for all evaluated mortars.

A higher sulfate-induced length change occurred for the mortars with 5 M NaOH than those made with 10 M NaOH. Sulfate-induced length expansion also decreased with increased sodium silicate-to-total solution ratio. Strength loss under sulfate attack was minimal, with the majority of the loss occurring during the first week of immersion. Overall, length expansion and strength loss were minimal due to the insufficient amount of calcium oxide found in class F fly ash. Total freezing and thawing mass loss of the studied alkali-activated fly ash mortars were found to decrease with increased sodium hydroxide concentration. In terms of sodium silicate-to-total solution ratio, its influence was found to be dependent on the sodium hydroxide

concentration. For the mortars containing 5 M NaOH, the total mass loss due to freezing and thawing regimens decreased with increases in sodium silicate-to-total solution ratio, whereas the contrary occurred for the mortars made with 10 M NaOH.

For a given sodium silicate-to-total solution ratio, the depth of wear of the studied alkali-activated fly ash mortars decreased with increased sodium hydroxide concentration. Resistance to abrasion results were found to be dependent on the sodium hydroxide concentration when the influence of varying sodium silicate-to-total solution ratios was evaluated. For the mortars containing 5 and 7.5 M sodium hydroxide, depth of wear decreased with increases in sodium silicate-to-total solution ratio. On the other hand, fly ash mortars activated with 10 and 12.5 M NaOH, the depth of wear increased with increased sodium silicate-to-total solution ratio.

The alkali-activated mortars made with 12.5 M NaOH and 0.20 sodium silicate-to-total solution ratio was found to offer the highest mechanical properties and most resistance to acid, sulfate and wear, while exhibiting the lowest transport properties.

6.2.2. Part II of Phase II

Part II of Phase II of this study focused on the properties of alkali-activated fly ash mortars using, sodium hydroxide and sodium silicate, moist-cured at ambient temperature. This was done by evaluating the mechanical, transport and durability properties of alkali-activated fly ash mortars containing 10 M sodium hydroxide with varying sodium silicate-to-total solution ratios of 0.20, 0.40 and 0.60.

6.2.2.1. Mechanical Properties

The evaluated mechanical properties were compressive and flexural strength, as well as modulus of elasticity. After 28 days of curing, compressive strength decreased with increased

sodium silicate-to-total solution ratio. The same results were found for flexural strength and modulus of elasticity.

6.2.2.2. Transport Properties

Absorption, density, void content, and rapid chloride migration were the evaluated transport properties. Absorption was found to increase with increased sodium silicate-to-total solution ratio. The same trend was found for apparent density, void content and rapid chloride migration. Dry bulk density and bulk densities displayed an opposite trend with an increase in sodium silicate-to-total solution ratio.

6.2.2.3. Durability Properties

The durability properties were resistance to sulfuric acid attack, sodium sulfate and wear. Sulfuric acid-induced mass loss increased with increases in sodium silicate-to-total solution ratio, with the maximum mass loss of nearly 3%. Compressive strength was found to increase with immersion age in sulfuric acid solution. The same trend in compressive strength occurred when the studied alkali-activated fly ash mortars were immersed in a 5% sodium sulfate solution. These trends were found to be attributed to the lack of sufficient calcium oxide in the fly ash used. Depth of wear was found to increase with increases in sodium silicate-to-total solution ratio. The alkali-activated fly ash mortars containing 0.20 sodium silicate-to-total solution ratio was found to be optimum in terms of mechanical properties (highest); resistance to acid and sulfate attacks and wear (highest); and transport properties (lowest).

6.2.2.4. Comparison of Oven-Cured and Moist-Cured Alkali-Activated Fly Ash Mortars

The results obtained from Part II of Phase II were compared to the results obtained for the matrices containing the same alkaline solution from Part I. For all evaluated properties, oven-cured matrices outperformed matrices moist-cured at ambient temperature.

6.3. Recommendations on Future Research

Although much was discovered in this study by evaluating fresh, mechanical, transport, and durability properties of alkali-activated fly ash mortars, more needs to be investigated to better understand the behavior of alkali-activated fly ash mortars. Studies on micro-properties of alkali-activated fly ash mortars made with different concentrations of sodium hydroxide and sodium silicate are needed in order to better explain geopolymerization and macro-properties changes with increasing activator concentration. In addition, future studied should be directed toward evaluating properties of alkali-activated fly ash concrete as a more sustainable alternative to ordinary Portland cement concrete used in the precast industry.

APPENDIX A

CONVERSIONS

1 mm = 0.03937 in

1 g/cm^3 = 1.6856 lb/yd^3

1 g/cm^3 = 0.0624 lb/ft^3

1 MPa = 145 lb/in^2

1 m^3 = 35.3147 ft^3

REFERENCES

(2014)Retrieved March 23, 2015, from http://www.epa.gov/climatechange/ghgemissions/gases/co2.html

Arioz, E., Arioz, O., Kockar, Mete. "An experimental study on the mechanical and microstructural properties of geopolymers". *Procedia Engineering Vol 42*, 2012, 100-105.

Bakharev, T. "Resistance of geopolymer materials to acid attack". *Cement and Concrete Research Vol. 35*, 2005, 658-670.

Chi, Maochieh, Huang, Ran. "Binding mechanism and properties of alkali-activated fly ash/slag mortars". *Construction and Building Materials Vol. 40*, 2013, 291-298.

Criado, M., Fernandez-Jimenez, A., Palomo, A. "Alkali-activated fly ash. Part III: effect of curing conditions on reaction and its graphical description". *Fuel Vol. 89*, 2010, 3185-3195.

Criado, M., Fernandez-Jimenez, A., Sobrados, I., Palomo, A., Sanz, J. "Effect of relative humidity on the reaction products of alkali activated fly ash". *Journal of the European Ceramic Society Vol. 32*, 2012, 2799-2807.

Criado, M., Palomo, A., Fernandez-Jimenez, A. "Alkali activation of fly ashes. Part 1: effect of curing conditions on the carbonation of the reaction products". *Fuel Vol. 84*, 2005, 2048-2054.

Dolezal, Josef, Skvara, Frantisek, Svoboda, Pavel, Sulc, Rostislav, Kopecky, Lubomir, Pavlasova, Simona, Myskova, Lenka, Lucuk, Martin, Dvoracek, Kamil. "Concrete based on fly ash geopolymers". *Alkali-activated materials – research, production and utilization 3rd conference, Prague, Czech Republic*, 2007, 185-197.

Fernandez-Jimenez, A., Garcia-Lodeiro, I., Palomo, A. "Durability of alkali-activated fly ash cementitious materials". *J Mater Sci Vol 42*, 2007, 3055-3065.

Fernandez-Jimenez, A., Palomo, A. "Composition and microstructure of alkali-activated fly ash binder: effect of activator". *Cement and Concrete Research 35*, 2005, 1984-1992.

Fernandez-Jimenez, Ana M., Palomo, Angel, Lopez-Hombrados, Cecilio. "Engineering properties of alkali-activated fly ash concrete". *ACI Materials Journal V. 103, No. 2, March-April 2006*, 2006, 106-112.

Görhan, Gökhan, Kürklü, Gökhan. "The influence of the NaOH solution on the properties of the fly ash-based geopolymer mortar cured at different temperatures". *Compsoite: Part B Vol 58*, 2014, 371-377.

Hardjito, Djwantoro, Wallah, Steenie E., Sumajouw, Dody M.J., Rangan, B. Vijaya. "Mechanical properties of fly ash-based geopolymer concrete". *ACI Materials Journal V. 101, No. 6, November-December 2004*, 2004, 467-471.

Joseph, Benny, Mathew, George. "Influence of aggregate content on the behavior of fly ash based geopolymer concrete". *Scientia Iranica A*, 2012, 1188-1194.

Katz, A. "Microscopic Study of Alkali-Activated Fly Ash". *Cement and Concrete Research Vol. 28, No. 2*, 2012, 197-208.

Komljenović, M., Baščarevič, Z., Bradić, V. "Mechanical and microstructural properties of alkali-activated fly ash geopolymers". *Journal of Hazardous Materials Vol. 181*, 2010, 35-42.

Kovalchuk, G., Pernandez-Jimenez, A., Palomo, A. "Alkali-activated fly ash: effect of thermal curing conditions on mechanical and microstructural development – part II". *Fuel Vol. 86*, 2007, 315-322.

Lee, N.K., Lee, H.K. "Setting and mechanical properties of alkali-activated fly ash/slag concrete manufactured at room temperature". *Construction and Building Materials Vol. 47*, 2013, 1201-1209.

Ma, Y., Hu, J., Ye, G. "The pore structure and permeability of alkali-activated fly ash". *Fuel 104*, 2013, 771-780.

Meyer, C. "The greening of the cement industry". *Cement and Concrete composites 31*, 2009, 601-605.

Mustafa Al Bakri, A.M., Kamarudin, H., BinHussain, M., Khairul Nizar, I., Zarina, Y., Rafiza, A.R. "The effect of curing temperature on the physical and chemical properties of resulting geopolymer". *Ceramics International Vol. 37*, 2011, 285-291.

Pacheco-Torgal, Fernando, Castro Gomes, Joao, Jalali, Said. "Alkali-activated binders: a review part I. Historical background, terminology, reaction mechanisms, and hydration products". *Construction and Building Materials 22*, 2008, 1305-1314.

Pacheco-Torgal, F., Abdollahnejad, Z., Camoes, A.F., Jamshidi, M., Ding, Y. "Durability of alkali-activated binders: a clear advantage over Portland cement or an unproven issue?". *Construction and Building Materials 30*, 2012, 400-405.

Panias, Dimitrios, Giannopoulou, Ioanna P., Perraki, Theodora. "Effect of synthesis parameters on the mechanical properties of fly ash based geopolymers". *Colloids and Surfaces A: Physicochem. Eng. Aspects Vol 301*, 2007, 246-254.

Rajamma, Rejini, Labrincha, Joao A., Ferreira, Victor M. "Alkali activation of biomass fly ash-metakaolin blends". *Fuel Vol. 98*, 2012, 265-271.

Rangan, Vigaya. "Fly ash-based geopolymer concrete". *Proceedings of the International Workshop on Geopolymer Cement and Concrete*, 2010, 68-106.

Ravikumar, Deepak, Peethamparan, Sulapha, Neithalath, Narayaran. "Structure and strength of NaOH activated concretes containing fly ash or GGBS as the sole binder". *Cement and Concrete Composites Vol. 32*, 2010, 399-410.

Ryu, Gum Sung, Lee, Young Bok, Koh, Kyung Taek, Chung, Young Soo. "The mechanical properties of fly ash-based geopolymer concrete with alkaline activators". *Construction and Building Materials Vol. 47*, 2013, 409-418.

Sagoe-Crentsil, K., Weng, L. "Dissolution processes, hydrolysis and condensation reactions during geopolymer synthesis: part II. High Si/Al ratio systems". *J Mater Sci Vol 42*, 2007, 3007-3014.

Shi, Caijun, Fernandez-Jimenez, A., Palomo, Angel. "New cements for the 21st century: the pursuit of an alternative to Portland cement". *Cement and Concrete Research 41*, 2011, 750-763

Silva de Vargas, Alexandre, Dal Molin, Denise C.C., Vilela, Antonio C.F., da Silva, Felipe Jose, Pavao, Bruno, Veit, Hugo. "The effects of Na_2O/SiO_2 molar ratio, curing temperature and age on compressive strength, morphology and microstructure of alkali-activated fly ash-based geopolymers". *Cement and Concrete Composites Vol. 33*, 2011, 653-660.

Thokchom, Suresh, Ghosh, Dr. Partha, Ghosh, Dr. Somnath. "Acid resistance of fly ash based geopolymer mortars". *International Journal of Recent Trends in Engineering, Vol. 1, No. 6*, 2009, 36-40.

Weng, L., Sagoe-Crentsil, K. "Dissolution processes, hydrolysis and condensation reactions during geopolymer synthesis: part I – low Si/Al ratio systems". *J Mater Sci Vol 42*, 2007, 2997-3006.

Xie, Jiting, Kayali, Obada. "Effect of initial water content and curing moisture conditions on the development of fly ash-based geopolymers in heat and ambient temperature". *Construction and Building Materials*, 2013.

Xin, Luo, Jinyu, Xu, Erlei, Bai, Weimin, Li. "Systematic study on the basic characteristics of alkali-activated slag-fly ash cementitious material system". *Construction and Building Materials Vol. 29*, 2012, 482-486.

Yang, Keun-Hyeok, Song, Jin-Kyu, Ashour, Ashraf F., Lee, Eun-Taik. “Properties of cementless mortars activated by sodium silicate”. *Construction and Building Materials 22*, 2008, 1981-1989.

CURRICULUM VITAE

Graduate College
University of Nevada, Las Vegas

Kimberly J. Sierra

Email Address: sierrak@unlv.nevada.edu

Degrees:

Bachelor of Science in Entertainment Engineering Design, 2012
University of Nevada, Las Vegas

Thesis Title: Alkali-Activated Fly Ash Binders: Feasibility as a Sustainable Alternative to Ordinary Portland Cement for Precast Systems